View metadata, citation and similar papers at core.ac.uk
brought to you by CORE
provided by Wits Institutional Repository on DSPACE

THE EFFECT OF COAL COMPOSITION ON CARBON DIOXIDE ADSORPTION

Siboniwe Bhebhe

A dissertation submitted to the Faculty of Engineering and the Built Environment, University of the Witwatersrand, in fulfillment of the requirements for the degree of Master of Science in Engineering.

Johannesburg, 2008

I declare that this dissertation is my own, unaided work. It is being submitted for the degree of Master of Science in the University of the Witwatersrand, Johannesburg. It has not been submitted before for any degree or examination in any other University.

(Signature of candidate)

_____day of _____ (year) _____

ABSTRACT

Greenhouse gas emissions due to fossil fuel combustion and gasification are recognized as the major contributor to climate changes. South Africa is ranked the 12th highest emitter of carbon dioxide in the world and accounts for 38 % of carbon dioxide emissions in Africa. Carbon dioxide sequestration in unminable coal seams is one of the options available for the reduction of carbon dioxide emissions in South Africa.

The adsorption behavior of carbon dioxide on four parent coal samples from major coal fields in South Africa was studied. Heavy media separation was used to concentrate coal macerals and mineral matter. The effect of the coal macerals, mineral matter and coal rank on the carbon dioxide adsorption of the samples was evaluated. The coal samples covered a maturity range from 0.69 % to 2.28 %. The maceral compositions of the fractions varied from 92.8 % to 0.4 % vitrinite and 78.8 % to 0.4 % inertinite. Half of the samples had 0 % liptinite and the maximum liptinite obtained for the rest of the samples was 9.2 %. Mineral matter content ranged between 0.4 % and 93.0 %. Adsorption measurements were performed on 2.0 g samples with a grain size of 300 – 600 µm. The adsorption isotherms were measured at 303-304 K and a pressure range of 250kPa to 1500 kPa using the volumetric method. The volumetric system was specifically designed and constructed for this research work.

The adsorption capacity was determined by fitting the data with a Langmuir equation. The model provided very good fits, the relative error between the measured value and the predicted value over the entire pressure range was less than 5.0 % for all the samples.

The carbon dioxide adsorption capacity appears to positively correlate to the vitrinite content and negatively correlate to the mineral matter content. There appears to be no relationship between the inertinite content and gas adsorption capacity. The highest adsorption capacity obtained was for the highest rank vitrinite-rich coal sample, and the mineral matter-rich sample had the lowest adsorption capacity.

Repeatability tests generated similar adsorption isotherms to the original experiments, thus showing that the equipment and the experimental procedures used are valid for the purposes of this analysis.

ACKNOWLEDGEMENTS

I would like to extend my sincere gratitude to Dr. Nikki Wagner, Senior Lecturer in the School of Chemical and Metallurgical Engineering, for sponsoring this project and for her guidance, support and for carrying out the petrographic analysis of the samples.

Many thanks also go to the different organisations who supplied the samples. I would also like to thank the staff at Johannesburg Valve and Fitting Company for constructing the equipment. My sincere gratitude also goes to the staff at the Potchefstroom campus for conducting the surface area analysis. Many thanks also go to Bruce and Doctor for assistance with laboratory equipment.

Last but not least I would also like to thank my parents and siblings for their support during my period of study.

CONTENTS

LIST OF FIGURES

LIST OF TABLES

Table

LIST OF SYMBOLS

cP	centipoise
^{o}C	degrees Celsius
Gt	Gigatonne
kPa	kilopascal
n	number of moles
nm	nanometer
PJ	Petajoule
pH	logarithm of the hydrogen ion concentration in solution
Pc	critical pressure (bar)
ppm	parts per million
Pr	reduced pressure
R	gas constant (J. mol^{-1}.K)
s.g	specific gravity
Tc	critical temperature (K)
Tr	reduced temperature
% v/v	volume percent
Vm	molar volume (m^3/mol)
Z	compressibility factor

LIST OF ABBREVIATIONS

CARMA	Carbon Monitoring for Action
CDM	Clean Development Mechanism
CSLF	Carbon Sequestration Leadership Forum
ECBM	Enhanced Coal Bed Methane
EOR	Enhanced Oil Recovery
IPCC	Intergovernmental Panel on Climate Change
IUPAC	International Union of Pure and Applied Chemistry
KZN	KwaZulu-Natal
NGO	Non-Governmental Organisation
SSN	South South North
TGA	Thermogravimetric Analyser
UNFCC	United Nations Framework Convention on Climate Change

CHAPTER 1: INTRODUCTION

1.1 BACKGROUND AND MOTIVATION

Greenhouse gas emissions due to fossil fuel combustion and gasification are recognized as the major contributor to climate change. Carbon dioxide, which is the main anthropogenic greenhouse gas, is believed to be responsible for enhancing the greenhouse effect leading to global warming, a rise in sea level and changes in rainfall patterns. Fossil fuel combustion and coal gasification, which are the main sources of carbon dioxide emissions, are likely to continue to provide a large proportion of the world's commercial energy for the foreseeable future. Therefore there is urgent need to develop technology for reducing carbon dioxide emissions (Flory, 2005).

Since the beginning of the industrial revolution in the mid-nineteenth century, atmospheric concentrations of carbon dioxide have increased by nearly 30 % (Birol and van Hulst, 2006) and this has enhanced the heat trapping capability of the earth's atmosphere. Global energy-related carbon dioxide emissions are predicted to increase further by 55 % between 2004 and 2030 and carbon dioxide emissions could reach an alarming 40 Gt in 2030 if measures are not taken to control emissions. Developing countries are expected to account for 50 % of the emissions in 2030; this is mainly due to the low calorific value and high carbon content of their primary source of energy, coal (Birol and van Hulst, 2006).

In South Africa, the growth of the economy has led to an increase in energy demand. The total primary energy supply increased from 3,933 PJ in 1993 to 5,241 PJ in 2004 (Van Wyk et al., 2006). The abundance of low-cost coal, which has higher environmental impacts than the other fossil fuels i.e. oil and gas, led to coal providing approximately 68 % of South Africa's primary energy in 2004 (Van Wyk et al., 2006). Although the impact on the environment would be considerably less if the energy economy were based on natural gas, or hydro-electric power, the presence of large and easily-exploitable coal reserves

suggests that coal will continue to be the mainstay of the energy sector for the foreseeable future (Van Wyk et al., 2006).

These alarming statistics on carbon dioxide emissions in South Africa call for immediate intervention by the South African government and industry to reduce carbon dioxide emissions into the atmosphere. Carbon dioxide sequestration in unminable coal seams is one of the possible mitigation options that South Africa can employ in its quest to reduce emissions. Carbon dioxide sequestration is a process which involves carbon dioxide capture, transportation and subsequent injection into the desired storage site. The data from this study could guide selection of suitable sites as well as optimization of the sequestration process in South Africa.

Coal seams provide one of the most attractive geological storage options due to the large coal reserves in South Africa, and the fact that carbon dioxide adsorption onto coal is high. Carbon dioxide adsorption onto coal displaces the adsorbed methane from the coal surface (Saghafi et al., 2006). This concept can be employed to enhance coal bed methane extraction at the same time reducing carbon dioxide emissions. Revenue from enhanced coal bed methane recovery can offset the costs associated with carbon dioxide capture, transport and storage. This study is aimed at providing data for optimising storage in coal seams, by identifying compositional factors which affect the carbon dioxide adsorption capacity.

The macerals that make up the organic fraction of coal are; vitrinite, inertinite and liptinite. Vitrinite is a product of the decomposition of cellular plant material while inertinite is fossilized charcoal and liptinite is a product of decayed leafy matter, spores, pollen and algal matter. The three macerals exhibit different physical and chemical characteristics hence their gas adsorption capacities are expected to be different. Gas adsorption occurs mainly on the surfaces of pores and coal porosity varies depending on the maceral composition and rank i.e. vitrinite predominantly contains micro pores while inertinite contains meso- and macro-pores (Karacan et al., 2003). The adsorption of carbon dioxide onto coal is a function of the coal porosity; therefore the variation of coal porosity with rank and

maceral composition is expected to affect carbon dioxide adsorption capacity onto coal.

Studies conducted by Karacan and Mitchell (2003) as well as Day et al. (2007) show that inertinite rich coals adsorb more carbon dioxide than vitrinite-rich coals. Inertinite-rich coal mainly consists of macropores and mesopores, and these pores have larger diameters hence gas molecules can easily be adsorbed onto the surface of these molecules. The vitrinite-rich coal contains micropores which prevent ease of movement of gas particles to the coal surface. Karacan and Mitchell (2003) also concluded that the mineral matter in coal allows gas molecules to easily pass through the matrix before it gets adsorbed on the organic surfaces. Hence mineral matter rich coal can adsorb more gas.

The adsorption isotherm is the most widely used technique to describe gas adsorption by coal. The Langmuir adsorption model is widely used for the assessment of low pressure gas adsorption on coal (Simeons et al., 2007).

1.2 PROBLEM STATEMENT

Due to the complexity of the chemistry of coal and its variability, different researchers have reported conflicting results on studies conducted to determine the effect of coal rank and coal composition on carbon dioxide adsorption for coal samples. In order to optimize the carbon dioxide sequestration process in South African coal seams, there is need to conduct studies on the carbon dioxide uptake behavior of South African coals. Therefore the purpose of this study is to determine the effect of coal rank, maceral composition and mineral matter on the carbon dioxide adsorption capacity for South African coals i.e. Witbank, Waterberg and Kwazulu Natal coals. The results of the study will be used to create a database for carbon dioxide sequestration modeling and upscaling in South African coal seams.

1.3 HYPOTHESIS

1. Inertinite rich coals have the ability to adsorb a greater amount of carbon dioxide than vitrinite-rich coals.
2. There is a correlation between coal rank and carbon dioxide adsorption capacity.
3. Mineral matter in coal has an effect on the carbon dioxide adsorption capacity of the coal.

1.4 AIM AND OBJECTIVES

The aim of this dissertation is to study the carbon dioxide adsorption capacity of South African coals with different compositions.

The objectives are;

1. To design and construct experimental equipment for adsorption measurements.
2. To use this equipment to determine:
    i. the maceral with the greatest capacity for carbon dioxide adsorption.
    ii. the effect of mineral matter on the adsorption capacity of coal.
    iii. the effect of rank on carbon dioxide adsorption capacity.
    iv. the suitability of the Langmuir adsorption model in representing the adsorption of carbon dioxide onto coal.

1.5 OUTLINE OF THE DISSERTATION

The structure of the dissertation is as follows:

Chapter 2 is an overview of global greenhouse gas emissions and its effects on climate change as well as carbon dioxide sources and sequestration options.

Chapter 3 describes coal formation, composition and unminable coal seams.

Chapter 4 outlines the properties of carbon dioxide as well as the principle of its adsorption onto coal and results of similar research conducted in other countries.

Chapter 5 is a description of the detailed design, construction and testing of the adsorption equipment.

Chapters 6 describes sample preparation and sample characterisation results, a detailed description of the adsorption experimental procedure is also given.
Chapter 7 presents the adsorption experimental results and discussion.
Chapter 8 lists the conclusions of the investigation and recommendations for continued research in this area.

CHAPTER 2: CARBON DIOXIDE EMISSIONS AND CLIMATE CHANGE

This chapter describes the role played by anthropogenic carbon dioxide emissions on climate change. It also gives an overview on legislation for the reduction of carbon dioxide emissions. The last part of the chapter lists the various sources of carbon dioxide, as well as the mitigation options that are available.

2.1 THE GREENHOUSE EFFECT

The earth is surrounded by a thin layer of gases called the atmosphere, which is held in place by gravity. The composition of the atmosphere is given in Table 2.1 below:

Table 2.1 Composition of the Atmosphere in 2001 (Houghton, 2004).

Gas	Composition
Nitrogen (N_2)	0.78 %v/v
Oxygen (O_2)	0.21 %v/v
Water vapor (H_2O)	0.02 %v/v
Carbon dioxide (CO_2)	370 ppm
Methane (CH_4)	1.8 ppm
Nitrous oxide (N_2O)	0.3 ppm
Chlorofluorocarbons	0.001 ppm
Ozone (O_3)	1000 ppm

The earths' overall temperature is determined by the strength of the incident radiation from the sun and the amount of heat retained within the atmosphere. During the day the incoming solar radiation (shortwave radiation) is absorbed by the ground and at night the ground emits this heat into space as infrared radiation (long wave radiation). Nitrogen and oxygen are transparent to both solar and infrared radiation, however the minor constituents of the atmosphere

called greenhouse gases are only transparent to the solar radiation but strongly absorb the infrared radiation (Houghton, 2004).

Greenhouse gases include water vapor, carbon dioxide, methane, nitrous oxide, chlorofluoro carbons and ozone. The radiation absorbed by these greenhouse gases is re-emitted in all directions, resulting in warming of the earths' surface. This process is called the green house effect (Fig. 2.1), and is a natural process that plays a major role in the earths' climate. It is responsible for creating a relatively warm environment on the earths' surface which supports life on the planet (Houghton, 2004).

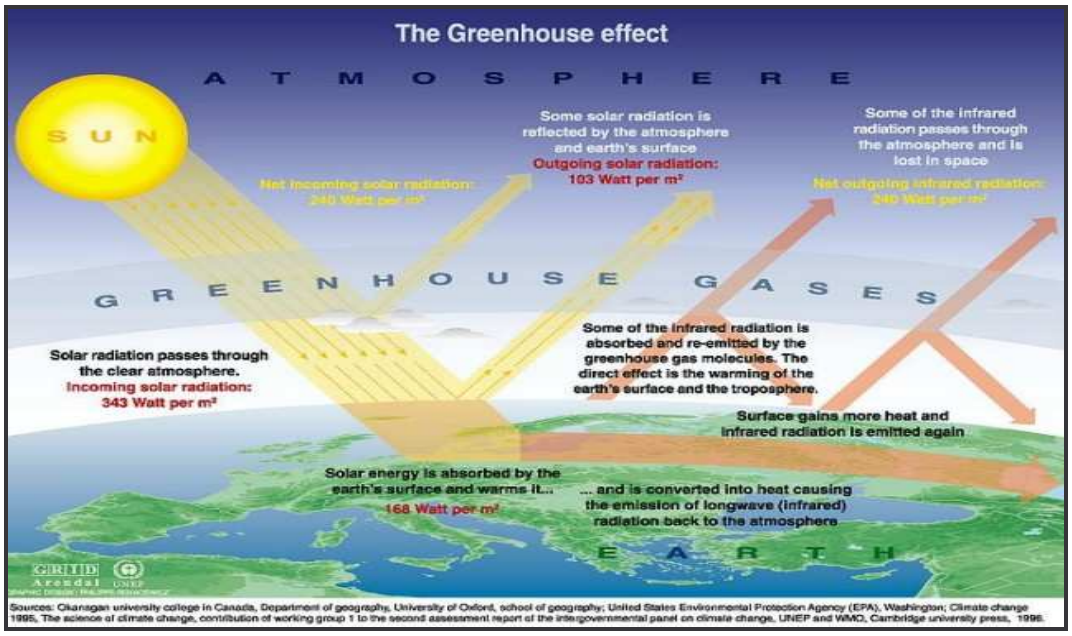

Fig. 2.1 The Greenhouse Effect (Rekacewicz, 2002).

A study of climate on other planets shows the effect of atmospheric carbon dioxide concentration on average surface temperatures. The planet mercury which is closest to the sun compared to all other planets experiences extremely hot and extremely cold temperatures. According to studies conducted it was discovered that mercury has no atmosphere therefore its main source of heat is solar radiation which is subsequently re-emitted into space as infrared radiation. Venus which is much further from the sun has a mean surface temperature of 464 ^{o}C, this is attributed to the extremely dense and carbon dioxide rich

atmosphere, which absorbs and re-emits infrared radiation to the planets' surface (BOM, 2003).

Since the industrial revolution in the mid-nineteenth century human activities have been responsible for altering the composition of the atmosphere by releasing more greenhouse gases. These activities include the accelerated use of fossil fuels for energy, broad scale deforestation for agricultural purposes and land use changes for infrastructural development. The global atmospheric concentration of carbon dioxide has increased from a pre-industrial concentration of 280 ppm to 379 ppm in 2005 (IPCC, 2007). This concentration far exceeds the natural variability of increase in carbon dioxide concentration over the last 8,000 years prior to industrialisation.

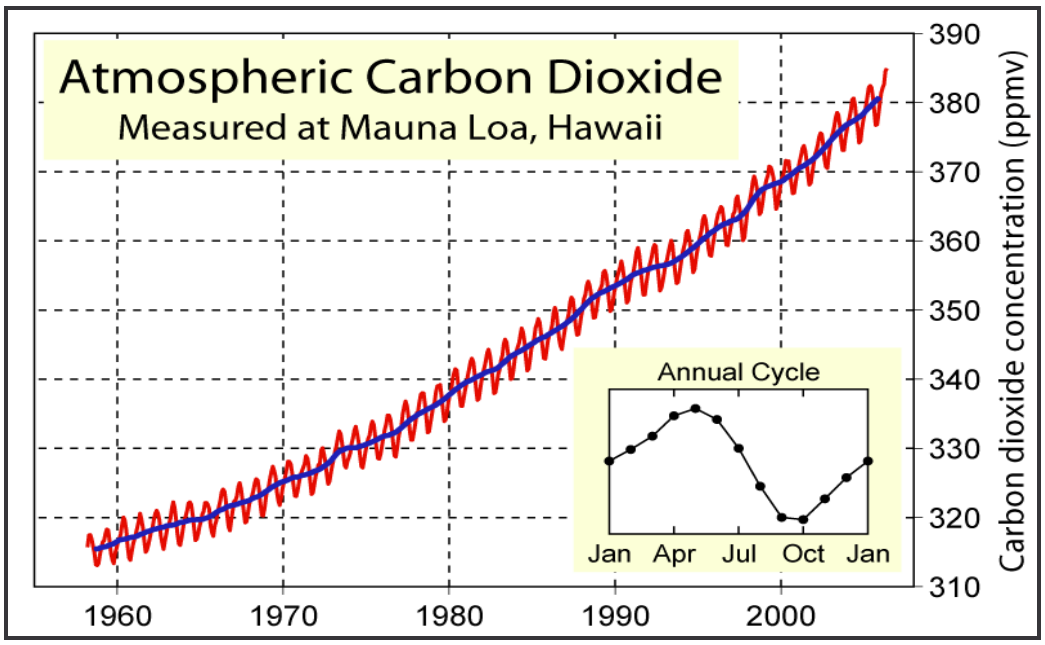

Fig. 2.2 Atmospheric Carbon Dioxide Concentration (Handly, 2006).

The annual rate of increase of carbon dioxide concentration between 1965 and 2005 also confirms the contribution of human activities to carbon dioxide concentrations in the atmosphere (Fig. 2.2). According to the Intergovernmental Panel on Climate Change (IPCC) 2007 report (IPCC, 2007) the average annual rate of increase of carbon dioxide concentration from 1965 was 1.4 ppm and it rose to 1.9 ppm in 1995. This is a direct reflection of the rate of growth of

industrialization since 1965 with a very high growth rate experienced in the last 12 years. Further evidence shows that about 1.3 times as much carbon dioxide is entering the atmosphere annually compared with just 20 years ago (Pearce, 2007). This enhances the greenhouse effect.

2.2 GLOBAL WARMING AND CLIMATE CHANGE

Climate is defined as an average of weather conditions experienced over a long period of time including extreme weather events (BOM, 2003). The six major factors that influence climate are;

- The strength of the incident radiation which determines the surface temperature;
- The shape of the earth and orientation of its axis;
- The greenhouse effect which is determined by the composition of the air;
- The global energy balance, water balance, carbon cycle and other bio-geochemical cycles;
- The rotation of the earth;
- The distribution of continents and oceans (BOM, 2003).

These factors are not constant but are always changing, some quicker than others, resulting in a change of climate. A study of the earths' climate since pre-historic times shows that climate is not static but changes over a range of geological time frames. However the natural variability of the earths' climate has always been a very slow process which allows for adaptation and evolution of life on earth. The general belief with regards to the rapid climate change currently being experienced is that anthropogenic influences are overriding the natural variability of climate. Although human activities cannot influence most of the climate determining factors, they can influence the composition of the air, the global energy balance, water balance, carbon cycle, and the bio-geochemical cycles. It is therefore believed that it is this ability to interfere with the natural factors that is leading to a rapid change of climate.

The increase in earths' surface temperatures is the most significant indicator of a changing climate. The unprecedented increase in carbon dioxide concentrations

in the atmosphere is enhancing the greenhouse effect resulting in high global mean temperatures. This phenomenon is known as global warming, which is causing a possibly irreversible change in the earths' climate. Studies of global mean temperatures over the last 120 years show an undisputed and rapid rise in global mean temperatures (Fig. 2.3).

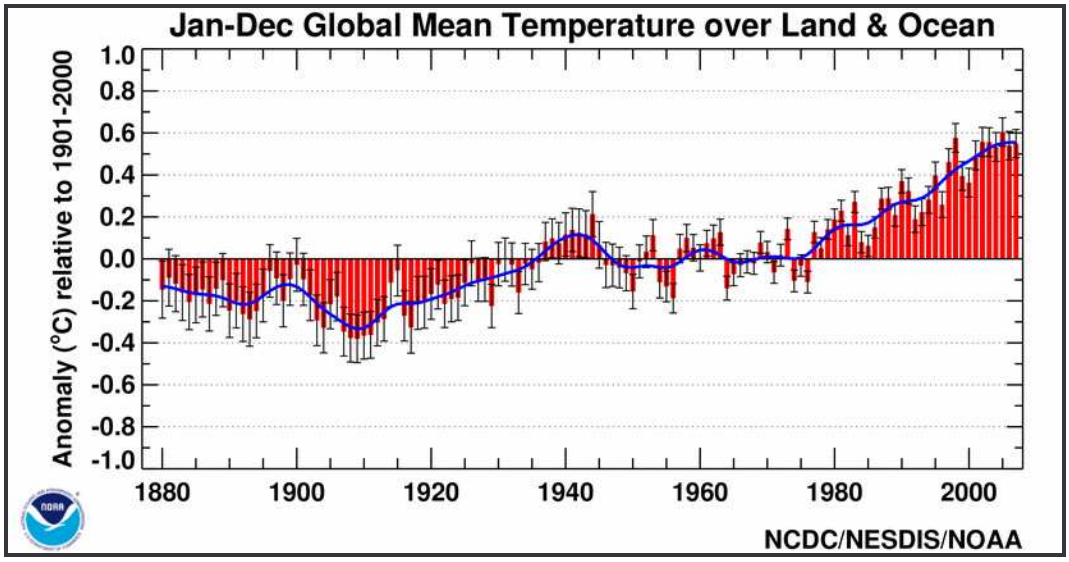

Fig. 2.3 Global Mean Temperatures Over Land and Sea (NCDC, 2006).

Records show that the atmosphere is warming at a rate of 0.13 ^{o}C per decade (Pearce, 2007). The two warmest years over the last century were 1998 and 2005 (IPCC, 2007), and the linear warming trend over the last 50 years is nearly twice as that of the last 100 years (IPCC, 2007). The scientific data on global temperature increase is supported by the adverse changes in climate. Generally land masses are warming up faster than oceans, and widespread changes in extreme temperatures have been observed with cold days and nights becoming less frequent while hot days and nights become more frequent. Heat waves have increased in frequency and duration since the latter half of the century. The heat wave which occurred in Europe in August 2003 was the worst ever experienced, claiming a record 35,000 lives (Larsen, 2003).

The high temperatures experienced are also causing the melting of snow and ice as well as rising sea levels. The sea level is rising by 3.1 mm per decade (IPCC, 2007); this is mainly attributed to the melting of mountain glaciers and snow

cover. This is posing a serious threat of flooding in coastal areas (Levin and Pershing, 2006). Records of data collected since 1961 show an increase in the average sea temperature up to a depth of 3,000 m and that the ocean is absorbing more than 80 % of the excess heat in the atmosphere.

Fig. 2.4 Portage Glacier (Alaska U.S.A) in 1914 (Braasch, 2008).

Fig. 2.5 Portage Glacier (Alaska U.S.A) in 2004 (Braasch, 2008).

Mountain glaciers and snow are melting due to the high atmospheric temperatures. Figs 2.4 and 2.5 above show pictures taken during the winter months of 1914 and 2004 of the Portage Glacier, in the state of Alaska, United States of America. The pictures show a substantial decrease in snow cover. The Arctic sea ice is also believed to be contracting by 7 % per decade (Pearce, 2007) and a sharp decline of ice has been recorded in the Antarctic Peninsula where the ice sheet is cracking.

Water vapour is also increasing in the atmosphere due to more evaporation from the oceans as a result of the higher ocean temperatures and the warmer air which is able to hold more moisture. This high moisture content in the atmosphere is resulting in excessive rainfall in some areas leading to flooding. However, in sub tropical areas more intense and longer droughts are being experienced due to higher temperatures and a decrease in precipitation. In these areas the decrease in precipitation is due to the low moisture content in the atmosphere. The droughts being experienced particularly in Africa are causing a decline in crop yields leaving millions of people without food or water (Levin and Pershing, 2006).

Ecosystems are particularly vulnerable to climate change and a number of species face extinction should global temperatures continue to rise unabated. Ocean acidification due to absorption of more carbon dioxide by sea water, leading to low pH will have a negative impact on the marine ecosystem (Levin and Pershing, 2006). The effects of global warming on life on the planet and the environment in general cannot be overemphasized.

2.3 LEGISLATION ON GREENHOUSE GASES

The drive towards sustainable development has led to drafting of legal frameworks for greenhouse gas emissions control. Concern regarding the possibility of irreversible climate change due to carbon dioxide emissions started in the 1950s, leading to the establishment of the Mauna Loa monitoring station in Hawaii in 1957 (BOM, 2003). Records of carbon dioxide emissions showed an annual increase in carbon dioxide concentrations and growing public concern on environmental issues led to the climate change issue being part of the political agenda.

The World Meteorological Organisation convened the first World Climate Conference in 1979 (BOM, 2003). The conclusion of the conference was to use present knowledge and improve it, as well as to be able to predict and prevent possible effects of climate change. These recommendations triggered a global interest and responsibility to monitor and predict climate change. This led to the

establishment of the IPCC in 1988, whose key role is to assess scientific, technical and socio-economic information in relation with the risk of climate change. In order to function more effectively the IPCC was divided into three working groups, each focusing on a specific area. Working Group 1 assesses information on the climate system and climate change, while Working Group 2 focuses on the impacts of climate change and adaptation, and Working Group 3 is responsible for identifying mitigation options (BOM, 2003). Each Working Group is expected to release an assessment report that consists of a summary for policy makers and a detailed technical summary (BOM, 2003).

The assessment reports are submitted to the Conference of Parties to the United Nations Framework Convention on Climate Change (UNFCC). The UNFCC is an international treaty which entered into force on March 21, 1994. Its member states are divided into three categories that are Annex 1 (industrialized countries), Annex 2 (developed countries which pay for costs of developing countries) and Annex 3 (developing countries). The parties meet annually at a Conference of the Parties, to assess progress and to make new resolutions. The Conference of the Parties held in Kyoto Japan 1997 was a landmark conference where specific greenhouse gas emissions reduction targets were set leading to the adoption of the Kyoto Protocol (BOM, 2003).

2.3.1 The Kyoto Protocol

The ultimate objective of the Kyoto Protocol is to stabilize atmospheric concentrations of greenhouse gases at levels that would prevent dangerous anthropogenic interference with the climate system. Member states that ratify this protocol commit to reduce their emissions of carbon dioxide and other greenhouse gases, or engage in emissions trading if they fail to reduce emissions. The requirements of the protocol differ for Annex 1 and Non-Annex 1 countries, the main reason being that per capita emissions of Annex 1 parties are higher than those of most developing countries and they have greater financial and institutional capacity to address climate change mitigation requirements.

Annex 1 countries are expected to adopt national policies that will ensure that they reduce the overall emissions to at least 5 % below the 1990 levels. These

countries are expected to have national systems for the estimation of anthropogenic emissions as well as to submit annual inventories of their greenhouse gas emissions. Further to that Annex 1 parties are expected to submit national communications, detailing their climate change policies and measures. In the case where countries fail to reduce emissions they may purchase carbon credits, according to the emissions trading requirements (BOM, 2003).

Developing countries (Non-Annex 1) on the other hand are not expected to fund carbon dioxide reduction projects but to participate in the clean development mechanism and submit national communications. South Africa acceded to the Kyoto protocol in March 2002 as a Non-Annex 1 country (Engelbrecht et al., 2004).

2.3.2 Clean Development Mechanism

According to the requirements of the Kyoto Protocol South Africa may participate in the Clean Development Mechanism (CDM), which is a flexible emissions reduction option in which Annex 1 countries provide financial support to Non–Annex 1 countries, for greenhouse gas emissions reduction projects. This mechanism aims to assist South Africa to reduce carbon dioxide emissions and thus alleviate the impacts of climate change; given that it is a semi-arid country and particularly vulnerable to the impacts of climate change (BOM, 2003).

The low-cost housing project in Khayelitsha, Cape Town is one of the sixteen CDM projects under development in South Africa. Eight low-cost houses and two crèches were retrofitted with insulated ceilings, high efficiency light bulbs and solar water heaters, reducing carbon dioxide emissions by 2.85 tons per building per year. The project will be expanded to include 2,000 other households. This project was made possible through funding from the City of Cape Town and South South North (SSN), which is an international Non-Governmental Organisation (NGO). The project was awarded gold standard recognition by the (UNFCC), and it earned carbon credits (Alexander, 2005).

Besides the Kyoto Protocol South Africa, is also a member of the Carbon Sequestration Leadership Forum (CSLF) which was formed in 2003. An annual CSLF meeting was held in Cape Town in April 2008. These and other greenhouse gas emissions reduction programmes that South Africa is embarking on present a challenge for South Africa to consider the different mitigation options available, of which carbon dioxide sequestration in coal seams is one.

2.4 CARBON DIOXIDE SOURCES

In order to be able to control carbon dioxide emissions it is important to identify the different sources of CO_2 as well as to quantify the amount of carbon dioxide emitted at these points. Anthropogenic carbon dioxide is a by-product of many commercial processes which include the combustion of fossil fuels for power generation and steam production, coal gasification, hydrogen production, fermentation, limestone calcination and other chemical synthesis processes (Kirk and Othmer, 1991[b]).

2.4.1 Power Generation

Coal is the major source of energy in South Africa. Although other fossil fuels like petroleum and natural gas are in use, coal is the cheapest and most abundant source of energy, and hence it is used at a larger scale compared to the other fossil fuels. In 2004, the energy supply in South Africa was as follows: 68.0 % coal, 19.0 % oil, 3.0 % nuclear, 2.0 % natural gas and 8.0 % renewables (Van Wyk et al., 2006). The high consumption of coal leads to higher carbon dioxide emissions. The South Africa Environment Outlook report states that in 1994 the energy sector was responsible for 91 % of carbon dioxide emissions in South Africa (DEAT, 2006).

The power generation industry in South Africa is the highest emitter of green house gases. Data collected by the Carbon Monitoring for Action (CARMA) group shows that the South African power company Eskom, is the second largest emitter of carbon dioxide out of more than 4,000 power utilities in the world (CARMA, 2007).

2.4.2 Gasification and Hydrogen Production

Approximately 35 % of South Africa's' liquid fuel is obtained from coal through the coal liquefaction process (Van Wyk et al., 2006). This process generates gas emissions with a high concentration of carbon dioxide; hence it presents a good capture point. Secunda is the largest single point source emitter of carbon dioxide globally. The projected increased production of low-carbon energy carriers such as hydrogen sourced from coal could result in more gasification plants being built, thus producing more carbon dioxide. The advantage is that the carbon dioxide is concentrated therefore the plants are considered capture ready.

2.4.3 Other Industry

The combustion of fossil fuels as a source of energy in industry and use of carbon based materials for reduction in metallurgical processing are major sources of air pollution including carbon dioxide emissions. These emissions are substantial, accounting for 18 % of the total carbon dioxide emissions (DEAT, 2006). Boiler plant operations involve the combustion of fossil fuels, particularly coal to produce steam for process operations. Coal has been the backbone of South Africa's industrial development, as the major source of energy. Coal mining started in 1870 and coal utilisation has been the foundation of the mining industry in South Africa providing a low cost source of energy (Barker, 1999).

In the iron and steel industry, apart from carbon dioxide emissions in the boiler plant, further emissions are encountered during the burning of coke as a fuel and its use as a reductant of iron ore in the blast furnace. In the steel making process further carbon dioxide is produced during the reduction of carbon.

The production of clinker in the cement industry and the production of quicklime are major sources of industrial carbon dioxide emissions.

Apart from the heavy industry, carbon dioxide emissions also occur on a smaller scale from the transport industry. The growth of the South African economy has resulted in more people owning cars hence more emissions of carbon dioxide. The use of fossil fuels for heating and cooking purposes in households is another

source of emissions. However, the disadvantage with these small scale emissions is that they can not be captured for storage purposes, hence the need to introduce other sources of energy for use at this scale. The use of hydrogen powered cars is one of the options currently under development, as well as the use of solar power for lighting, heating and cooking purposes in households (Schlumberger, 2008).

2.5 CARBON DIOXIDE MITIGATION OPTIONS

The need to reduce carbon dioxide levels in the atmosphere cannot be overemphasized. According to the IPCC special report (Metz et al., 2005) , there is need to use all the possible mitigation measures possible as there is no option that can be the universal answer to this problem.

There are a number of possible mitigation options that can be employed; these include efficient use of energy, use of renewable sources of energy, promotion of near zero emissions technology, mineral carbonization of carbon dioxide and carbon dioxide capture and storage.

2.5.1 Energy Efficiency, Near Zero Emissions Technology and Renewable Sources of Energy

The American Council for an Energy Efficient Economy Report of May 2007 (Pringle and Eldridge, 2007) states that energy efficiency and renewable energy are the twin pillars of a sustainable energy policy. The rapid development of these technologies will go a long way in the stabilization and reduction of carbon dioxide emissions.

Efficiency is the extent to which input is converted to output; for example the efficiency of energy generation can be increased by using less fuel to generate the same amount of energy. The efficient use of energy reduces the production of carbon dioxide from the onset as less fuel will be required thus reducing the pressure of dealing with enormous carbon dioxide emissions. End-user efficiency can also be improved by using less energy to achieve a desired effect such as the use of low-watt light bulbs for lighting purposes, and the use of insulated

geysers for water heating. Eskom, which is the largest emitter of greenhouse gases in South Africa, has embarked on a number of energy-efficiency initiatives as possible mitigation options. In 2006 a total of 271 Kt of carbon dioxide emissions were avoided by application of energy-efficient technology (Eskom, 2007).

The underground coal-gasification pilot plant at Majuba is an example of a low emissions technology that Eskom is embarking on. This option allows Eskom to continue to use the cheap and abundant coal resources, thereby producing affordable electricity for the people of South Africa with limited carbon dioxide emissions.

Renewable energy is generated from the naturally occurring non-depletable sources of energy such as solar, wind, biomass, hydro, and geothermal. The use of renewable energy ensures a clean environment as most of the sources of energy are carbon-neutral. The white paper on renewable energy policy of South Africa sets out principles, goals and objectives for renewable energy. This paper reflects the governments support for the use of renewable energy sources (DME, 2003).

2.5.2 Carbon dioxide Capture and Storage

Carbon dioxide sequestration and storage is listed as one of the key mitigation options for emissions from the power supply sector by the IPCC special report (Metz et al., 2005). Fig. 2.7 provides a summary of possible carbon dioxide sequestration options.

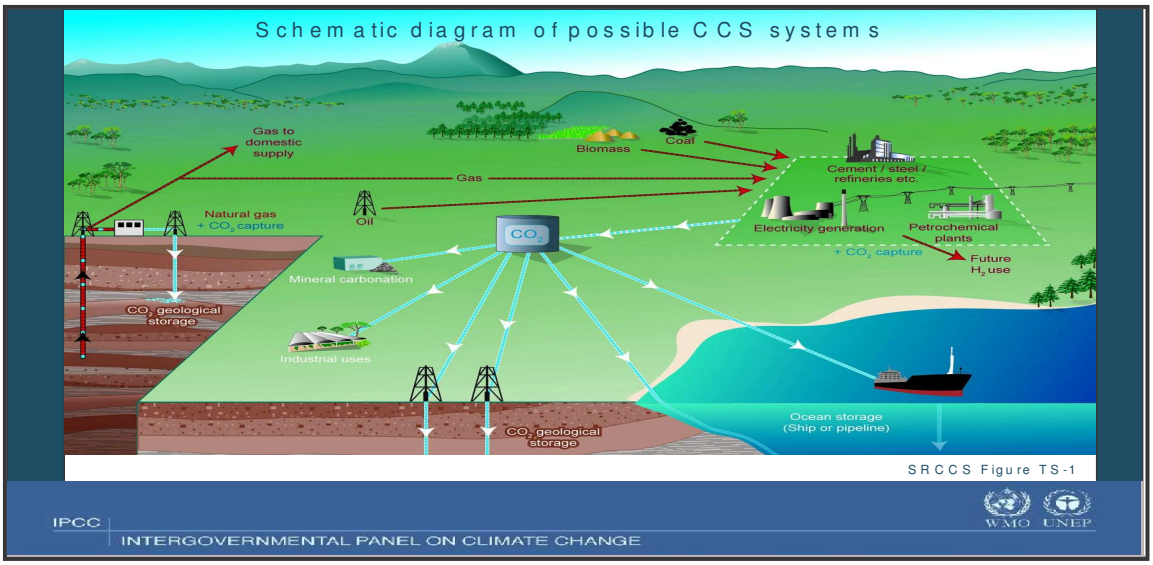

Fig. 2.7 Carbon Dioxide Storage Options (Metz et al., 2005).

2.5.3 Carbon Dioxide Capture And Transportation

Carbon dioxide capture is the first step in the carbon dioxide sequestration process. The purpose of capture is to produce a carbon dioxide rich stream at high pressure that can be subsequently transported to the storage site. Carbon dioxide capture can only take place at large point sources such as power stations and industry.

2.5.3a) Pre-Combustion Capture

In pre-combustion capture, the carbon in the fossil fuel is removed from the fuel before it is used for the purposes required. This process generally involves partial oxidation of the fuel in a gasifier to produce carbon monoxide and hydrogen. The gas composed of carbon monoxide and hydrogen undergoes further reaction with steam to produce more hydrogen and carbon dioxide. The carbon dioxide is then separated from the gas mixture and is compressed to the required pressure and transported to the storage site. Hydrogen is then used as a carbon-free energy carrier and is used to generate power and heat (Metz et al., 2005).

2.5.3b) Oxy-Fuel Combustion

In oxy-fuel combustion the fuel is burned in a pure oxygen stream. The flue gas produced consists mainly of water vapour and carbon dioxide, the water vapour is subsequently removed from the flue gas by cooling and compression. This

process gives rise to very high flame temperatures, and in order to control these temperatures to normal operational temperatures, the cooled flue gas is injected into the combustion chamber. This gives rise to a flue gas with a very high carbon dioxide concentration, which can then be transported to the storage site (Metz et al., 2005).

2.5.3c) Post- Combustion Capture

Post-combustion capture involves removal of carbon dioxide from flue gas in a conventional combustion process. The process uses a solvent to separate carbon dioxide from the flue gas; the most common solvent used for this operation is monoethanolamine (Metz et al., 2005).

2.5.3d) Methods of Transportation

Captured carbon dioxide is compressed to a pressure above 7.83 MPa, and then it is transported to the storage site. The most developed method of transport is the pipeline; however this method is feasible only for short distances. In the case of a capture plant being far away from the storage site a marine tanker may be used for transportation (Metz et al., 2005).

2.6 CARBON DIOXIDE STORAGE

Fig. 2.7 indicates several carbon dioxide capture and storage options, the main ones being geological storage, ocean storage and mineral carbonization.

2.6.1 Mineral Carbonization

Reaction of carbon dioxide with naturally occurring minerals is one of the options that offer permanent sequestration of the gas. Carbon dioxide is reacted with magnesium silicates to form stable environmentally friendly carbonates according to the following reaction;

$$(Mg, Ca)_x Si_y O_{x+2y} + xCO_2 \longrightarrow x\,(Mg, Ca)\,CO_3 + ySiO_2 \quad \text{---------- 2.1}$$

Although this process is very attractive, the main holdback is the rate of the reaction which is naturally too slow, as well as the huge amount of materials

handling associated with the process. The main challenge is to identify conditions that will allow the reaction to be carried out at high rates (Metz et al., 2005).

2.6.2 Ocean Storage

The transfer of carbon dioxide from the atmosphere to the surface of the sea is a natural part of the global carbon cycle. The high concentration of carbon dioxide in the atmosphere is leading to more carbon dioxide dissolving in the ocean causing ocean acidification. This creates a very high pH in the water which has a negative impact on marine organisms that reside in the subsurface.

The natural ability of the ocean to store carbon dioxide can be used to develop man made carbon dioxide storage. The ocean offers the largest carbon dioxide storage capacity, and the two processes that can be used include direct injection and indirect sequestration through the enhancement of carbon dioxide uptake on the ocean surface. Carbon dioxide can be injected into the water column of the ocean or at the sea floor. As the carbon dioxide dissolves in the sea water it increases in density and the carbon dioxide rich water sinks to the bottom of the sea and forms a carbon dioxide lake. The carbon dioxide injected into the water column, dissolves and disperses in the water and eventually becomes part of the global carbon cycle (Metz et al., 2005). A major concern with this sequestration option is the impact on marine and ocean floor organisms. In addition warm and cold ocean currents circulate the earth and carbon dioxide may become mixed and escape to the atmosphere.

2.6.3 Geological Storage

Geological storage is one of the main options for storage of captured carbon dioxide. The purpose of storage is basically to keep carbon dioxide locked away by injecting dense carbon dioxide into a rock formation below the earths' surface. This method is best suited to porous rocks that have previously been used to hold fluids such as oil, gas or brine. Current research is not able to completely explain what happens to the stored carbon dioxide, and how long the carbon dioxide will stay locked at the storage site, although large scale tests are underway.

The three types of possible geological storage are

(i) oil and gas reservoirs,

(ii) deep saline formations,

(iii) unminable coal seams.

(i) *Oil and Gas Reservoirs*

Storage in active and depleted oil and natural gas reservoirs is the most attractive option at the moment given the advanced technology and experience associated with enhanced oil recovery (EOR) as well as the economic benefits of oil production. In EOR operations carbon dioxide is injected into oil reservoirs to increase the mobility of the oil by reducing the viscosity of the oil. This technique is used to increase the production capacity of oil reservoirs. Some of the injected carbon dioxide remains in the reservoir; this technique can be modified for the sequestration of large amounts of carbon dioxide. An example of a carbon dioxide sequestration project with enhanced oil recovery is the Weyburn project in Saskatchewan, Canada. Carbon dioxide injection started in September 2000 and the project is proving to be a success (NETL, 2008). The oil and gas reservoirs are natural strata graphic traps that have held oil over time and they have a cap rock above the storage area that can trap the carbon dioxide. When the carbon dioxide is pumped deep underground, it will be in a liquid or supercritical state, its density is 50 to 80 % the density of water. This will result in buoyancy forces that drive carbon dioxide upwards leading to concerns of breakthrough. However, the presence of a cap rock traps this carbon dioxide and prevents it from escaping the storage site. Although enhanced gas recovery is not currently employed, studies show that it is possible to use carbon dioxide for enhanced gas recovery (Metz et al., 2005).

(ii) *Deep Saline Formations*

Saline aquifers are carbonate and sandstone based sedimentary rocks whose pores are filled with saline water. These aquifers are widely distributed below the continents and the ocean floor; therefore they are within easy reach to most industrial plants. Studies also show that they have a high storage capacity for carbon dioxide. When carbon dioxide is injected into an aquifer it can either dissolve in the salty water or can react with minerals in the surrounding rocks to

form carbonates, thus permanently sequestering the carbon dioxide. The water with dissolved carbon dioxide in it tends to be heavier than the surrounding water therefore it sinks to the bottom of the rock formation, thereby trapping the carbon dioxide (Metz et al., 2005).

(iii) *Unminable Coal Seams*

Unminable coal seams present another possible storage option. Studies show that carbon dioxide adsorption onto coal is the mechanism for gas storage in coal seams and that coal has a very high adsorption capacity for carbon dioxide. The adsorption of carbon dioxide favours the desorption of coal bed methane therefore the economics of enhanced coal bed methane (ECBM) recovery make this is a very attractive storage option (Metz et al., 2005). This aspect is explored further in this study and other studies being undertaken at the University of the Witwatersrand, and other organisations discussed later.

2.7 SUMMARY

In summary this chapter considered the contribution of carbon dioxide emissions to climate change as well as the different mitigation options available for carbon dioxide reduction.

CHAPTER 3: COAL

In Chapter 2 unminable coal seams were suggested as a suitable storage site for carbon dioxide emissions. In this chapter coal itself is explored further, with a specific focus on its formation, petrographic composition, and a description of unminable coal seams.

3.1 COAL FORMATION

Coal can be defined as a compact stratified mass of plant debris which is a result of combined biological, chemical and physical degradation of accumulated plant matter interspersed with smaller amounts of inorganic matter (Francis, 1961). It is formed by the burial of plant material in swampy areas. This plant material, termed peat, is compacted, hardened, chemically altered and metamorphosed by heat and pressure over time. As the depth of burial increases the plant material under goes coalification, releasing volatile matter as it forms coal (Fig. 3.1).

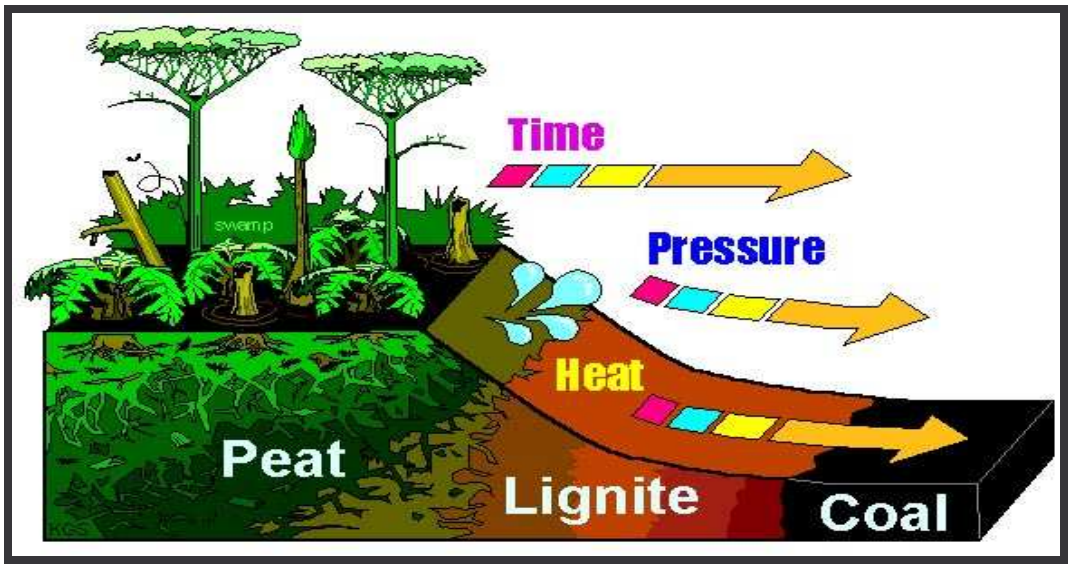

Fig. 3.1 Coal Formation Process (DMP, 2008).

3.1.1 Conditions Required For Peat Formation

(i) Accumulation of plant material

(ii) Favourable climatic conditions

(iii) High water level

(iv) Tectonic control and sedimentary environment (Falcon, 1986a).

(i) The accumulation of plant matter is the first step required for peat formation and this can occur in either of the two methods given below;

- Autochthonous/In situ accumulation – this is the accumulation of vegetation which grows on the deposition area.
- Allochthonous/Drift accumulation – this is the accumulation of vegetation that is transported from source to the area of deposition, by flood water (Francis, 1961).

The evolution of flora is also important as it influences the organic composition of the resultant coal. The Witbank coal seams belong mainly to the Ecca group and the later part of the Dwyka group, during this period the vegetation consisted mainly of the Glossopteris and Gangamopteris plant species with a very small proportion of conifer. The Waterberg coal seam belongs to the Ecca and early Beaufort group, during which the only the Glossopteris and Gangamopteris plant species were deposited (Falcon, 1986[a]).

(ii) Climate plays a major role in the formation of peat as it affects the rate of plant degradation. The climate has to favor the excessive growth of flora or else minimise its degradation. The type of climate also determines the types of flora that will flourishes in a swamp. In warmer and wetter climate forest swamps tend to be more dominant compared to reed and moss swamps. In a period of 7-9 years trees in tropical swamps can grow up to 30 m in height, while within the same period trees in temperate zone only grow up to a height of 6 m in average (Stach et al., 1982). Raised ombrogeneous bogs which are generally poor in nutrients can support tree growth in the tropics, while in the temperate zone only moss can grow on bogs.

In the geological past during the Upper Carboniferous time peats predominated in warm climatic zones and that is when the formations richest in coals were

deposited in the Northern Hemisphere. However in the Southern Hemisphere, the coal deposits accumulated in cold to cool temperate climate such as the inter- and post- glacial Permo-Carboniferous Gondwana coals. Coal seams formed from peat deposited in moist warm climate are generally thick and contain many broad bands of bright coal while peat deposited in temperate climate produced coal with relatively little bright coal. Post-glacial Gondwana coals, which frequently formed from a relatively stunted flora, are usually finely detrital. The finely divided clay minerals are believed to have blown into treeless swamps from surrounding mountains that had no vegetation (Stach et al., 1982).

(iii) Water is an important prerequisite for the preservation of plant debris; this could either be ground water or precipitation. The level of water is important in determining the type degradation of plant matter. A low water level exposes plant matter to the atmosphere hence aerobic degradation will occur, however if the water level is high very little or no oxygen will be able to reach the plant matter This is normally achieved if there is submergence of plant matter below water. The purpose of the water is to cover the dead plant material and prevent it from decaying (Francis, 1961).

(iv) The sedimentary depositional environment is the last requirement for the formation of peat. After the plant debris has accumulated on the floor of a swampy area, there is need for immediate cover of the plant debris with limnic or marine sediments to prevent decay. The rapid subsidence of the basin due to a rise in the ground water level is the final requirement for peat deposition. This is mainly affected by tectonic factors, which determine the rate of sediment influx and rate of basin subsidence. It is only those areas where the two rates are balanced that peat can be converted to coal. Common coal forming areas environments include; alluvial plains, deltaic plains and coastal plains (Stach et al., 1982). In Gondwana coals the peat deposition occurred in stable continental depressions. These include shallow cratonic basins as well as intercratonic and fault bounded grabens. Deposition also occurred along shorelines in margins of shallow inter-continental seas. Tectonic movement of the South Pole to the East caused resulted in melting of ice thereby creating swamps which supported the growth of vegetation. River channels which ran through the swamps deposited

fine sediment during periodic flooding. Due to the cold climatic condition degradation of plant matter was very slow resulting in coal seams rich in oxidized plant matter (Falcon, 1986 [a]).

3.1.2 Peat to Coal conversion

After burial of plant debris, the plant matter undergoes some biochemical and geochemical degradation. The biochemical decomposition converts the plant matter to peat while geochemical decomposition converts peat to coal.

3.1.2a) Peatification

The biochemical decomposition of plant matter involves microbial and chemical changes. The action of fungi and aerobic bacteria on plant matter that is either exposed to the atmosphere or in aerated water completely decomposes the plant matter. This normally occurs at the peat surface, as the depth of the peat increases different reactions take place due to the restriction of oxygen, in which case the decay of plant matter is incomplete (Stach et al., 1982). In this zone only anaerobic bacteria are active, and plant protoplasm, proteins, starches and cellulose are digested. Cellulose and lignin are partially digested because they are very resistant to attack.

The waxy protective layers are the most decay-resistant plant parts and these include cuticles, spore, pollen walls and the resins. When the plant matter has been completely digested, the microorganisms are reduced and with time they completely die.

The formation of humic substances is the most important process during peatification. Humification is promoted by oxygen supply, increased peat temperatures and alkaline environments (Stach et al., 1982).

3.1.2b) Coalification

This is the development from peat to coal. Exposure to pressure and heat during the geochemical stage caused the differences in the degree of coalification that are observable in the coal series; peat, brown coal and lignite, sub bituminous coal, bituminous coal and anthracite.

The sedimentary cover causes pressure build up on the peat and insulates it from the atmosphere. This insulation ensures that the earths' internal heat is retained within the peat and does not escape, thereby leading to very high temperatures. This temperature increase is between 4 and 8 ^{o}C/100 m (Stach et al., 1982). The pressure causes water to be squeezed out of the peat, hence the reduction in moisture content with increasing coal rank i.e. from the peat to anthracite. The loss of moisture causes change in the chemical composition of the coal, as some of the compounds decompose under high temperatures to form water. This chemical decomposition leading to the formation of water which is subsequently removed causes a decrease in the oxygen and hydrogen content while the carbon content increases (Kirk and Othmer, 1991[c]). The volatile matter also decreases while the calorific value of coal increases; these two properties are the main criteria used for commercial classification of coal.

Besides pressure and temperature, time is also an important factor in the coalification process. Most of coals in South Africa were deposited over 200 million years ago. The prolonged application of pressure and temperature on a particular coal seam is required for coal to progress through the low volatile bituminous, high volatile bituminous and finally to anthracite. Tectonic plate movements also provide more pressure and volcanic activity also provides more heat and pressure for further conversion. Most anthracitic coals are formed under one or both of these conditions.

The table below (Table 3.1) shows the classification of coal based on its vitrinite reflectance and reactives content (ISO 11760, 2005 and Falcon, 1986[b]).

Table 3.1 Classification of South African Coals (ISO 11760, 2005 and Falcon, 1986 [b]).

Rank	% R_oV_{Mr}	%Total Reactives	Description and Uses
Lignite	X<0.4		-lowest rank of coal. -fuel for electric power generation.
Sub-bituminous	0.4<X<0.5	20<Y<100	-high volatile bituminous coal. -fuel for steam-electric power generation. -source of light aromatic hydrocarbons for the chemical synthesis industry.
Bituminous	0.5<X<2.0	20<Y<100	-medium to low volatile bituminous coal. -coke making
Anthracite	2.0<X<4.6	20<Y<100	-highest rank coal. -residential and commercial space heating.

3.2 COAL COMPOSITION

Coal is made up of C, H, O, N and S. These elements are bonded together to make up different functional groups and the arrangement of these functional groups determines the structure of coal.

The oxygen containing functional groups include carbonyl, hydroxyl, carboxylic acid and methoxy. The nitrogen containing groups are aromatic nitriles, pyridines, carbazoles, quinolines and pyroles. Sulphur is mainly found in thiols, dialkyl and aryl-alkyl thioethers, thiophene groups and disulphides (Kirk and Othmer, 1991 [c]).

The presence and amount of each functional group differs for each coal maceral and also differs with coal rank. Some groups tend to dominate in a specific coal type while other groups exist in insignificant quantities, or do not exist at all.

The aromacity of coal molecules increases with coal rank and the number of aromatic carbons per cluster varies from 9 in lignites to 20 in low volatile bituminous coal (Kirk and Othmer, 1991[c]).

3.3 COAL MACERALS

Coal is not homogenous; it is made up of organic and inorganic components. Coal macerals are the building blocks of the carbonaceous component of coal. They are microscopically recognizable components of coal and have different chemical compositions and different physical properties. Macerals are distinguished from each other on the basis of their morphology, hardness, optical properties and chemical characteristics (Stach et al., 1982). Coal macerals owe their differences to the parent plant matter and conditions of deposition of the plant matter. The three coal maceral groups are; vitrinite, inertinite and liptinite. Vitrinite is a product of the decomposition of cellular plant material while inertinite is a product of fossilized charcoal and liptinite is a product of decayed leafy matter, spores, pollen and algal matter (Stach et al., 1982).

3.3.1 The Vitrinite Group

3.3.1a) Formation

Vitrinite is the coalification product of woody tissue derived from stem and roots of trees and vascular tissues of leaves. The formation of vitrinite from these plant tissues occurs in two processes i.e. humification and gelification. Humification is the microbiological degradation of lignin and cellulose in the plant matter giving rise to humic substances. The humic substances are dark-coloured compounds of complex composition, which contain carbon, oxygen, hydrogen and nitrogen. Cellulose ($C_6H_{10}O_5$) is the structural component of plant cell walls, while lignin fills the space between the cell walls. Lignin and cellulose are both decomposed by fungi, bacteria and other microorganism and converted to humic substances. Humic acid is one of the major components of humic substances. Due to

chemical attack humic acids loses its acidity by the removal of –OH and –COOH groups, thus converting humic acids to humins (Stach et al., 1982).

These humic acids are linked in a defined manner and undergo a drying process leading to the formation of gels.

Vitrinite normally occurs in the form of bands, lenses and matrix in coal. The thickness of vitrinite bands varies from less than 1 mm to 300 mm. This variation is dependant on the source material, thicker bands are generally due to the decomposition of roots, bark and stem of tress while twigs and leaves result in the formation of thin bands. Vitrinite is subdivided into telinite, collinite, corpocollinite and vitrodetrinite based on the internal structures. Vitrinite occurs mostly in the Carboniferous seams and very little can be found in the Gondwana coal seams (Stach et al., 1982 and ICCP, 1994 [a]).

3.3.1b) Chemical Composition and Structure

Vitrinite has a relatively high oxygen content compared with the other macerals. Its elemental composition is as follows;

Table 3.2 Composition of Vitrinite (ICCP, 1994 [a]).

Element	% Composition Range
Carbon (C)	77 - 96
Hydrogen (H)	6 - 1
Oxygen (O)	16 - 1

During coalification of vitrinite, carbon increases and oxygen decreases. The humins in vitrinite consist of an aromatic nucleus surrounded by aliphatic groups. With increasing rank these groups are lost and the aromatic nuclei become larger. The number of aromatic carbons per cluster varies from nine in lignite to twenty in low volatile bituminous coal. The main oxygen containing groups are phenolic hydroxyl and conjugated carbonyls. The macromolecules consist of a number of small aromatic clusters each with one to four benzene rings. These

clusters are partly linked together by hydro aromatic and alicyclic ring structures. The entanglement between these molecules leads to difficulties in molecular-weight determinations and changes in properties when heated. Irregularities in packing are mainly due to the different molecular shapes and sizes. This gives vitrinite its amorphous nature and extensive ultra fine porosity (Kirk and Othmer, 1991 and ICCP, 1994 [a]).

3.3.1c) Physical Properties

Vitrinite is very brittle, that is it fractures angularly and conchoidally, leaving a glossy or pitchy lustre on the fractured surface. Under pressure it fractures to form rectangular prisms or cubes and also forms splinters which are normally found concentrated in the coal fines. Fissures and cleats caused by shrinkage and tectonic forces can be seen under the microscope. The density of vitrinite varies between 1.3 and 1.8, depending on the rank of coal. The resistance to polishing decreases with increasing rank. The pore volume of vitrinite also decreases with coal rank. The reflectance of vitrinite is intermediate compared with other maceral groups. It increases with coal rank and hence it is used as a rank indicator (Stach et al., 1982).

3.3.2 The Inertinite Group

3.3.2a) Formation

This group of macerals is also formed from the decomposition of cellulose and lignin from plant material. The difference to vitrinite is that the plant matter undergoes fusinisation either before deposition or on the peat surface. Fusinisation can include a number of material degradation processes such as charring, oxidation, mouldering and fungal attack. These processes produce substances that have very high carbon content, low hydrogen content and a high O/C ratio. During the coalification process inertinites alter very little because they are already degraded before deposition. These macerals are less reactive than liptinite and vitrinite. During coalification inert macerals may lose the remnant oxygen and hydrogen becoming more enriched in carbon (Stach et al., 1982). Inert maceral subgroups include fusinite, semifusinite, funginite, secretinite, macrinite, micrinite and inertodetrinite (ICCP, 1994 [b]).

3.3.3 The Liptinite Group

This group of macerals are products of relatively hydrogen-rich plant materials and bacterial degradation products of proteins, cellulose and carbohydrates. They are derived from resinous and waxy materials of plants, including resins, cuticles, spore, pollen, exines and algal remains. The source material is the basis of subdivision of the macerals into sporinite, cutinite, resinite, alginate and liptodetrinite (Stach et al., 1982).

3.3.4 Microlithotypes

Coal macerals rarely occur as single macerals, they are normally associated with other macerals. These maceral combinations are termed microlithotypes and the can occur as monomacerals, bimacerals and trimacerals. The physical and chemical properties of the monomaceral microlithotypes are usually similar to the main maceral group. In bimaceral microlithotypes the properties are a combination of the two main maceral groups in relation to their proportion.

3.4 UNMINABLE COAL SEAMS

Carbon dioxide storage in unminable coal seams is regarded as a possible sequestration option for South Africa. The advantage of this option is that the injection of carbon dioxide into coal seams enhances the extraction of coal bed methane, which is an economically valuable and relatively low carbon fossil fuel. Revenue from ECBM recovery can offset the costs associated with carbon dioxide capture, transport and storage.

Studies show that the adsorption capacity of carbon dioxide onto coal is twice that of methane (Cui et al., 2004), hence for every molecule of methane extracted two molecules of carbon dioxide can be stored in the coal seam. This indicates that coal has the potential to store very large quantities of carbon dioxide. With respect to technology development a similar technology is currently being employed in EOR and minor modifications are required for the purposes of ECBM recovery.

Although coal seams offer a possible storage option for carbon dioxide, this relies heavily on the availability of unmineable coal seams. The classification of coal seams as “unmineable” is based on the cost of extraction and market availability for the type of coal to be mined. Due to its low calorific value compared to other fossil fuels a large amount of coal is required for most applications. This means that the cost per tonne of extracting coal should be kept as low as possible if the deposit is to be economically viable. The quality of coal is also an important factor in determining whether the coal deposit is economic (Ward, 1984). Coal deposits can generally be classified into;
Coal reserves – this is material that is of suitable quality and can be economically extracted using available technology.
Total coal resources – this includes all coal deposits i.e. currently minable and unminable deposits (Ward, 1984).

These unminable coal seams are basically deposits that cannot be economically extracted using the available technology but can be possibly mined in the future with improved technology and demand. This includes coals seams that are either too deep or too thin, or too poor in quality (high ash for example) to be mined economically. It also includes deposits on which too little geological data is available to assess their economic feasibility (Ward, 1984).

Another economical advantage of sequestering carbon dioxide in unminable coal seams is that there may be significant reductions in the cost of carbon dioxide transportation. This is because most coal-fired power stations are located within major coal basins where there is potential to inject carbon dioxide into unminable seams (Day et al., 2007).

A major risk associated with geological sequestration is the possibility of carbon dioxide leakage from the geological strata. This necessitates extra long-term costs for monitoring the site for any possible leakages as well as taking remedial action. Storage in deep unminable coal seams offers lower risk of leakage of carbon dioxide as the potential of leakage to the surface is minimised due to the thickness of overburden.

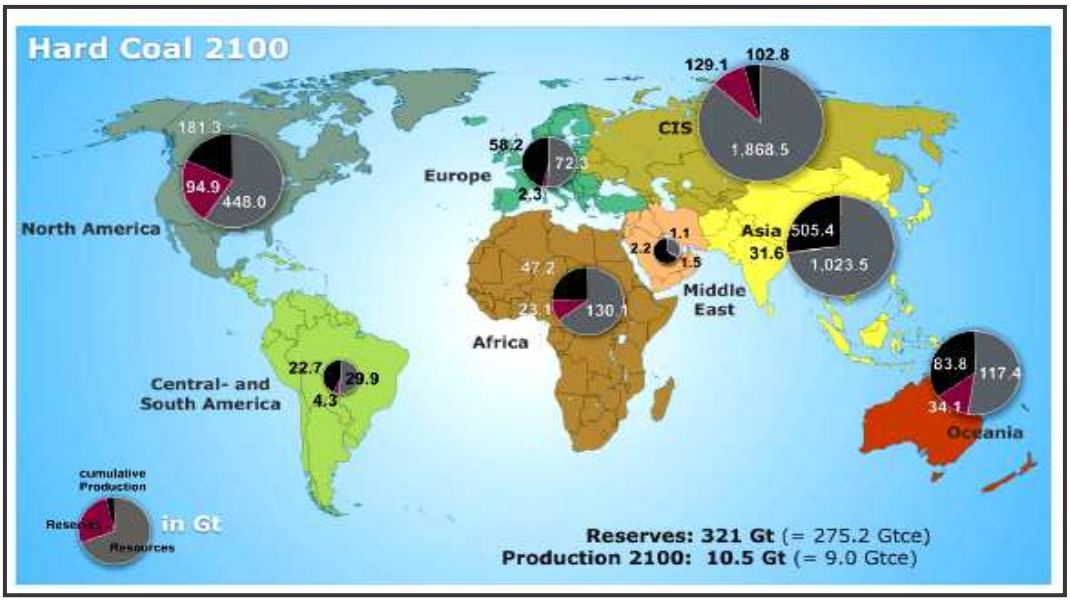

Fig. 3.2 World Coal Resources and Reserves in 2100 (Thomas et al., 2007)

The map above (Fig. 3.2) is a forecast of the distribution of coal resources and coal reserves around the globe in the year 2100. According to the map there is a greater proportion of unminable coal seams than minable coal seams in Africa which indicates a possible large storage capacity for carbon dioxide.

Due to the advancement in the technology of carbon dioxide injection into carbonaceous rock, carbon dioxide storage in coal seams can provide the quickest and cheapest solution to the carbon dioxide emissions reduction problem. However a number of concerns have been raised by policy makers about the possibility of mining these “so called” unminable coal seams in the future. The forecast of coal reserves and resources shown in the map (Fig. 3.2) above indicates that despite technological advances, by the year 2100 there will still be a very large proportion of unminable coal seams. At that time the world is expected to have switched to other forms of energy and fossil fuels will play a very minor role in energy supply, meaning that some of these coal seams will never mined, definitely not in the near future.

3.5 SUMMARY

In this chapter a description coal formation, coal properties, coal macerals as well as definition of unminable coal seams were provided. The next chapter provides a description of the principles of gas-solid adsorption, properties of carbon dioxide as well as results of similar research conducted by various scientists.

CHAPTER 4: ADSORPTION

In the previous chapter coal properties and composition were discussed, and in this chapter the principles of gas adsorption in coal seams are introduced. The properties of carbon dioxide which influence its adsorption onto coal are also listed as well as results of previous research work conducted on the subject.

4.1 PRINCIPLE OF ADSORPTION

Adsorption is a process that occurs when a film of gas or liquid (adsorbate) molecules adheres to the surface of a solid (adsorbent) (Kirk and Othmer, 1991[a]). There are two different types of adsorption i.e. physical adsorption and chemical adsorption. Physical adsorption occurs when non-balanced physical forces appear at the boundary of the adsorbate and adsorbent. Chemical adsorption occurs when molecules from adjacent phases form chemical bonds at the interface.

The adsorption of carbon dioxide onto coal is physical adsorption. Physical adsorption is caused by van der Waals and electrostatic forces between the adsorbate molecules and the atoms on the adsorbent surface. Adsorbents are therefore characterized by surface properties such as surface area and polarity. A large surface area is therefore required to provide a large adsorption capacity (Kirk and Othmer, 1991[a]).

Adsorption of an adsorbent onto a heterogeneous surface like coal is dependant on the surface area available for adsorption. During the adsorption of carbon dioxide onto coal, three phases can be identified; that is the solid phase, gas phase, and the adsorbed phase. The solid phase has a potential energy field on its surface and the gas molecules contain kinetic energy.

The amount of gas adsorbed depends on the energy of the free gas, which is a function of temperature and pressure (Kirk and Othmer, 1991[a]).

4.2 CARBON DIOXIDE ADSORPTION ONTO COAL

The main mechanism of gas storage in coal is adsorption; this is because coal is a highly porous material with a very high surface area to volume ratio. Carbon dioxide is strongly adsorbed onto coal and the volume of gas that coal can adsorb exceeds its open pore volume by an order of magnitude. The volume of pores in coal is small (less than 10 % of the total volume for Sydney basin coals) (Saghafi et al., 2007).

Gas storage in coal occurs in both the adsorbed phase and free gas phase. The free gas is normally found in the meso pores, macro pores, cleats and fissures and it accounts for approximately 5 % of gas in coal. The majority of gas in coal exists in the adsorbed state, as mentioned earlier, which covers the surfaces of micro-pores. The pores in coal are classified by the International Union of Pure and Applied Chemistry (IUPAC) and are divided into three types based on their width and sizes. These are macropores (>50 nm), mesopores (2-50 nm) and micropores (<2 nm). The micropore surface area has been shown to be in the order of 20 to 200 m^2/g, therefore making large areas available for adsorption of gases (Saghafi et al., 2007).

The amount of gas adsorbed onto the coal surface does not only depend on the available surface area but is also dependent on the equilibrium state of the van der Waals forces, which are made up of surface attraction and repulsion forces.
Coal is a natural reservoir for gases including carbon dioxide and methane among others. During the coalification stage large amounts of carbon dioxide are generated by the following processes;

(i) decarboxylation reactions of soluble organic matter during burial heating of coal;
(ii) mineral reactions such as thermal decomposition and dissolution of carbonates;
(iii) bacterial oxidation of organic matter;
(iv) magmatic intrusion.

(Saghafi et al., 2007).

Although some of the gas is lost due to dissolution in mobile water and migration out of the coal seam, a substantial quantity still remains in the coal seams. This is evidenced by the carbon dioxide gas outbursts experienced during underground coal mining (Saghafi et al., 2007). It is the capacity to store gas as well as the ease of migration of the gas through the coal matrix that influences the release of gas during mining. Understanding the mechanism for natural carbon dioxide storage and migration in coal seams is the key to identifying factors that can affect the sequestration of anthropogenic carbon dioxide in coal seams. Gas transport in coal is considered to occur at two scales 1) laminar flow through the cleat system, 2) diffusion through the coal matrix (Yu et al., 2006).

Coal is made up of different macerals as described earlier, and these macerals have different physical properties and structures; hence they have different pore volume distributions and adsorption characteristics. Gas adsorption capacity in coal is closely related to the micropore development, which is a function of coal rank and coal composition (Crosdale et al., 1997). For coals of the same rank micropores tend to predominate in vitrinite while meso and macro pores are predominant in inertinite (Stefanska and Zarebska, 2005). Coal micro-pore surface area can reach several hundreds of square metres per gram of solid, making large areas available for gas adsorption.

The amount of gas adsorbed is not only dependent on the available surface area but also on the equilibrium state of surface attraction and repulsion forces. Equilibrium is reached when the total gas/solid surface potential energy is minimised. The adsorption of gas onto coal is a long range weak interaction called physical adsorption. In physical adsorption gas molecules lose kinetic energy and adhere to the coal surface, and energy is released during this process (Saghafi et al., 2007).

The selection of storage sites should target coal seams with high methane content as these coals have the potential to store a large quantity of carbon dioxide. Methane outbursts in South African underground coal mines such as the Twistdraai mine in the Highveld in 1993 indicate high gas content in the some of the coal seams (Saghafi et al., 2006). A study by Saghafi et al. (2006) shows that

igneous intrusions in South African coal seams can act as enclosures and gas traps for storage of gas, thereby reducing the possibility of gas leakage from the strata. This can also increase the volume of gas in the free phase giving the coal seam a greater overall storage capacity.

4.3 PROPERTIES OF CARBON DIOXIDE

Carbon dioxide is a colourless and odourless gas with an acid taste. It possesses excellent physical and chemical properties which make it a desirable material for use in many processes.

Carbon dioxide is a by-product of many commercial processes and exists in nature as a component of natural gas. It is recovered from the gas mixture and prepared for commercial use as a solid, liquid or gas (Kirk and Othmer, 1991[b]).

4.3.1 Chemical Properties

Carbon dioxide is a chemical compound composed of two oxygen atoms and one carbon atom and its chemical formula is CO_2. Each of the oxygen atoms are covalently bonded to the carbon atom, resulting in two double bonds (O=C=O). The carbon dioxide molecule is linear and it has no electrical charge. It has a molar mass of 44 g/mol.

Carbon dioxide is the final oxidation product of carbon and has moderate reactivity. It dissociates in water to give a weak acid, carbonic acid (H_2CO_3) which reacts with a base to give a salt. The pH of saturated carbon dioxide solutions varies from 3.7 at 1.0 bar to 3.2 at 23.4 bar.

It is non-flammable therefore it is a very safe gas to use (Kirk and Othmer, 1991[b]).

4.3.2 Physical Properties

At a temperature of 273.15 K and pressure of 1.01 bar, carbon dioxide is a gas with a density of 1.98 kg/m^3. The diagram (Fig. 4.1) below shows the equilibrium

conditions of the thermodynamically-distinct phases of carbon dioxide from 200 K to 400 K and pressure of 1 bar to 10 000 bar. This diagram is useful in determining the properties of carbon dioxide for sequestration purposes as the sequestration temperatures and pressure are within the given range.

For the adsorption tests conducted, an average temperature of 303 K and a pressure range from 0.25 bar to 1.5 bar was used. Carbon dioxide under these conditions is in sub-critical state. Although actual injection gas conditions are in the critical state, subcritical conditions are sufficient for comparative tests like the one conducted.

Supercritical carbon dioxide has a temperature above 304.25 K and a pressure above 73.830 bar. It is the preferred phase for carbon dioxide injection due to its unique properties. In this state carbon dioxide has physical properties intermediate to those of gases and liquids (Kirk and Othmer, 1991[b]).

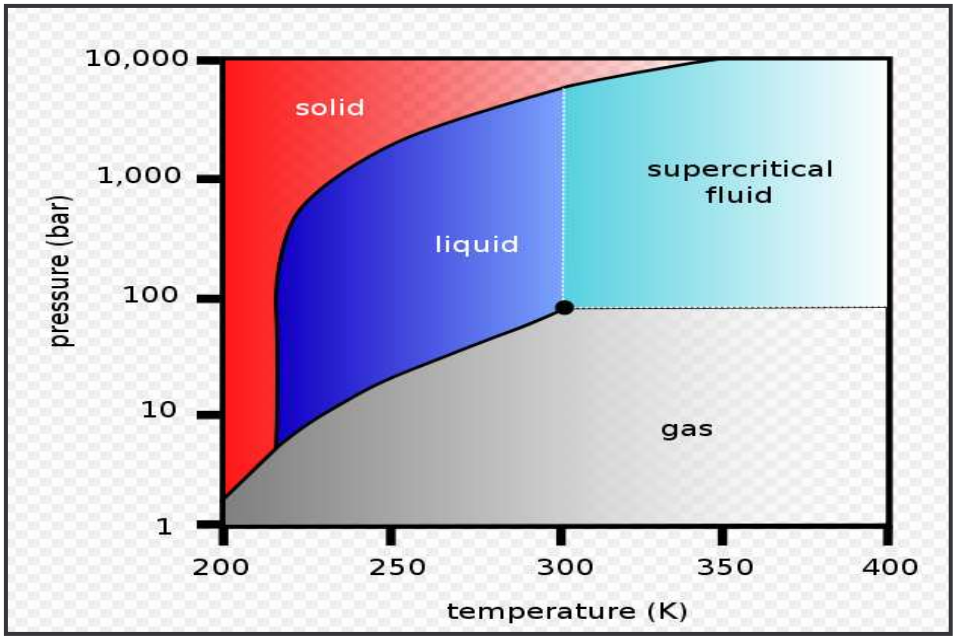

Fig. 4.1 Phase Diagram for Carbon Dioxide (Jacobs, 2005).

The table below gives values of physical properties of carbon dioxide under specific conditions.

Table 4.1 Physical properties of CO_2 (Kirk and Othmer, 1991[b]).

Property	Temperature (K)	Pressure (bar)	Value
Sublimation point	194.65	1.013	
Triple point	216.65	5.180	
Critical Point	304.25	73.830	
Critical density			467 kg/m^3
Gas density	@273.00	@1.013	1.976 kg/m^3
Viscosity	@298.00	@1.013	0.015 cP
Heat of formation	@ 298.00		393.7 kJ/mol

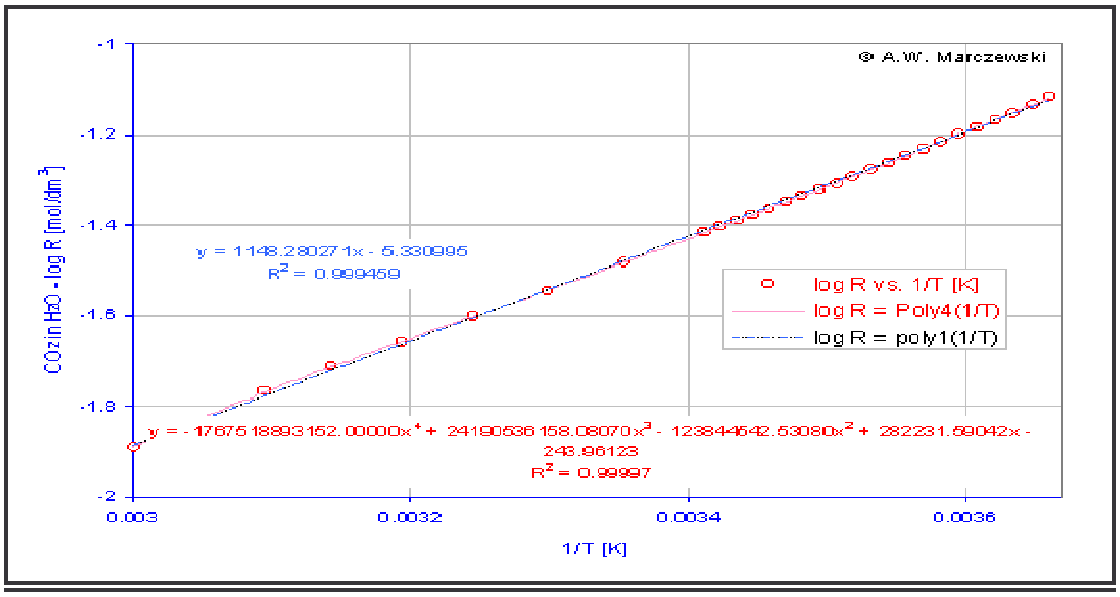

Fig. 4.2 Solubility Curve for Carbon Dioxide (Marczewski, 2004).

4.4 ADSORPTION ISOTHERMS

The adsorption isotherm is the most widely used technique to describe gas adsorption. The maximum quantity of gas that can be stored at low pressure in a given coal is mainly a function of its adsorption capacity (Saghafi et al., 2007). At higher pressures substantial quantities of gas can be stored in the free phase. In this study low pressure adsorption is considered therefore the main storage mechanism is assumed to be adsorption.

The Langmuir adsorption model is widely used for the assessment of gas adsorption onto coal (Siemons and Busch, 2007). Studies conducted by Saghafi et al. (2007) show that the Langmuir isotherm has a relative error of less than 2.7 % for pressures less than 6 MPa. The Langmuir isotherm describes the dependence of the surface coverage of an adsorbed gas on the pressure of the gas above the surface at a fixed temperature.

The model is based on the following assumptions

(i) the surface of the adsorbent is uniform,

(ii) adsorbed molecules do not interact,

(iii) the adsorption mechanism remains the same until equilibrium is established,

(iv) at maximum adsorption only a monolayer of adsorbate molecules is formed (Kirk and Othmer, 1991 [a]).

Assuming a dynamic equilibrium between the adsorption and desorption rate the Langmuir equation is described as;

$$Vads = \frac{K_L P Vm}{1 + K_L P} \qquad \ldots\ldots\ldots\ldots\ldots\ldots\ldots\ldots 4.1$$

Vads – volume of gas adsorbed/mass of adsorbate at pressure P

P – gas pressure

Vm – monolayer volume of gas

K_L – Langmuir constant

(Osborne, 2008)

Because the adsorption capacity is both a function of the amount and reactivity of surface area contained in pores, understanding the relationships of adsorption of carbon dioxide and coal composition require adsorption test data on representative coal samples of the same rank with different composition. Test data on the effect of rank on samples with similar composition will also be considered.

4.5 REVIEW OF PREVIOUS WORK

The adverse effects of global warming have drawn a lot of attention to the need for the reduction of carbon dioxide emissions. A number of researchers from different countries have conducted studies on the effect of coal composition and pressure on carbon dioxide adsorption. The complexity of the chemistry of coal and its variability has led to conflicting results in some cases.

Studies on the adsorption of coal bed methane onto coal samples from the Bowen basin in Australia were conducted by (Crosdale et al., 1997). The coal samples used had different maceral composition and mineral matter content. The

researchers concluded that maceral composition significantly affects gas adsorption. Vitrinite-rich coals exhibited a higher adsorption capacity than inertinite- rich coals of similar rank.

Adsorption experiments conducted on other samples from various sources including Australia, Poland, U.S.A and New Zealand show completely different results. According to (Day et al., 2007), the highest adsorption capacity observed was for a sample with a 23.9 % vitrinite, 74.5 % inertinite and 1.6 % inertinite. While the vitrinite-rich sample with a vitrinite-content of 95.5 % had the lowest adsorption capacity. Graphs from this study do not show a correlation between the maceral composition and adsorption capacity.

Results from the study of a Pittsburgh coal sample in the U.S.A show different results from the ones mentioned above. Karacan and Mitchell (2003) concluded that there is a very strong correlation between carbon dioxide adsorption capacity and maceral composition. Inertinite-rich samples exhibited the highest carbon dioxide adsorption rate compared to vitrinite-rich samples.

The effect of coal rank and depth of coal seam on the adsorption capacity of carbon dioxide was conducted on coal from the Sydney Basin in Australia. Results show that the deepest and highest rank coal had the highest adsorption capacity. The shallowest coal which was not necessarily the lowest rank exhibited the lowest adsorption capacity (Saghafi et al., 2007).

4.6 SUMMARY

In summary this chapter explored the principle of carbon dioxide adsorption onto coal and the results from other researchers. As discussed in section 1.4 the aim of this study is to determine the effect of maceral composition, mineral composition and coal rank on carbon dioxide adsorption for South African coals from the Witbank, Waterberg and KwaZulu-Natal basins. The next chapter is dedicated to the design of the equipment to be used for measuring adsorption.

CHAPTER 5: DESIGN OF ADSORPTION EQUIPMENT

In this chapter a discussion of the gravimetric and volumetric adsorption methods is given. The selection of the best method for the current research is also described. A detailed description of the design process and the construction of equipment are outlined.

5.1 INTRODUCTION

The adsorption experiments were conducted using a volumetric set-up which was designed by the author. The first set-up (Phase 1), which was constructed at the internal workshop had gas leaks, and hence no measurements were conducted on it. An external contractor was hired to construct the final set-up (Phase 2) which provided good measurements in the low pressures range.

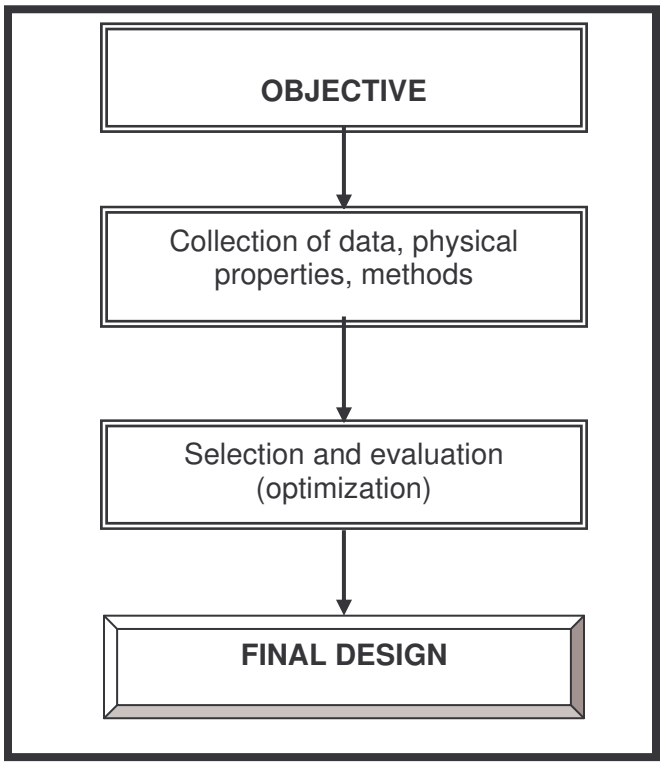

Fig. 5.1 Flow Diagram of the Design Process (Coulson et al., 1991).

The steps outlined in (Fig.5.1) were followed in designing the adsorption equipment.

5.2 OBJECTIVES OF THE DESIGN

- Design equipment that will be used to measure the adsorption of carbon dioxide onto coal. The coal sample will have a particle size range of between 300-600 µm and a mass of 2.0 g.
- The equipment should be gas tight because the system pressure is the most critical property for measurement.
- The equipment should also provide isothermal conditions as adsorption is highly dependant on the system temperature.
- The equipment should be able to withstand gas pressure of up to 5.0 bar.

5.3 ADSORPTION METHODS

The experimental techniques mainly used for the determination of gas adsorption isotherms are the gravimetric and volumetric methods.

5.3.1a) Volumetric method

There are different experimental set-ups that have been used by other researchers.

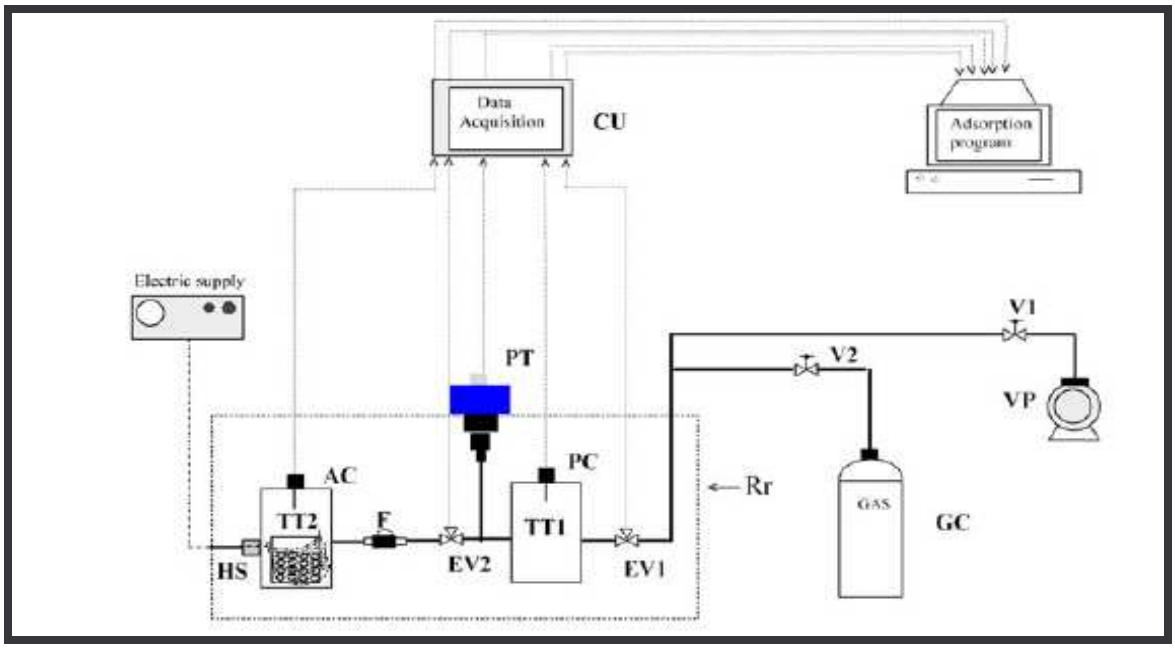

Fig. 5.2 Volumetric Set-up (Belmabkhout et al., 2004).

The diagram above (Fig. 5.2) shows the volumetric experimental set-up used by Belmabkhout (2004) for adsorption measurements. The main components of this system are the pressure cell (PC), adsorption cell (AC), pressure transducer (PT), two temperature probes, control unit (CU), heating system (HS) and a filter (F). The other pieces of equipment include a vacuum pump (VC), electronic valves (EV) and a gas cylinder (GC).

The method of adsorption includes introducing gas into the pressure cell, and quantifying the number of moles of gas using an equation of state. This known amount of gas is then introduced into the adsorption cell which contains the coal sample. Gas adsorption takes place with subsequent decrease of gas pressure in the system until the system pressure reaches equilibrium. The difference between the initial number of moles of gas and the number of moles of carbon dioxide remaining in the gas phase is calculated to be the quantity of gas adsorbed onto coal particles (Belmabkhout et al., 2004).

5.3.1b) Gravimetric method

Fig. 5.3 shows the set-up of the gravimetric apparatus used by Day et al. (2007) for adsorption measurements.

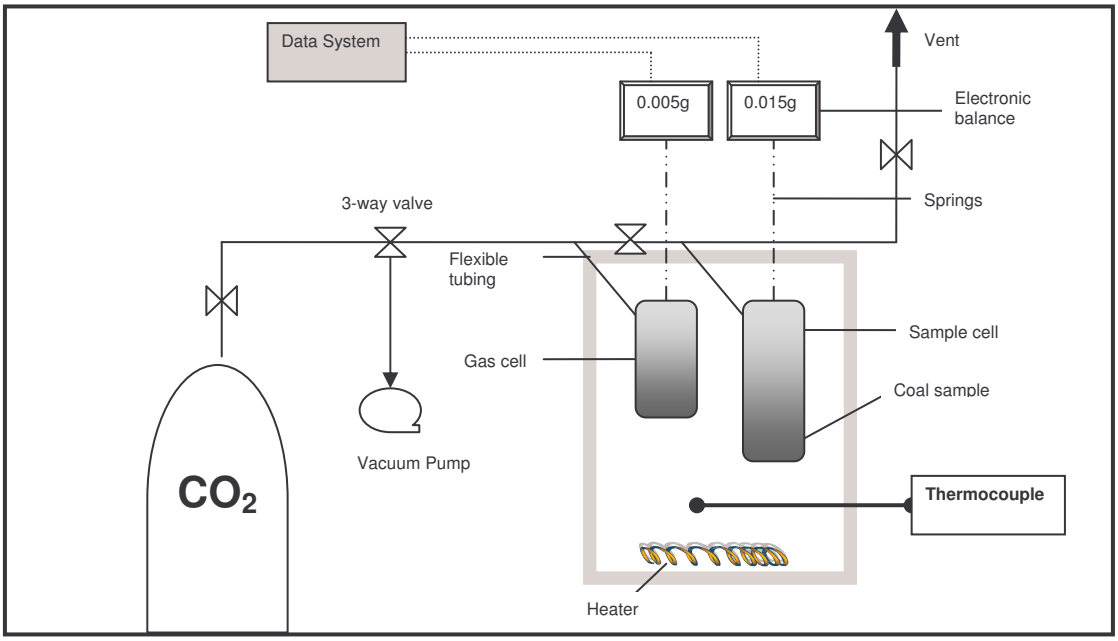

Fig. 5.3 Gravimetric Set-up (Day et al., 2007)

The set-up shown above consists of a gas cell and a sample cell, which are suspended from two balances by springs. The two cells are connected to the gas lines by flexible tubing. A heater is used to heat up the enclosure where these two are located and a thermocouple is used to measure the system temperature.

The method of adsorption measurement includes introducing gas into the pressure cell, and measuring the weight of the gas the gas density is determined. This known amount of gas is then introduced into the adsorption cell which contains the coal sample. Gas adsorption takes place with subsequent increase of sample weight in the system until the weight reaches equilibrium. The difference between the initial weight of sample and its final weight is the quantity of gas adsorbed (Day et al., 2007).

5.4 EVALUATION AND SELECTION OF BEST DESIGN

An evaluation matrix was used to evaluate and select the feasible method to use; that is volumetric vs. gravimetric. The evaluation matrix is a selection tool that is used to select the best option out of a number of given options. A number of important criteria are chosen and these are used to rank the options. The option which has the highest ranking is selected (Martin, 2008). This method was used to select the best set-up to use for adsorption measurements. The criteria used for selection includes; cost, time of construction, accuracy, availability of material and ease of maintenance.

5.4.1a) Cost

The cost of volumetric set-up was approximately R20 000 and while the cost of the gravimetric set-up was at least R150 000.

5.4.1b) Time of construction

The construction of the volumetric set-up only involves connecting the different pieces using standard fittings; hence it was a fairly easy set-up not requiring a lot of expertise. The suspension of cells from a balance requires technical expertise.

5.4.1c) Accuracy

The gravimetric method is a direct measurement of the weight of carbon dioxide adsorbed, whereas the volumetric method measures the pressure drop which could be a result of gas adsorption and leakage. However leakage tests have to be carried out as often as possible to ensure accuracy. Studies comparing the two methods at high pressure of up to 40 bar (Belmabkhout et al., 2004) show that the volumetric method has a 3 % error. In this study the error is expected to be much lower because very low pressures with a maximum of 1.50 bar were used.

5.4.1d) Availability of material

All the material required for construction of the volumetric set-up was readily available locally, whereas the magnetic suspension balances had to be imported from overseas.

5.4.1e) Maintenance

As mentioned earlier the volumetric method involves fitting the equipment pieces together using ordinary equipment but the gravimetric method requires more specialized technicians to repair the balance. The volumetric set-up can therefore be repaired by the user if the need arises.

Based on the information given above each method was given a score for each criterion using the following ranking:

5-excellent

4-very good

3-good

2-fair

1-poor

Table 5.1 Evaluation Matrix for Method Selection (Martin, 2008).

Criteria	Volumetric method	Gravimetric method
Cost	4	1
Time of construction	4	2
Accuracy	3	4
Availability of material	4	2
Maintenance	4	2
Total score	19	11

The matrix score for the volumetric method is higher than the gravimetric score. The main disadvantage of the gravimetric method is the high cost of the equipment and the availability. Based on the matrix score the volumetric method was selected as the best option.

5.5 DESIGN OF THE VOLUMETRIC SET-UP

The schematic diagram below is the volumetric set-up that was designed to measure the adsorption of carbon dioxide onto coal.

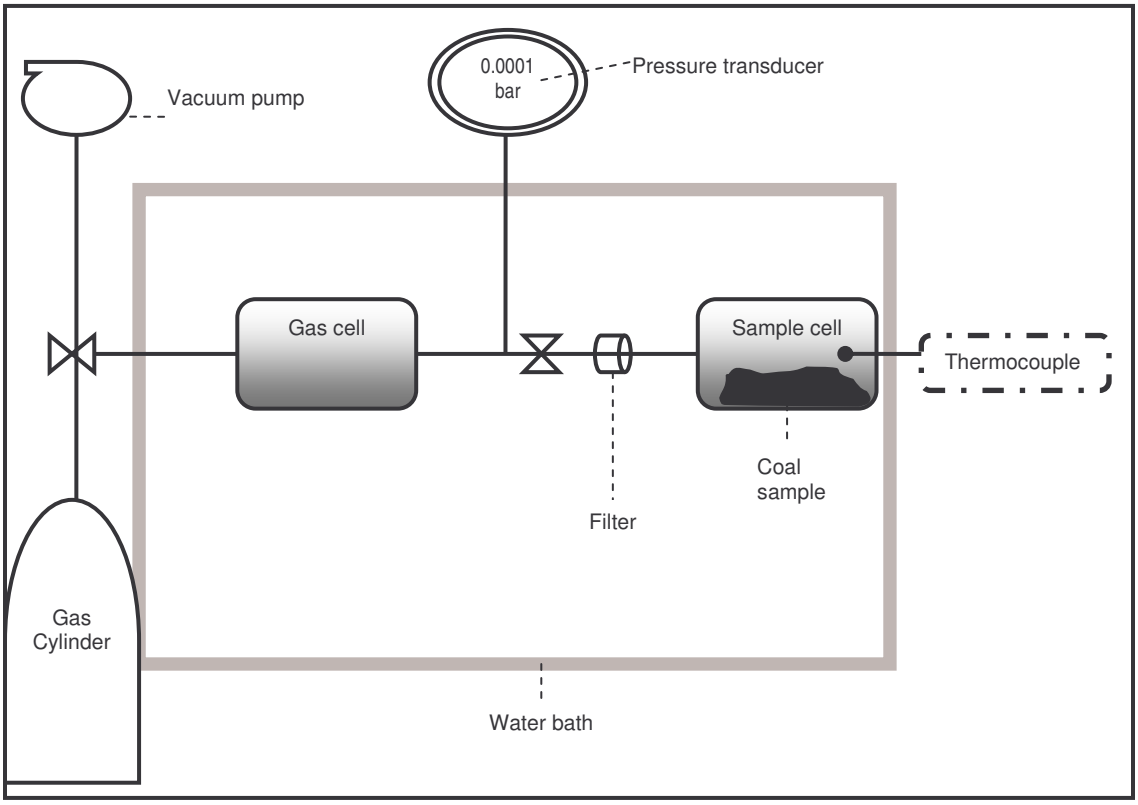

Fig. 5.4 Volumetric Equipment Set-up.

5.6 PHASE 1 OF CONSTRUCTION

The diagram above (Fig. 5.4) is the proposed set-up for the experimental equipment. The first phase of the experimental set-up was constructed at the School of Chemical and Metallurgical Engineering workshop at the University of the Witwatersrand, Johannesburg. Due to funding limitations relatively cheap material was used for the construction.

5.6.1 Equipment

5.6.1a)Gas Cell

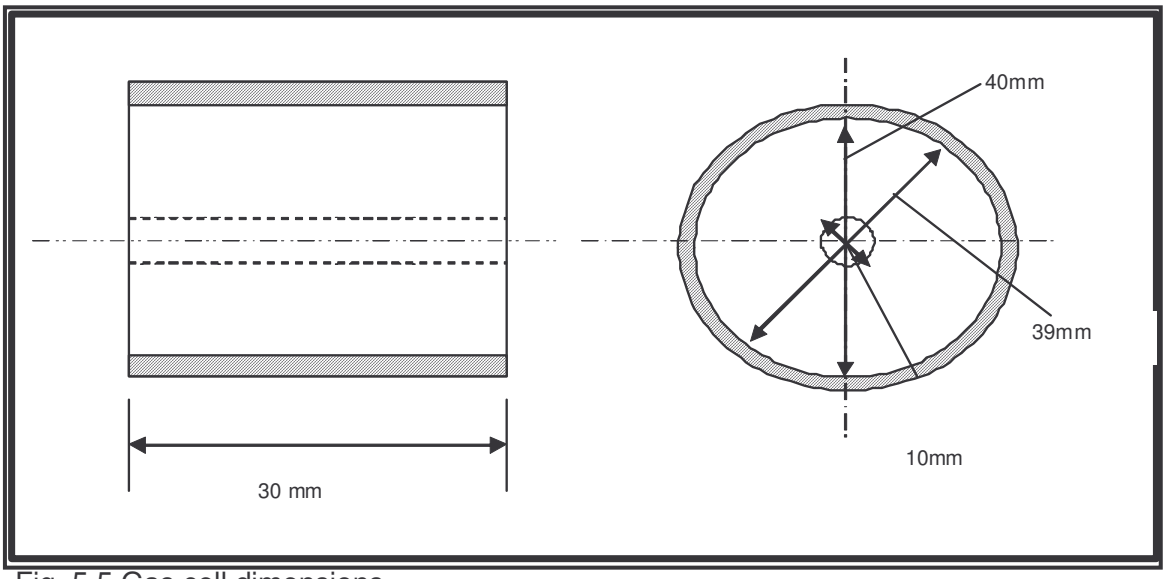

Fig. 5.5 Gas cell dimensions.

5.6.1b)Sample Cell

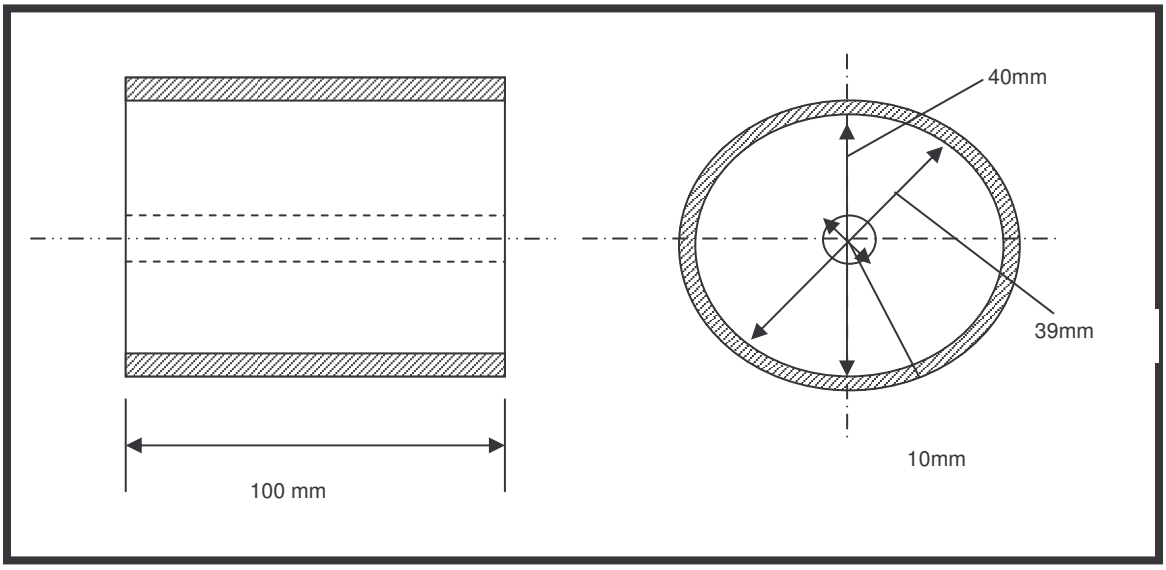

Fig. 5.6 Sample cell dimensions.

5.6.1c) Piping

A standard ¼ inch brass pipe was used for connecting all the pieces of equipment.

5.6.1d) Valves

Ball valves were selected for use in this system. These valves give a positive seal in the closed position and allow fluids to flow easily when open. The tight seal offered by the valve in the closed position is a very important for this study. Leakages of gas into or out of the system during operation will compromise the pressure measurements thereby introducing errors into the measurements. The valves used were made of brass.

5.6.1e) Fittings

All the connectors used for the equipment were also made of brass.

5.6.1f) Filter

The filter used consisted of a fitting made of poly-vinyl chloride (PVC) and a standard 2 µm filter paper.

Fig. 5.7 Phase 1 Equipment.

5.6.2 Equipment Pressure Test Results

After designing the equipment the first step is to test for leakages. The apparatus was connected to the gas lines and carbon dioxide gas was passed through the system. Soapy water was used to check for leaks, gas leaks are detected by a bubble forming at the connection. Several leaks were detected and the connections were tightened. Further tests were carried out and leaks were again detected in the system. Super glue was used to cover the openings; however this did not help as the system continued to leak. The main problem was due to poor machining of the cells and fittings that were of poor quality.

The results given below show the pressure drop of the system in the absence of a coal sample.

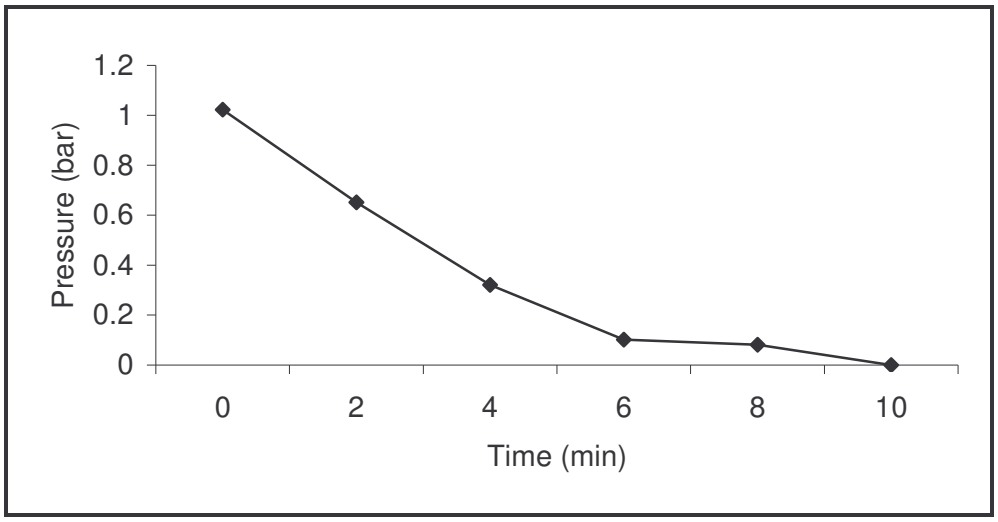

Fig. 5.8 Phase 1 Equipment Test Results- Pressure Decrease due to Leakage.

Measurements were also conducted on the three samples and the results were the same as above because all the gas escaped before any adsorption could take place.

Another design had to be made in order to be able to do the measurements.

5.7 PHASE 2 OF CONSTRUCTION

The same schematic diagram of the volumetric set-up (Fig. 5.4) was used for the equipment, however different material was used. Construction of the second design (Fig. 5.9) was contracted to the Johannesburg Valve and Fitting Company.

5.7.1 Equipment

5.7.1a) Water bath

Gas adsorption is strongly dependent on the system temperature. A heated water bath with a relative uncertainty in temperature of 0.1 ^{o}C was used to maintain a constant temperature in the system. The experiments were performed at 304 K which is the critical temperature of carbon dioxide.

5.7.1b) Gas cylinders

The carbon dioxide gas cylinder used was the one supplied by Afrox in which the compressed gas is stored. The gas pressure was controlled for the purposes of the experiment using a regulator.

5.7.1c) Gas cell

An open ended stainless steel cell was used capable of withstanding high temperatures and pressures of 473 K and 10 kPa respectively. Its internal volume is 50 cm^3.

5.7.1d) Pressure transducer

A high precision 261 PRESS.TX digital pressure transducer was used for pressure measurement. It has an operating range maximum pressure of 10 bar, with a precision of 0.1% of the full scale value. The pressure transducer is powered by a 24 V DC supply. Pressure transmission is ensured by a pressure transmission fluid (silicone oil). The pressure transducer can thus operate at process temperatures up to 473 K.

5.7.1e) Thermocouple

A K-type thermocouple connected to a digital temperature display was used for the measurement of temperature in the system. K-type thermocouples are made up of a mixture of chromel and alumel. It is the most commonly used general purpose thermocouple, mainly because it is fairly cheap. It has an operating temperature range of –200 °C to +1350 °C.

5.7.1f) Filter

A 2 µm in-line filter was used to prevent the coal particles from entering the valves.

5.7.1g) Sample Cell

A stainless steel flanged vessel was used, allowing temperatures between 223 and 473 K and pressures up to 10 000 kPa. Its internal volume is 50 cm^3.

5.7.1h) Vacuum pump

A Series N022_A18 diaphragm vacuum pump was used. The vacuum pump is a single-head dry running pump which can supply a vacuum of -4.0 bar.

5.7.1i) Valves and piping equipment

2 x standard two-way ¼ inch stainless steel ball valves and 1 x three-way ¼ inch stainless steel ball valve were used. Standard ¼ inch mild steel piping was used for connecting the pieces of equipment.

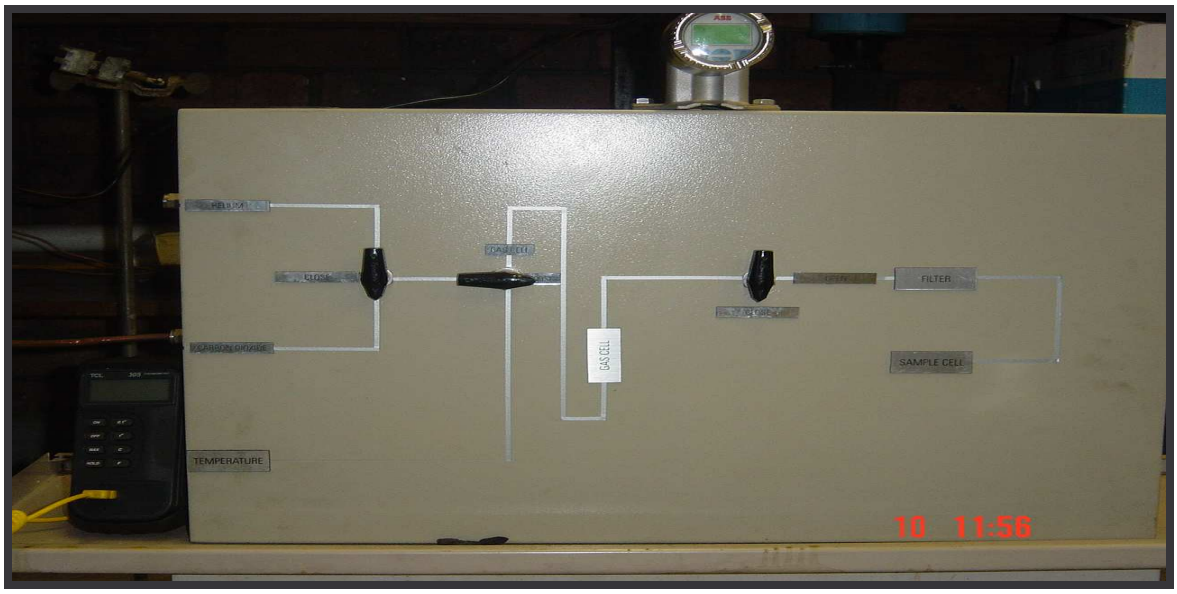

Fig. 5.9 Phase 2 Equipment.

To ensure accuracy of the experimental data the gas system was tested for leak-tightness. This was done by passing gas through the system at 1.75 bar pressure and using soapy water; no bubbles were detected in this pressure range.

5.7.2 Equipment Pressure Test Results

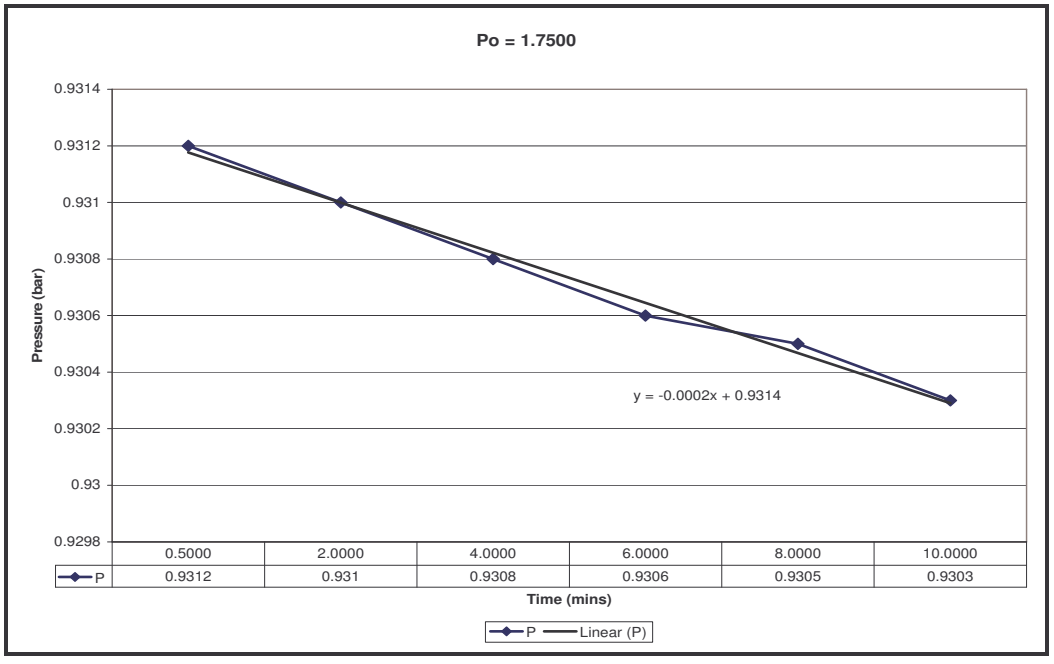

Fig. 5.10 Equipment Test Results.

The results show the pressure drop at an initial pressure of 1.75 bar. A pressure drop of 0.0002 bar every two minutes was measured. This pressure drop is very low as determined by the gradient of the equation 0.0002 ≈ 0, the system is therefore assumed to be gas tight.

5.8 SUMMARY

The gravimetric method is generally considered to be a more reliable method compared to the volumetric method. A comparative study of the two methods conducted by Belmabkhout et al. (2003) showed an average deviation of 3 % between the two methods. This shows that there is not much variation between data obtained from both methods, hence the volumetric method provides reliable data if gas leaks are minimised in the system.

A volumetric adsorption system was selected for the study. Despite initial design problems, the Phase 2 design appears to meet the requirements for this research project. Pressure tests were conducted, and the equipment appears to be reliable.

CHAPTER 6: EXPERIMENTAL WORK AND CHARACTERISATION RESULTS

In the previous chapter the equipment design and construction of the volumetric adsorption system was discussed. This chapter gives a description of all the experimental work including adsorption measurements using the equipment described in Chapter 5 (Fig. 5.9). Coal sample preparation and characterisation results are also presented.

6.1 INTRODUCTION

The four parent coal samples used in this study originate from the Witbank, Waterberg and Kwazulu Natal coal fields. These samples were selected because they represent major commercial coalfields in South Africa. The samples were crushed and sieved to give products with a particle size range between +1000 µm to -2800 µm for the beneficiation process. The fractions from beneficiation were further crushed to +300 µm to -600 µm for the adsorption tests. The remaining raw coal and beneficiation fractions were crushed to the appropriate sizes for sample characterisation, which include proximate, petrographic and surface area analyses. The technical programme is summarised in Fig. 6.1.

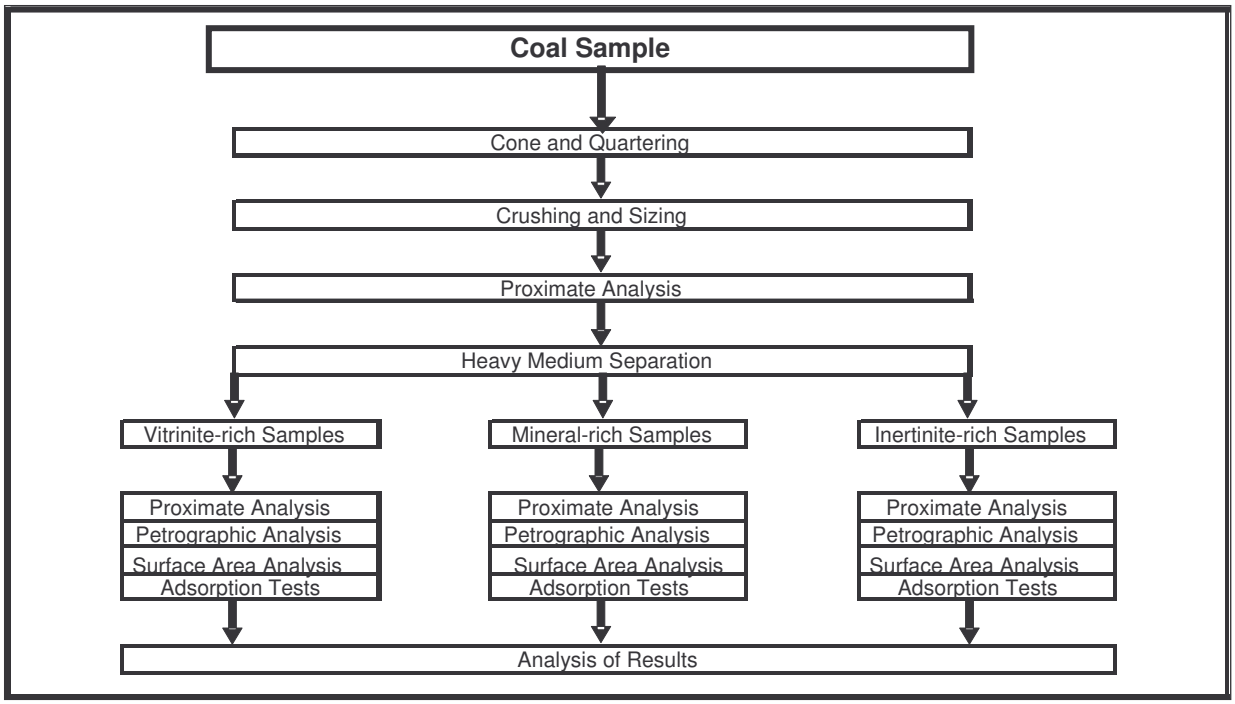

Fig. 6.1 Technical Programme.

6.2 SAMPLE PREPARATION

6.2.1 Cone and Quartering

The coal samples were each divided by using the cone and quartering method. This is a technique that is widely used to divide a sample, while ensuring that each portion is representative of the parent sample. This technique consists of pouring the material into a conical heap, which is flattened and divided into quarters. The method relies on the radial symmetry of a cone to give representative portions of the parent sample (Wills, 1992). Two opposite quarters are collected, mixed and the process is repeated until the required sample size is obtained.

6.2.2 Milling and Sieving

The main purpose of milling is to liberate the different components in the coal sample for effective separation of the components using the heavy medium separation technique. The smaller the particle sizes the greater the degree of liberation.

Each sample was sieved prior to milling to prevent over milling the smaller size fraction. In order to obtain the size fraction range of +1000 µm to -2800 µm, the coal sample was separated by passing each sample through 2800 µm and 1000 µm test sieves.

A vibrating sieve shaker was used to for efficient separation of the particles, because the vibrations aid in exposing all the particles to the openings in the sieve. The process of sieving takes place in two stages, where stage one involves the passage of particles much smaller than the screen apertures. The second stage is passage of “near size” particles, that is irregular particles whose equivalent diameter is close to the nominal aperture of the test sieve. The first stage occurs more rapidly with very little hindrance, while the second stage is more difficult requiring that the particle be presented to the aperture in a certain position before it is able to pass through. Induced vibration on the screens therefore gives particles a greater opportunity to attain this favourable position to pass through (Wills, 1992).

Particles less than 1000 µm were discarded while particles in the desired range were placed in a sample bag. Over-size particles, greater than 2800 µm were crushed using a ring mill. The ring mill uses a combination of impact and abrasion forces for particle size reduction. The mill consists of a cylindrical steel vessel, three rings of different diameter and a steel lid. The three rings are arranged concentrically inside the vessel, and the coal sample is charged into the spaces between the rings. The vessel is closed and clamped to a vibrator. During operation the vibrations cause the rings to vibrate and the impact and abrasion of the rings on the coal sample cause the particles to disintegrate. To avoid milling the sample to powder the milling time was maintained at one minute.

The product was sieved, separating over-size, undersize and the desired fraction, the over-size product returned to the mill was for further milling and the undersize discarded. The process was repeated until 200 g samples of +1000 µm to -2800 µm particles were obtained.

6.2.3 Heavy Medium Separation

In the heavy medium separation technique, the separation efficiency decreases with size due to the slower rate of settling of the particles. Hence a fairly coarse size range is required for effective separation, according to the recommended size range for process applications is >3 mm (Wills, 1992). For the purposes of this project the chosen size fraction was +1000 µm to -2800 µm which is fairly close to the recommended particle size. This size range strikes a perfect balance between maximizing the degree of liberation as well as the separation efficiency.

The heavy medium separation technique is a widely used method for separating particles based on the difference in their density. The principle of the process is to subject particles with different densities in a heavy liquid of suitable specific gravity (s.g), so that the lighter particles float while heavier particles sink. Coal macerals and mineral matter have different densities; hence this method was used to separate the coal particles into fractions with different maceral compositions and mineral-rich components.

The heavy liquids used were benzene (s.g 0.89), carbon tetrachloride (s.g 1.59) and bromoform (s.g 2.88). Mixtures of these liquids were prepared to give different solutions with different specific gravities. The solutions used had s.gs of 1.45, 1.60 and 1.90.

6.3.2a) Witbank Parent Sample – Bituminous Coal

The Witbank sample was composed of 56.8 % inertinite, 25.4 % mineral matter, 13.8 % vitrinite and 4.0 % liptinite (Appendix C). A solution of s.g 1.60 was used to separate the macerals from the inorganic matter. The sample was placed in the solution and allowed to stand for 2 minutes. The floats were collected as the inertinite-rich sample.

6.3.2b) Waterberg Parent Sample – Bituminous Coal

The Waterberg sample was mainly composed of vitrinite (46.2 %) and mineral matter (47.6 %) with inertinite and liptinite constituting only 6.2 % (Appendix C). Due to the very high mineral matter content, a solution with a very high density had to be used for separation. A solution of s.g 1.90 was therefore used to

separate the macerals from the inorganic matter. The Waterberg sample was placed in the solution and allowed to stand for 2 minutes. The floats were collected as the vitrinite-rich sample and the sinks were collected as the mineral matter-rich sample.

6.3.2c) KwaZulu-Natal (KZN) Parent Sample – Semi-anthracite A

The sample was mainly composed of vitrinite (80.0 %), inertinite (16.3 %) and mineral matter (3.7 %) (Appendix C). The sample was placed in the solution of s.g 1.45 and allowed to stand for 2 minutes. The floats and sinks fractions collected has different maceral compositions.

6.3.2d) KwaZulu-Natal (KZN) Parent Sample – Semi-anthracite B

The sample was composed of 49.8 % vitrinite, 45.6 % inertinite and 4.6 % mineral matter (Appendix C). The sample was placed in a solution of s.g 1.45 and allowed to stand for 2 minutes. Three fractions were obtained from the separation process that is the float, middling and the sink product.

A total of thirteen fractions were obtained using the heavy medium separation technique for use in this investigation.

Table 6.1 Sample Description

Sample I.D	Sample Identification	Description
Sample 1	Witbank float product @ 1.60 s.g	Inertinite-rich sample
Sample 2	Waterberg float @ 1.90 s.g	Vitrinite-rich sample
Sample 3	Waterberg sink @ 1.90 s.g	Mineral matter – rich sample
Sample 4	KZN Sample B float @ 1.45 s.g	Vitrinite-rich sample
Sample 5	KZN Sample B middling @ 1.45 s.g	Inertinite-rich sample
Sample 6	KZN Sample B sink @ 1.45 s.g	Inertinite-rich sample
Sample 7	Waterberg float @ 1.90 s.g	Vitrinite-rich sample
Sample 8	Witbank float @ 1.90 s.g	Inertinite-rich sample
Sample 9	Waterberg float @ 1.90 s.g	Mineral matter – rich sample
Sample 10	KZN Sample A float @ 1.45 s.g	Vitrinite-rich sample
Sample 11	KZN Sample A sink @ 1.45 s.g	Vitrinite-rich sample
Sample 12	Waterberg lower bench float @ 1.90 s.g	Inertinite-rich sample
Sample 13	Waterberg lower bench sink @ 1.90 s.g	Mineral matter – rich sample

6.3 PETROGRAPHIC ANALYSIS

6.3.1 Introduction

The analysis involves the determination of the coal maceral composition and the coal rank. Macerals are optically homogeneous and discrete; therefore they are easy to see under a microscope. There are two main methods of petrographic analysis namely reflected light and transmitted light techniques. For the purposes of this research the reflected (incident) light technique was used. This technique is widely used because of the relative ease in sample preparation and it can achieve a high resolution of the polished surface. The quantitative count of macerals is more accurate and the ability to measure reflectance of the macerals is enhanced. An incident light Leica DMP 4500 microscope with an oil immersion lens and total magnification of x500 was used for the analysis. The analysis was conducted by Dr N. Wagner in the School of Chemical and Metallurgical Engineering, University of the Witwatersrand. Under incident light vitrinites appear to be dark grey, light grey or white as the coal rank increases. Liptinites appear dark grey or grey while inertinites are bright to extremely bright (Karr, 1978).

6.3.2 Sample Preparation

When using the reflected light technique for analysis, samples can either be prepared in the form of polished blocks or as polished briquettes of crushed particles. Polished briquettes were used for this analysis since the separation method requires the use of small particle sizes. The procedure for the preparation of the blocks was conducted according to the ISO standard 7404 Part 2 (ISO 7404, 1985).

After separation of the macerals using heavy medium separation a representative 20 g portion of each sample was obtained using cone and quartering techniques. The samples were crushed using a pestle and mortar to give particles between + 600 µm and -1000 µm.

Plastic cups were used for preparing the mould. The cups were lined with a thin layer of vaseline to prevent binding of the briquettes to the cup. 5 g of each

sample was placed in the cup. A mixture of 7 parts epoxy resin to one part hardener was made and poured into each cup. The resin was mixed thoroughly to give a thick paste. A sample label was placed on top of the paste and the remaining resin was poured over to keep the label in place. The mould was left to set for 12 hours.

After 12 hours the mould was removed from the plastic cups in preparation for grinding and polishing. A Struers Tegrapol polishing machine was used for polishing. The samples were ground under a force of 15 N, for 1 and 2 minutes using the SIC 500 and 1000 papers respectively with water as the medium. Polishing was done at 10 N, for 2 minutes, using allegro largo and MD Dac as the mediums.

After polishing the samples were washed with soap and water and dried in preparation for the analysis.

6.3.3 Sample Analysis

The polished briquettes were mounted onto glass slides using a levelling press, before placing them under the microscope. The microscope was used for determining the percentage maceral content in each of the polished briquettes as well as the mean random reflectance.

6.3.3a) Maceral determination

An incident light Leica DMP 4500 microscope with an oil immersion lens and total magnification of x500 was used for the analysis. The light source for the microscope is a tungsten lamp with a power output of 30 to 100 W. The microscope is also equipped with a rotating object stage and an attachable mechanical stage for point counting. The proportions of each maceral were determined by a point counting procedure and expressed in volume % based on a minimum of 500 point counts. The maceral analysis was determined according to ISO 7404 part 3 (Karr, 1978 and ISO 7404, 1994).

6.3.3b) Reflectance measurements

Reflectance is a measurement of the degree of metamorphism or coalification. The reflectance of coal samples is based on the reflectance of vitrinite. Vitrinite exhibits a wide reflectance range from 0.2 to 2.5 % from brown coal to anthracite respectively; therefore it is a more reliable source of determining coal rank (Karr, 1978).

6.3.4 Results

Vitrinite measurements were done according to ISO standard 7404 part 5 (ISO 7404, 1994). Mean random reflectance was measured using a J and M spectroscopic system attached to the Leica microscope.

Table 6.2 Petrographic Composition of the Samples.

Sample I.D	Petrographic Analysis Results (%)				
	Vitrinite	Inertinite	Liptinite	Mineral matter	RoVmr
Sample 1	8.00	73.4	9.2	9.4	0.72
Sample 2	92.0	0.4	4.4	3.2	0.69
Sample 3	2.60	3.6	0.8	93.0	0.69
Sample 4	65.6	32.4	0	2.0	2.21
Sample 5	42.2	52.8	0	5.0	2.21
Sample 6	9.60	66.2	0	24.2	2.21
Sample 7	76.8	8.6	2.4	12.2	0.69
Sample 8	28.6	58.4	4.2	8.8	0.72
Sample 9	4.2	3.0	0.2	92.6	0.69
Sample 10	92.8	6.8	0	0.4	2.28
Sample 11	67.6	25.4	0	7.0	2.28
Sample 12	4.2	78.8	2.6	14.4	0.69
Sample 13	0.4	19.8	0.2	79.6	0.69

Table 6.2 above presents the results of the petrographic analyses. Samples 2 and 10 have very high vitrinite contents of above 90.0 %. Except for sample 1 which has liptinite content of 9.2 %, the rest of the samples have relatively little liptinite or none at all; this maceral will therefore not be considered in the adsorption analyses procedure. Samples 1 and 12 have inertinite contents of over 70.0 %, while samples 5, 6 and 8 have moderate contents of inertinite. The samples provide a very good maceral variation which can be used effectively to assess the influence of each maceral on the adsorption capacity of coal samples.

The samples studied generally fall into two coal rank categories, the Waterberg and Witbank parent coals are medium rank C bituminous coals and the Kwazulu Natal parent coals are high rank C anthracites. The reflectance measurements were conducted on the float samples and the same value was used for the sink since the fractions originate from the same parent coal.

6.4 PROXIMATE ANALYSIS

The proximate analysis for a coal sample is the determination of the moisture, volatile matter, fixed carbon and ash content of the sample. These are the most common coal properties used in coal trading. Moisture analysis involves the determination of the surface and inherent moisture, the volatile matter content involves determination of the volatile gases in coal, fixed carbon indicates the approximate carbon content and ash content indicates the amount of non-combustible material in coal. A Perkin Elmer STA600 thermo gravimetric analyzer with Pyris software housed in the School of Chemical and Metallurgical Engineering, University of the Witwatersrand, was used for the proximate analysis of the coal samples.

6.4.1 Thermo gravimetric Analysis

Thermogravimetric analysis is an analytical technique which is used to determine a materials' fraction of volatile and combustible components by monitoring its weight change, as the sample is heated in an inert or oxidizing atmosphere. This method relies heavily on a high degree of precision for mass and temperature change measurements.

The Perkin Elmer ST600 analyzer that was used consists of a high-precision balance with a platinum weighing pan. The pan is placed in a small electrically heated oven with a thermocouple to accurately measure the temperature. The equipment has a built-in mass flow controller, with inputs for two different gases which allows for automatic switching between nitrogen and oxygen.

The following in-house procedure was loaded onto the computer for the determination of moisture, volatile matter, fixed carbon and ash.

A 15 mg sample with particle size of +300 µm to -600 µm was placed in the sample cup, at a temperature of 30 ^{o}C under an inert atmosphere; nitrogen was used as the inert gas.

6.4.1a) Moisture

For percentage moisture determination the sample was heated at a rate of 50 ^{o}C/minute to a temperature of 110 ^{o}C and held at constant temperature for 3 minutes. The weight loss corresponded to moisture loss, which is expressed as a percentage of the original weight of the sample.

Moisture in coal occurs in four possible forms and these are;

i) Surface moisture – this is extraneous water held as films on the surface of the coal particles, which readily evaporates when dried out in the open.

ii) Hygroscopic moisture – this is water held inside the capillaries of the coal matrix.

iii) Decomposition moisture – this is water incorporated in some of coal's organic compounds.

iv) Mineral moisture – water which forms part of the crystal structure of clays and other minerals present in coal (Karr, 1978).

6.4.1b) Volatile Matter

The sample was heated further at a rate of 50 ^{o}C/minute to a temperature of 900 ^{o}C and this temperature was maintained for a further seven minutes to ensure complete release of all volatile matter. The weight loss between 110 ^{o}C and 900 ^{o}C was expressed as a percentage of the original sample weight to give percentage volatile matter

Volatile matter in coal consists of components in coal that are liberated as gas or vapor at high temperatures in the absence of air. The sources of the material are both the inorganic and the organic components of coal (Karr, 1978).

6.4.1c) Fixed Carbon

After seven minutes had elapsed the temperature remained at 900 ^{o}C. However the gas in the chamber was changed to oxygen and these conditions were maintained for a further 20 minutes. The oxygen atmosphere supported complete combustion of the carbonaceous matter. The percentage fixed carbon was calculated as the weight loss between the points of addition of oxygen and at the end of the 20 minute period as a percentage of the initial sample weight.
This is carbon found in coal after all the volatile matter has been expelled. It represents the decomposition of the coal's organic components and contains N, S, H and O_2 as absorbed or chemically combined material.

The fixed carbon content gives a good indication of expected coke yield after coal carbonization. It is also used to determine the solid combustible material in coal combustion processes. When quoted on an ash free basis the fixed carbon is used in coal classification and determination of the coal rank (Karr, 1978).

6.4.1d) Ash

The percentage ash is the weight of the remaining material as a fraction of the initial weight of the sample.

This is the non-combustible inorganic residue that remains after complete combustion under strictly controlled conditions. During the course of combustion there is alteration of the original mineral matter, carbon dioxide escapes due to decomposition of mineral carbonates. Water of hydration also escapes from hydrated silicates, while pyrites are converted to ferric oxide resulting in the loss of sulphur (Karr, 1978).

The final step of the TGA procedure is to reintroduce the inert gas and cool the equipment using water as a coolant at a rate of 50 ^{o}C down to the initial temperature of 30 ^{o}C.

The Pyris software program in the system generates a percentage weight loss curve which is used to determine the different analysis. A typical weight loss curve is shown below (Fig. 6.2).

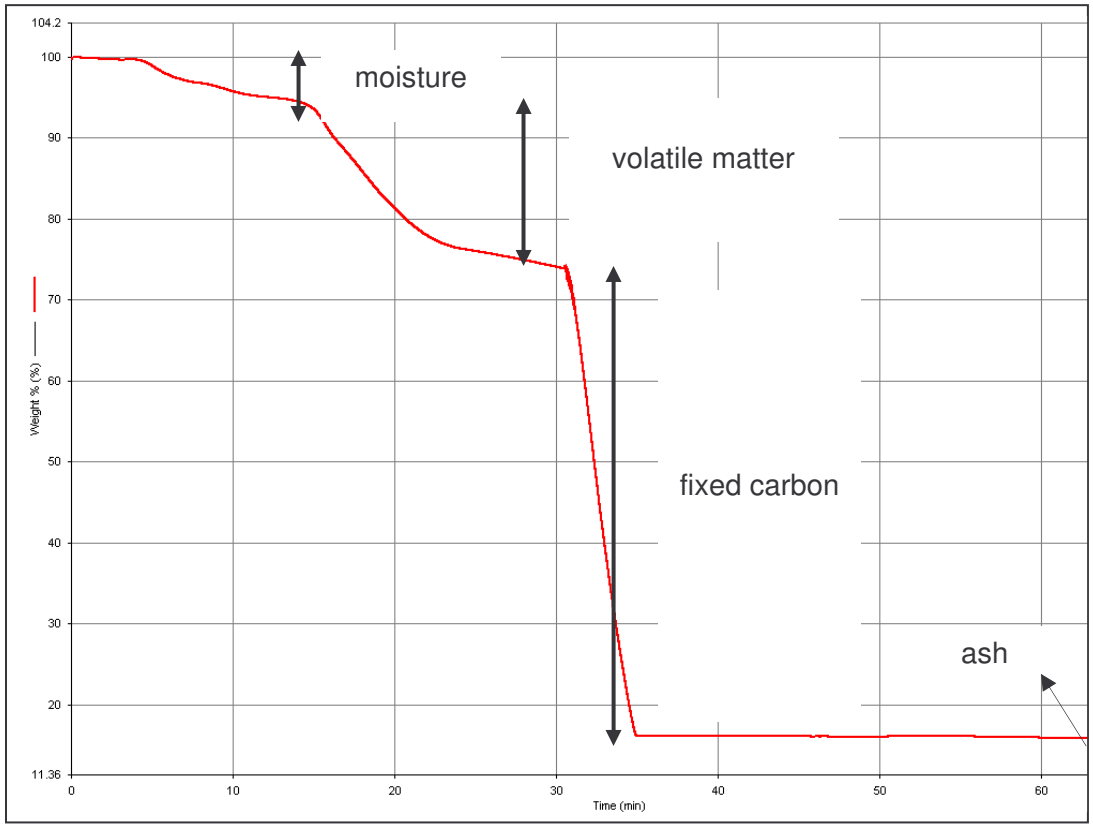

Fig. 6.2 Typical Weight Loss Curve as Obtained from a TGA.

Table 6.3 Proximate Composition of the Samples

Sample I.D	Proximate Analysis Results (%)			
	Moisture	Volatile Matter	Fixed Carbon	Ash
Sample 1	3.28	33.85	53.95	8.9
Sample 2	1.94	35.95	56.54	5.6
Sample 3	1.50	16.32	3.59	78.6
Sample 4	0.81	12.88	80.53	5.8
Sample 5	0.89	12.62	74.24	12.3
Sample 6	1.34	12.73	55.35	30.6
Sample 7	2.32	31.79	49.56	16.3
Sample 8	2.20	32.53	25.97	12.3
Sample 9	1.98	15.97	4.45	77.6
Sample 10	0.91	11.85	85.84	1.4
Sample 11	0.98	11.32	80.70	7.0
Sample 12	1.92	31.43	52.25	14.4
Sample 13	1.95	17.25	15.40	65.4

The proximate analysis of the coals is presented in Table 6.3. The moisture content of the coal samples ranges from 0.81 to 3.28 %. The volatile matter content of the anthracite samples is between 11.32 and 12.88 %, while the bituminous samples with low ash content have a volatile matter content ranging from 31.43 to 35.95 %.

The results show that the low rank coals have high volatile matter compared with the high rank coals; as mentioned in Section 3.1.2 b) the volatile matter of coal decreases with increase in rank. The fixed carbon ranges from 25.97 to 85.84 % for low ash samples, while the high ash samples have very low fixed carbon levels as expected.

The ash levels are very high for the sink fractions samples 3, 9 and 13 ranging between 65.4 and 78.6 %. The rest of the samples have ash levels below 20.0 %.

These results along with the petrographic results confirm that the required separations were achieved in order to meet the objectives of the investigation.

6.5 SURFACE AREA AND MICROPORE VOLUME ANALYSIS

The determination of the surface area was conducted at the North-West University (Potchefstroom Campus), using a Micromeritics ASAP2020 BET analyser. The equipment consists of a sample tube which is maintained at 273.15 K for the adsorption tests. Carbon dioxide gas was introduced into the system and the isotherm plotted by the software. The isotherm was then used to determine the micropore surface area.

The surface area of coal particles is a product of the monolayer capacity and the area occupied by a single adsorbed molecule. The monolayer capacity is the number of molecules necessary to cover the surface of the adsorbent with a complete monolayer (Karr, 1978). The monolayer capacity was determined by the Dubin-Radushkevich equation. This equation was found to be more appropriate compared with the BET equation because it is based on the

adsorption of carbon dioxide; therefore it is expected to give results which relate well with the adsorption measurements since the adsorbate is the same.

The Dubin-Radushkevich surface area was determined from carbon dioxide adsorption isotherms measured at 273 K.

$$\log V = \log Vo - (0.434BT^2/\beta^2)[\log (p_s/p]^2 \quad \text{6.1}$$

V – volume of gas adsorbed at equilibrium pressure p,
Vo – micropore capacity,
p_s – saturation vapor pressure of the adsorbate,
β – affinity coefficient of the adsorbate relative to CO_2,
B – constant which is a measure of the micropore size.

A plot of log V and $[\log (p_s/p]^2$ gives the micropore capacity Vo as the intercept, which is multiplied by the cross-sectional area of an adsorbed molecule to give the micropore surface area.
The cross sectional area of the adsorbed molecule is calculated by using the Emmet-Brunauer equation. This equation assumes hexagonal packing of close-packed spheres;

$$\sigma_m = 3.464 \times 10^{16} (M/4 \sqrt{2} N_A \rho_s)^{2/3} \quad \text{6.2}$$

M – molecular weight
N_A – Avogadro's number
ρ_s – density of adsorbed phase

Table 6.4 Surface Area Analysis Results

Sample I.D	Surface Area Analysis Results		
	Micropore Surface Area (m^2/g)	Monolayer Capacity (cm^3/g)	Maximum Pore Volume (cm^3/g)
Sample 3	36.06	7.89	0.007
Sample 4	164.41	35.99	0.033
Sample 6	110.52	24.19	0.023
Sample 7	76.78	16.81	0.015
Sample 10	297.54	65.13	0.033

Table 6.4 above shows the results for surface area analysis for 5 selected samples. These samples were selected as the representative samples for the parameters under investigation. Sample 4, 7 and 10 are high vitrinite samples of different rank, while sample 6 and sample 3 represent high inertinite and high mineral matter samples.

The high vitrinite samples 4 and 10 have the highest micropore surface area available for adsorption, with the highest rank sample having the highest micropore surface area. Samples 3 and 6 have much lower micropore surface area as is expected for mineral matter rich and inertinite rich samples. Sample 7 was found to have a low micropore surface area despite having a high vitrinite content of 76.8 %, since only one sample was run for these tests this unexpected result can be attributed to an experimental error.

6.6 ADSORPTION MEASUREMENTS

6.6.1 Introduction

As previously discussed in section 5.3, the experimental techniques mainly used for the determination of gas adsorption isotherms include the gravimetric and the volumetric methods. To recap, the gravimetric method is a direct determination of the quantity of gas adsorbed as it measures the increase in the mass of the coal sample when the gas is in equilibrium with coal. The volumetric method provides an indirect measurement of the quantity of gas adsorbed. It is based on the assumption that the decrease in the quantity of gas in a closed system at equilibrium is a result of the adsorption of the gas onto the coal surface. The volumetric system was used in this research.

A full description of the components of the volumetric equipment used is given in Chapter 5. The adsorption measurement procedure consists of two major parts that is:

(i) Sample degassing and

(ii) Carbon dioxide adsorption onto the degassed sample.

These two procedures are discussed in detail in the following sections.

6.6.2 Sample Degassing

Sample degassing is the pre-treatment required for the adsorption tests. The purpose of degassing is to remove any surface moisture and any adsorbed gases in the coal. The process does not remove the volatile matter. The degassing process was performed by heating the sample under vacuum. A flat bottomed flask was used for the degassing process. The flask was placed on a hot plate and it was connected to a vacuum pump Fig. 6.3.

A 10 g coal sample with a particle size range of +300 µm to -600 µm was weighed and placed in the flask. The sample was heated to a temperature of 120 ^{o}C and the system was subjected to a vacuum of -1.5 bar for 1 hour.

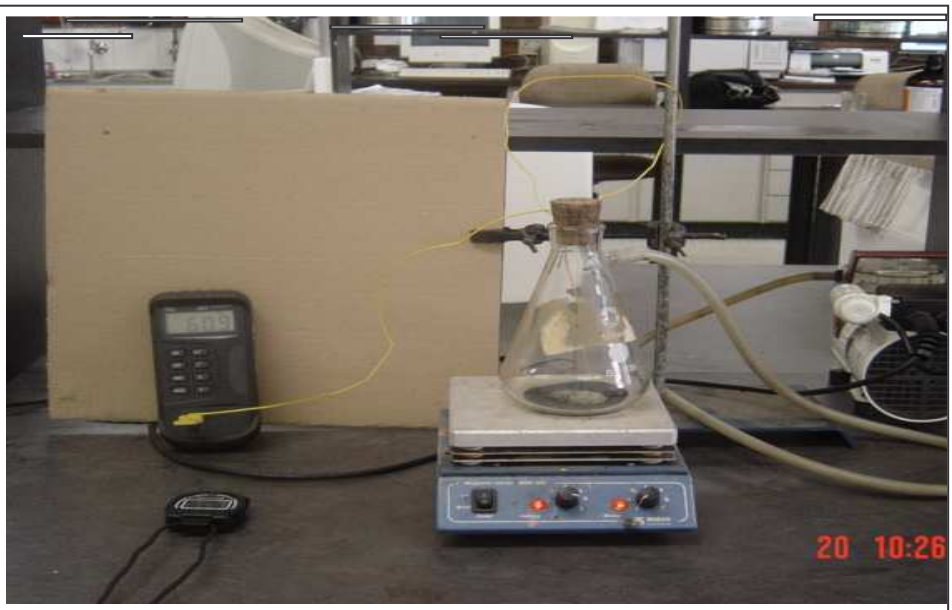

Fig. 6.3 Degassing Set-up.

6.6.3 Adsorption Experimental Procedure

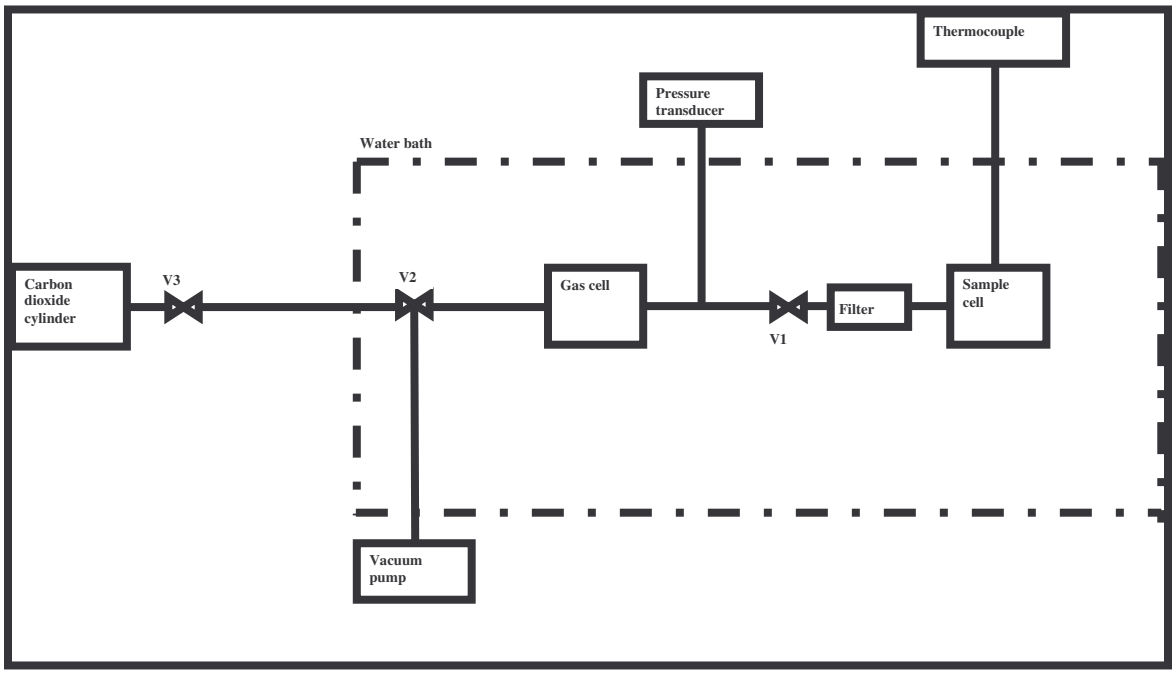

Fig. 6.4 Schematic Diagram of the Equipment Set-up.

The method described below is based on the schematic diagram above (Fig. 6.4).

i. After degassing a pre-weighed 2.0 g of the coal sample was quickly transferred to the sample cell and the adsorption chamber was tightly closed. The whole system is then evacuated to ensure that there are no gasses in the whole system before adsorption, and to establish a defined starting point.

ii. System volume

The internal volume of the gas cell V_{cell} = 50 cm^3.

The sample cell internal volume $V_{sample,cell}$ = 50 cm^3

The void volume is the space occupied by the gas

The void volume i.e. the volume not occupied by the sorbent is

$V_{sample,cell} = V_{sample} + V_{void}$ …….. ……6.3

iii. The sample cell is isolated from the rest of the system by closing valve V1.

iv. A certain amount of carbon dioxide is admitted into the gas cell by opening valves V3 and V2 respectively. Valve V2 is closed as soon as the gas cell pressure reached 0.25 bar.

v. After closing the valve 30 seconds were allowed for pressure equilibration in the gas cell.

vi. The number of moles of gas admitted into the gas cell is calculated by using the Redlich-Kwong equation of state (6.4) based on the gas pressure, volume and temperature measurements.

An equation of state is a thermodynamic equation describing the state of matter under a given set of physical conditions. It provides a mathematical relationship between the system temperature, pressure, volume and internal energy. It is used to describe the properties of a gas (Perry et al., 1997).

The basic and simplest equation of state is the ideal gas law; this law can be applied for gas properties at low pressure and very high temperatures where the gas approaches an ideal state. In the ideal gas state there are no intermolecular forces. However, this equation becomes increasingly inaccurate at higher pressures and lower temperatures because under these conditions intermolecular forces are present. Gases which exist under these non ideal conditions are called real gases. A number of equations of state have been developed to predict the properties of a real gas. At present, there is no single equation of state that accurately predicts the properties of all substances under all conditions.

The Redlich-Kwong equation (Perry et al., 1997) was chosen for this purpose as it is the most widely used equation of state for real gases.

$$P = [RT/ Vm - b] - [a/\sqrt{T}Vm(Vm+b)] \quad \text{.....} \quad \text{.....} \quad 6.4$$

$$a = 0.4278\, R^2 Tc^{2.5}/Pc$$

$$b = 0.0867\, RTc/Pc$$

The Redlich-Kwong equation of state is adequate for calculation of gas phase properties when the ratio of the pressure to the reduced pressure is less than about one-half of the reduced temperature. The system temperature used was the critical temperature for carbon dioxide hence Tr/2 is 0.5000.

$$Pr < (1/2)Tr$$

$$Pr = (P/Pc)$$

Tr = (T/Tc)

Table 6.5 Ratio of Pr to Tr.

P (bar)	Pc (bar)	Pr		Tr/2 = (T/Tc)
0.25	73.83	0.003386	<	0.500000
1.75	73.83	0.023703	<	0.500000

Table 6.5 shows that the reduced pressure for the upper and lower limit of the gas pressure is less than half of the reduced temperature; hence the equation can be used to give a good prediction of the system properties.

$V_{void} = n(ZRT/P)$ …….. 6.5

vii. Valve V1 is opened and carbon dioxide is admitted into the sample cell.

viii. In order to monitor the establishment of equilibrium, several pressure measurements were recorded every 2 minutes until the difference for three subsequent measurements was 0.0002 or less.

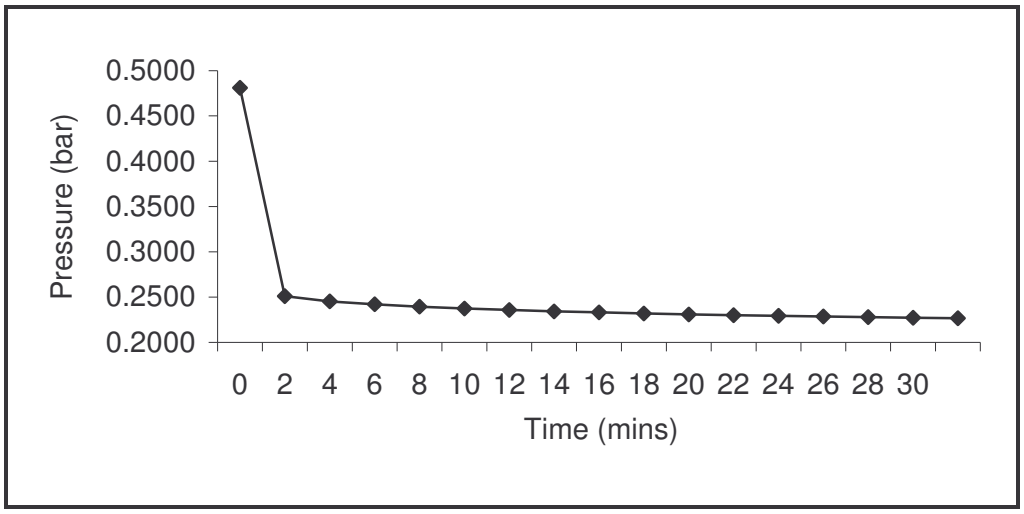

Fig. 6.5 Attainment of Equilibrium.

Fig. 6.5 shows the establishment of equilibrium for the gas adsorption process. The high pressure peak represents the initial gas cell pressure when gas is admitted into the system. When valve V1 is opened the pressure drops by a

factor of 0.47 due to the volume expansion as the gas occupies more space; this usually takes 30 seconds to equilibrate. Further pressure drop is due to adsorption of gas onto coal; this is represented by the rest of the pressure measurements.

ix. After equilibrium was achieved the system temperature and pressure were recorded and the equation of state was used to calculate the number of moles of gas remaining in the gas phase.

Mass balance on carbon dioxide gas molecules

$$n_{gascell} = n_{void} + n_{adsorbed} \quad \text{..... 6.6}$$

Gas volume (Fig. 6.6)

$$V_{gascell} = V_{void} + V_{adsorbed} \quad \text{.....6.7}$$

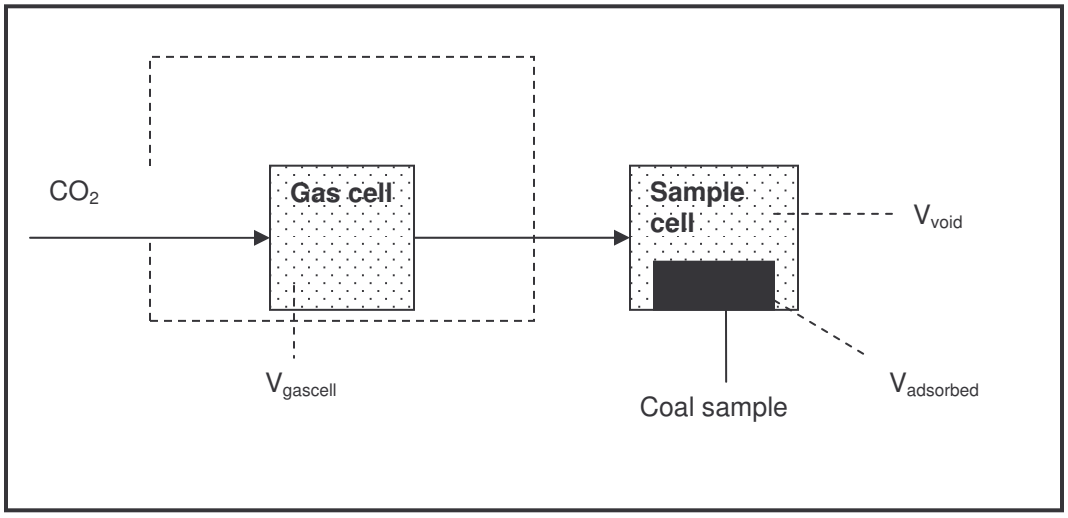

Fig. 6.6 Mass balance of CO_2 in the system.

The volume of gas in the system before adsorption is calculated using the Redlich-Kwong equation of state (equation 6.4).

x. The process was repeated again by closing valve V1 and following steps iii to step ix, to obtain 0.50 bar, 0.75 bar, 1.00 bar, 1.25 bar and 1.50 bar pressure in the gas cell.

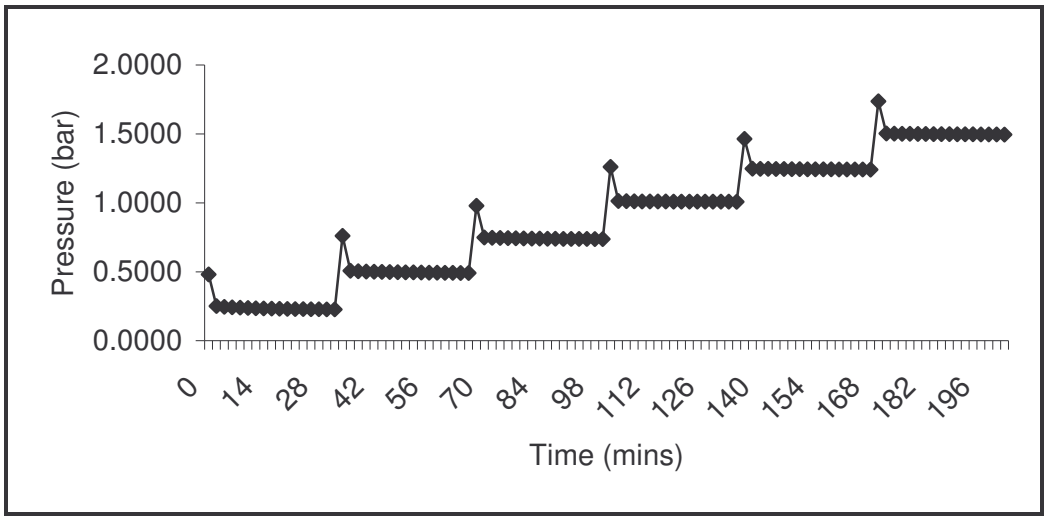

Fig. 6.7 Pressure-step graph.

The graph above shows the attainment of equilibrium at different initial gas cell pressures.

xi. The cumulative quantity of gas introduced through the gas cell into the previously evacuated sample cell is evaluated by summing up the quantities introduced into each step.

6.7 SUMMARY

The adsorption experimental procedure follows the schematic diagram given in Fig. 6.1. The table below summarises the results of the key sample characteristics used in this study.

Table 6.6 Summary of the Key Sample Characterisation Results.

Sample ID	Vitrinite (%)	Inertinite (%)	RoVmr (%)	Volatile Matter (%)	Mineral matter (%)	Micropore Surface Area (m^2/g)
Sample 1	8.00	73.4	0.72	33.85	9.4	-
Sample 2	92.0	0.4	0.69	35.95	3.2	-
Sample 3	2.60	3.6	0.69	16.32	93.0	36.06
Sample 4	65.6	32.4	2.21	12.88	2.0	164.41
Sample 5	42.2	52.8	2.21	12.62	5.0	-
Sample 6	9.60	66.2	2.21	12.73	24.2	110.52
Sample 7	76.8	8.6	0.69	31.79	12.2	76.78
Sample 8	28.6	58.4	0.72	32.53	8.8	-
Sample 9	4.2	3.0	0.69	15.97	92.6	-
Sample 10	92.8	6.8	2.28	11.85	0.4	297.54
Sample 11	67.6	25.4	2.28	11.32	7.0	-
Sample 12	4.2	78.8	0.69	31.43	14.4	-
Sample 13	0.4	19.8	0.69	17.25	79.6	-

CHAPTER 7: ADSORPTION EXPERIMENTAL RESULTS AND DISCUSSION

In Chapter 6 sample preparation, characterisation results as well as the adsorption procedure were discussed; in this chapter the results of the adsorption experiments are presented and discussed.

A total of 4 parent coal samples were used in the experiments originating from Witbank, Waterberg and Kwazulu Natal coalfields. These samples were separated into 13 fractions by using heavy media separation and the key characteristics of the samples are summarised in Table 6.6. Adsorption tests were conducted on the 13 samples. Fig. 7.1 shows the adsorption isotherms of the coal samples and a general description of the isotherms is given. In the latter sections detailed descriptions of the differences in the shapes of the isotherms is given.

Repeatability tests were also conducted on 4 selected samples to assess the suitability of the procedure used to conduct the tests.

The Langmuir model was used to fit the adsorption experimental data.

Summarised tables and figures are provided in the text; details are found in the Appendices.

7.1 ADSORPTION ISOTHERM

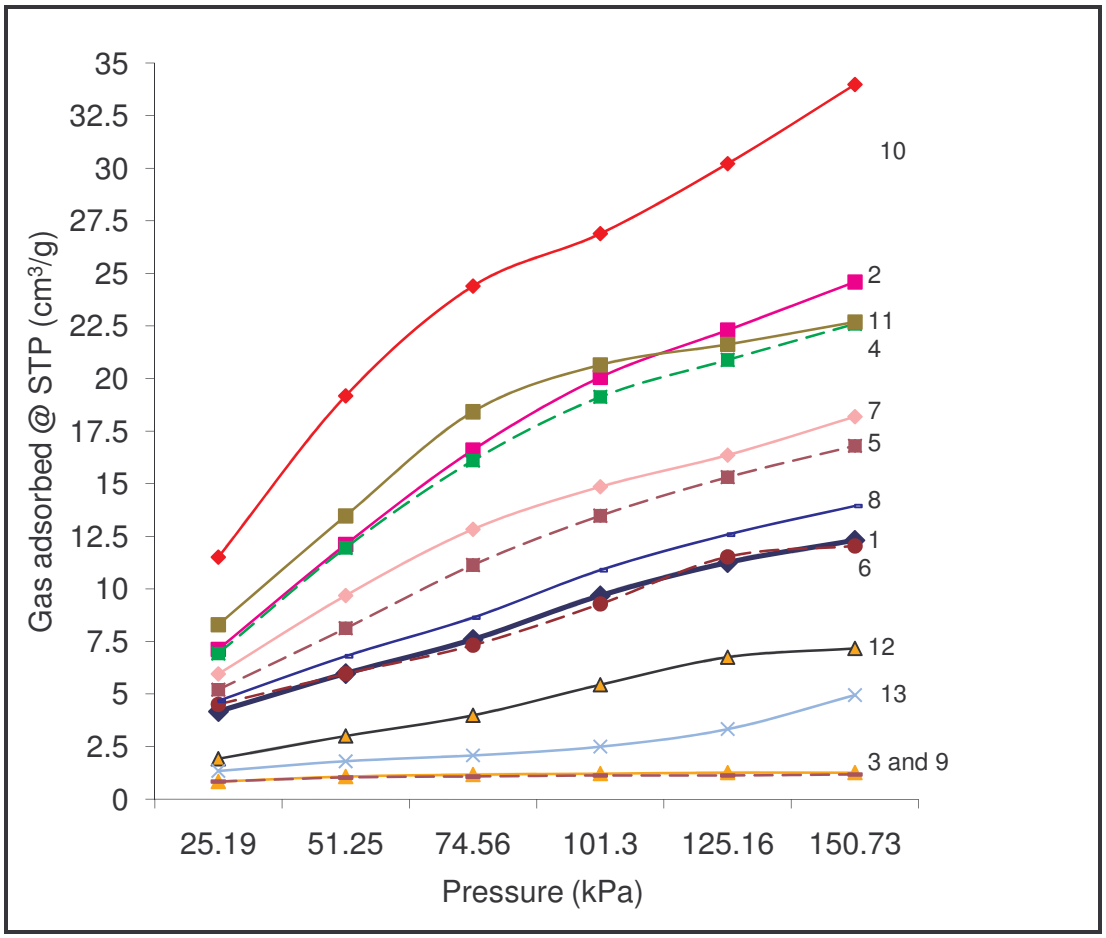

Fig. 7.1 Carbon Dioxide Adsorption Isotherms for the 13 Samples Tested.

The results of the adsorption measurements performed are shown in Fig. 7.1. The isotherms show distinct differences in the adsorption capacities and in the shapes of the isotherms.

The isotherms for samples 2, 4, 5, 7 and 10 show an almost linear increase up to the final pressure, with a reduction in gradient at higher pressures. These coal samples generally have a substantial amount of vitrinite (42.2 to 92.8 %), hence the gas adsorption is mainly vitrinite controlled. The isotherms do not seem to reach a limit suggesting that there were still some vacant sites for more adsorption to take place at higher pressures. The importance of vitrinite shall be discussed further in the chapter.

Isotherms for samples 1, 6, 8 and 12 show a linear increase at lower pressures and subsequently approach a limit as the isotherms flatten out at higher pressures. These samples are mainly composed of inertinite.

Adsorption isotherms for samples 3 and 9 show the lowest adsorption capacity and after the first adsorption step no substantial adsorption takes place as the isotherm remains level throughout the pressure steps. These samples were high ash samples, and the isotherms suggest that after the initial pore filling there were no more vacant sites for adsorption to take place.

7.2 THE EFFECT OF COAL COMPOSITION

The relationship between the composition of coal and its adsorption capacity has been studied by different researchers and different results have been obtained as discussed in section 4.5. In this study 13 samples were used and the graphs below show the relationship between coal composition and adsorption capacity of these coals.

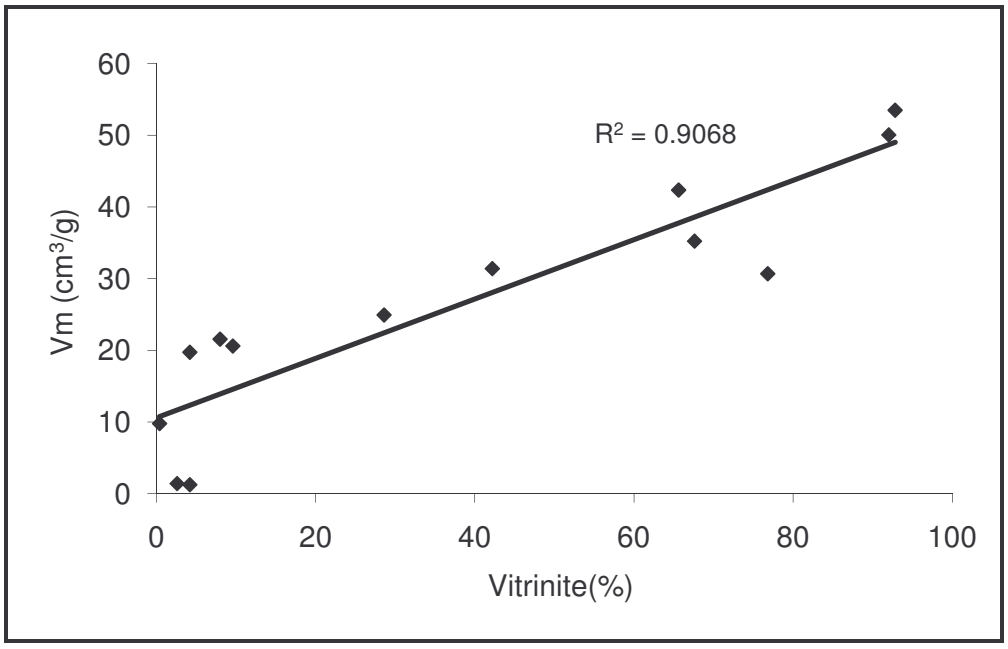

Fig. 7.2 Effect of Vitrinite Content on Carbon Dioxide Adsorption Capacity.

Fig. 7.2 suggests a very strong correlation between the vitrinite content of a coal sample and its adsorption capacity for the 13 samples studied. Samples with a low vitrinite content exhibit a low adsorption capacity while samples with a high vitrinite content exhibit a high adsorption capacity. The lowest adsorption capacities obtained were 1.42 cm^3/g and 1.26 cm^3/g and these correspond to samples 3 and 9 whose vitrinite contents are 2.6 % and 4.2 % respectively. The samples with the highest adsorption capacities were samples 2 and 10. These samples have vitrinite contents of 92.0 % and 92.8 % respectively and their adsorption capacities are 50.06 cm^3/g and 53.50 cm^3/g. These results are in agreement with results obtained by Crosdale et al. (1997).

The adsorption of carbon dioxide gas onto coal is largely dependant on the pore size of the coal sample. According to Stefanska (2005), for coals of the same rank that is isorank coals, micropores tend to predominate in vitrinite while meso and macro pores are predominant in inertinite. Gas adsorption in coal has been found to occur mainly on the surface of micropores because the micropore surface area is very large (Saghafi et al, 2007). Since vitrinite is mainly made up of micropores, it is therefore expected to provide a very large surface area for gas adsorption and thus adsorb more gas. The strong correlation that was obtained in the experimental work carried out, confirms that the vitrinite-rich coal samples used provided a higher surface area for gas adsorption, hence more gas was adsorbed in these samples.

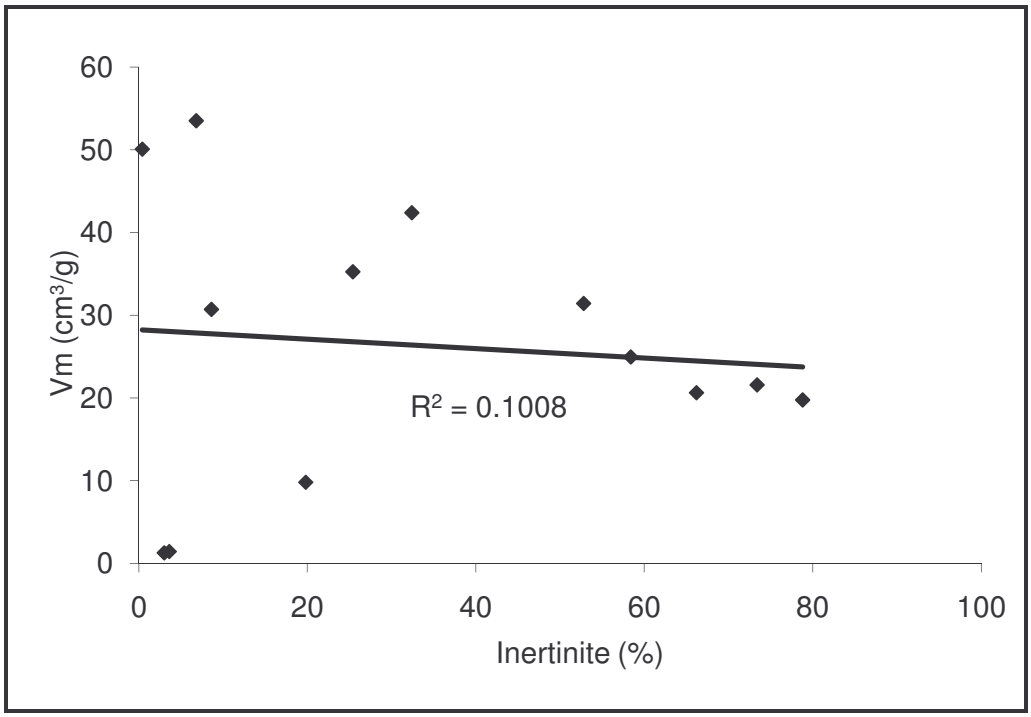

Fig. 7.3 Effect of Inertinite Content on Carbon Dioxide Adsorption Capacity.

Fig. 7.3 above is a plot of inertinite content against adsorption capacity for the 13 samples used in the study. The graph shows a very weak relationship between these two parameters. The inertinite component of a coal sample is mainly composed of mesopores and macropores. According to studies conducted by Saghafi (2007) gas adsorbed in mesopores and macropores accounts for less than 5 % of the total gas adsorbed in coal. The studies conducted therefore confirm that the inertinite component of coal has very little influence on the gas adsorption capacity.

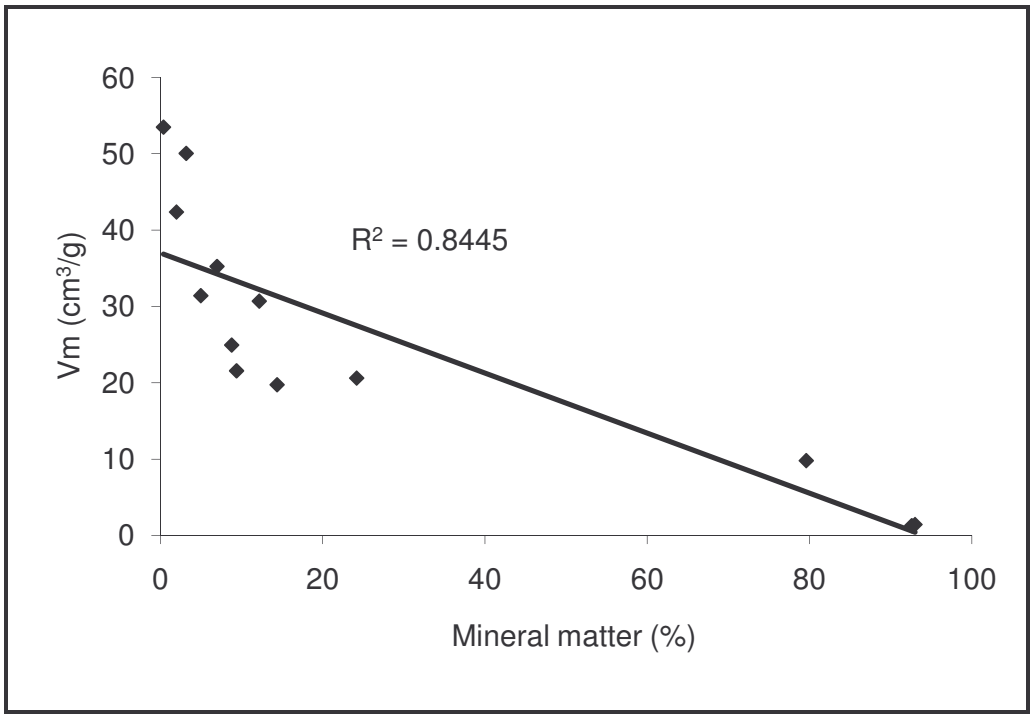

Fig. 7.4 Effect of Mineral Matter Content on Carbon Dioxide Adsorption Capacity

Fig. 7.4 above shows the relationship between mineral matter content on the adsorption capacity of coal. A fairly strong negative correlation exists between mineral matter content and adsorption capacity. The graph shows that higher adsorption capacities were obtained in samples with very low mineral matter content while samples with high mineral matter content had very low adsorption capacities. This proves that gas adsorption occurs mainly on the organic surfaces of coal and the presence of mineral matter reduces the adsorption capacity of a coal sample.

The isotherms in the Figs 7.5 to Fig 7.7 below show the effect of coal composition in isorank coals.

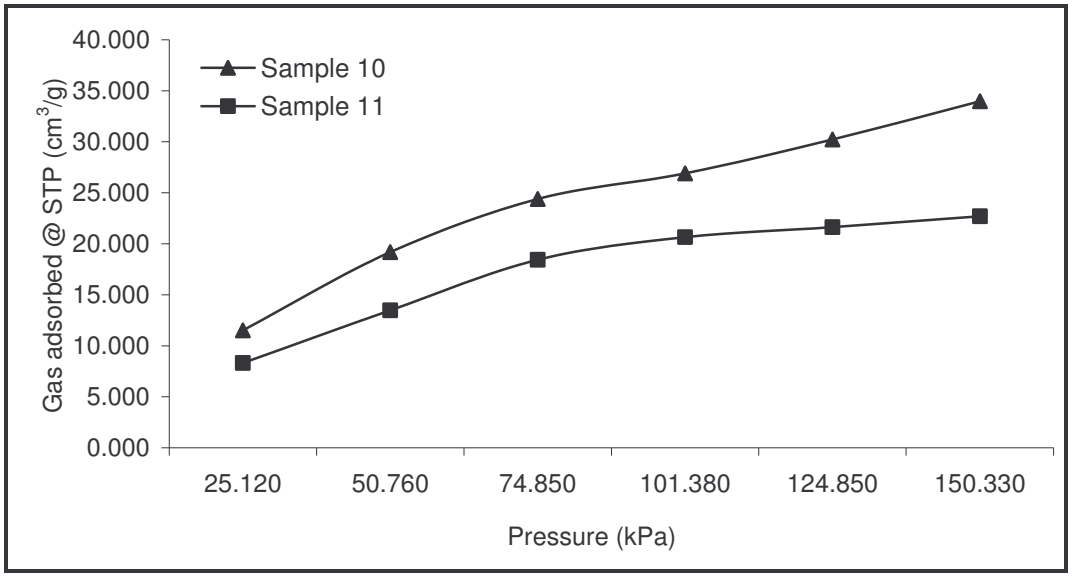

Fig. 7.5 Effect of Maceral Composition of High Rank C Coal Samples ex- KZN Sample A.

Fig. 7.5 confirms the relationship between vitrinite content and adsorption capacity for isorank coals. The two coal samples, that is, samples 10 and 11, are the float and sink fractions obtained from the heavy media separation of a high rank C parent sample from the Kwazulu Natal coal field, with a vitrinite reflectance of 2.28 %.

Sample 10 (float fraction) reported a vitrinite content of 92.8 % and its adsorption capacity is 53.5 cm^3/g; sample 11 (sink fraction) had a vitrinite content of 67.6 % and an adsorption capacity of 35.24 cm^3/g. A 25 % difference in the vitrinite content caused a reduction of the adsorption capacity from 53.5 to 35.24 cm^3/g which is 35 % of 53.5 cm^3/g. This result shows that when modeling carbon dioxide sequestration it is important to consider the vitrinite content as this has a profound effect on the quantity of carbon dioxide that can be stored.

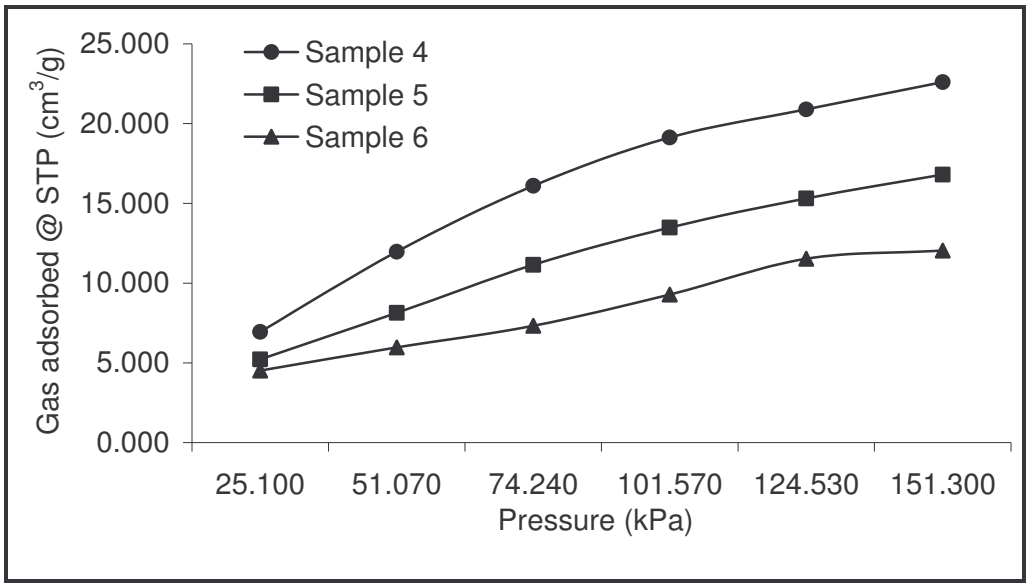

Fig. 7.6 Effect of Maceral Composition of High Rank C Coal Samples ex-KZN Sample B.

Fig. 7.6 presents the adsorption isotherms of samples 4, 5 and 6. These isorank samples are fractionation products of heavy media separation of a high rank C sample with a vitrinite reflectance of 2.21 %.

Sample 4 is the float fraction with a vitrinite content of 65.6 %, sample 5 is the middlings fraction with a vitrinite content of 42.2 % and sample 6 is the sink fraction with a vitrinite content of 9.6 %. The variation in the vitrinite led to different adsorption capacities that are 43.27, 31.41 and 20.61 cm^3/g respectively (Table 7.1). A 35 % reduction in the vitrinite content for samples 4 and 5 resulted in a 25 % reduction in the adsorption capacity.

For samples 5 and 6 a reduction of vitrinite content by 77.3 % resulted in a 34.4 % reduction of the adsorption capacity. The adsorption capacity of sample 6 is much higher than expected, this suggests that the although the inertinite content does not in general have an effect on carbon dioxide adsorption as shown in Fig. 7.3, this might not be true for all coal samples. Studies conducted by Karacan and Mitchell (2003) report that inertinite adsorbs more carbon dioxide than vitrinite. Although this might not be true for sample 6, which shares the

same parent coal as samples 4 and 5. The inertinite in these samples could be playing a role in the adsorption of carbon dioxide.

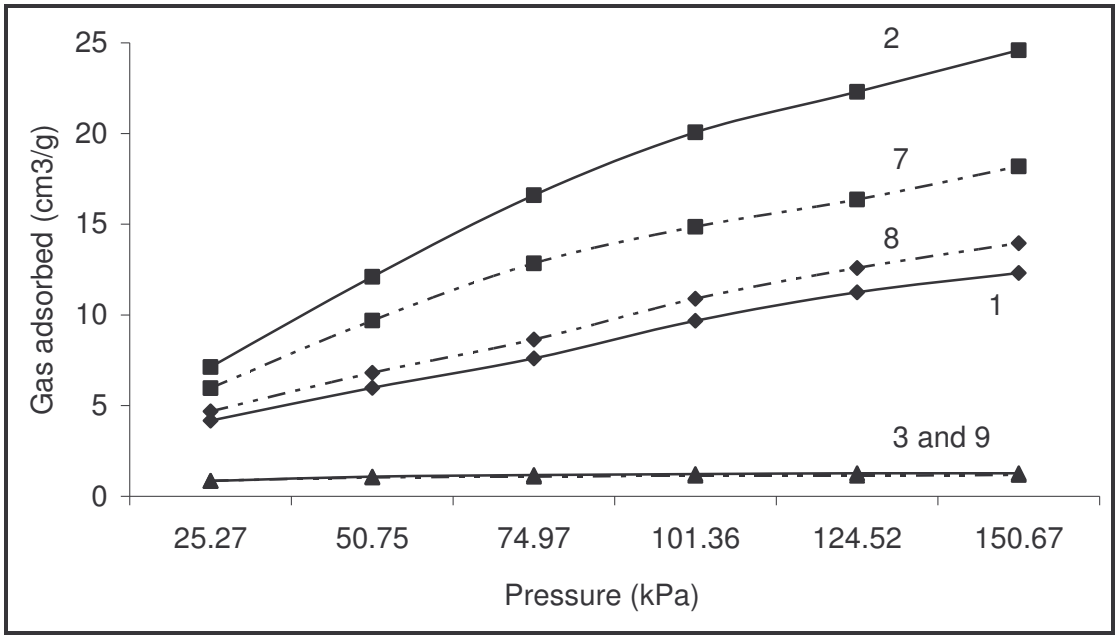

Fig. 7.7 Effect of Maceral Composition of Medium Rank C Coal Samples ex-Witbank and Waterberg.

The isotherms shown in Fig. 7.7 are for medium rank C coal samples with vitrinite reflectances of 0.69 and 0.72 %. From the graph it can be seen that the isotherms are divided into three parts, this division is a result of the sample composition.

The two top isotherms correspond to samples 2 and 7 which are both vitrinite rich samples with vitrinite contents of 92.0 and 76.8 % respectively. These samples are both float fractions obtained through heavy media separation of a Waterberg sample. Analyses of the results shows that a vitrinite difference of 16 % resulted in a 39 % reduction in adsorption capacity. This reduction is much higher the adsorption reductions obtained with high rank C coal samples discussed above. This shows that the effect of vitrinite content is much higher in medium rank coals than in high rank coals. This is due to the fact that although coalification results in more formation of micropores, the micropores formed during vitrinite formation account for a greater percentage of micropores in coal.

Samples 1 and 8 correspond to the second set of isotherms shown in Fig. 7.7. These samples are inertinite rich samples originating from the Witbank sample with a vitrinite reflectance of 0.72 %. Sample 1 with a higher inertinite content of 73.4 % has a lower adsorption capacity of 21.56 cm^3/g while sample 8 has an inertinite content of 58.4 % and an adsorption capacity of 24.94 cm^3/g. This shows that the inertinite component of this coal sample does not have much effect on the adsorption capacity as shown in Fig. 7.3.

Samples 3 and 9 correspond to the last set of isotherms, these two samples are mineral matter rich with mineral matter contents of 93.0 % and 92.6 % respectively. Most of the adsorption took place during the first and second pressure steps probably filling the micropores in the vitrinite component of the sample and nothing was adsorbed at higher pressures since the micropore surface was small and therefore there were no more vacant sites.

7.3 EFFECT OF RANK

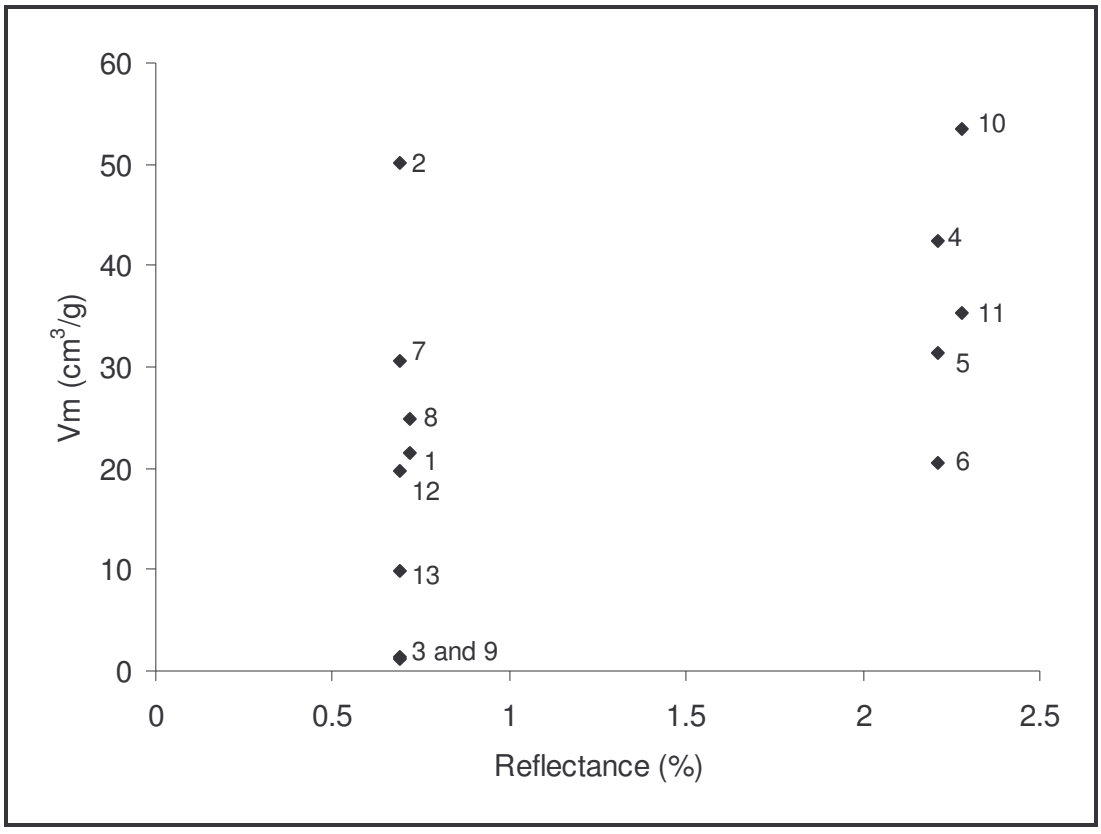

Fig. 7.8 Effect of Vitrinite Reflectance (Rank) on Adsorption Capacity.

Fig. 7.8 shows the relationship between the adsorption capacity and the coal rank. Crossdale (1997) stated that the gas adsorption of coal is closely related to its micropore development which is a function of coal rank and coal composition.

Micropore development in the vitrinite component of coal is strongly dependant on the rank of coal; higher rank vitrinite-rich coals tend to be more microporous than lower rank coals with a similar vitrinite composition. As mentioned before in section 7.1 gas adsorption mainly occurs on the surfaces of micropores and during coalification micropore development increases in the vitrinite component as coal rank increases.

Samples 2 and 10 have high vitrinite content of 92.0 and 92.8 % respectively. In the graph above (Fig. 7.8) it can be seen that sample 10 adsorbs more gas than sample 2 because it is a high rank coal. Sample 5 and 7 have similar adsorption capacities despite that fact they have different vitrinite contents of 42.2 and 76.8 % respectively. This can be explained by the fact that the vitrinite component of sample 5 has a higher micropore development because it is a high rank sample while sample 7 is a medium rank sample.

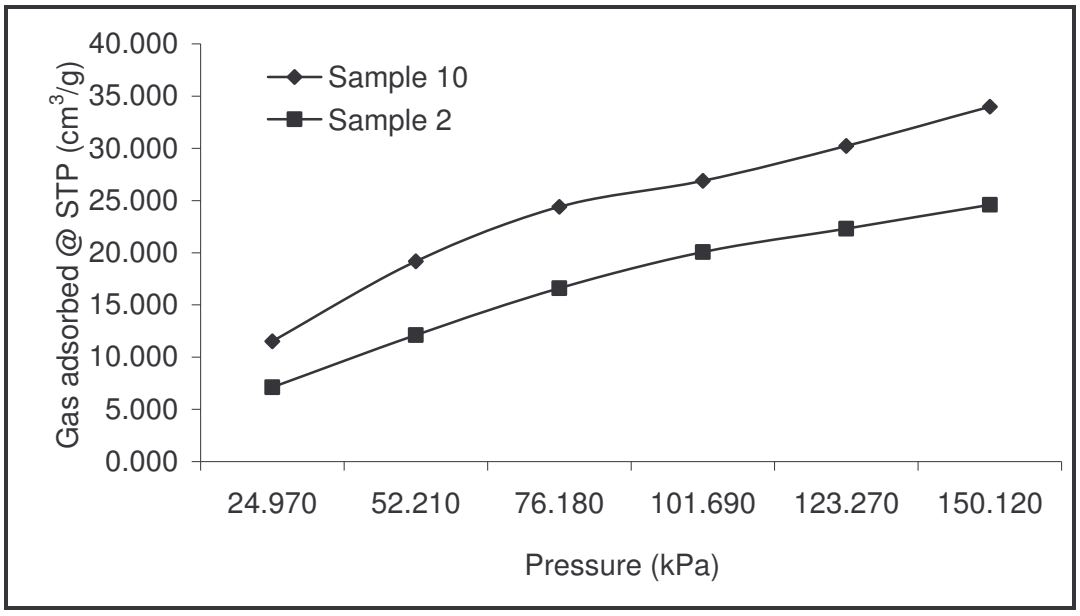

Fig. 7.9 Effect of rank on vitrinite-rich samples of different rank, ex-KZN Sample A and Waterberg.

Fig. 7.4 shows isotherms for two vitrinite-rich samples of different rank. Sample 10 is a high rank C coal with a vitrinite reflectance of 2.28 % while sample 2 is a medium rank C coal with a vitrinite reflectance of 0.69 %. Both samples have comparable vitrinite contents of 92.0 for sample 2 and 92.8 % for sample 10. The similarity in the sample compositions is a good basis for comparison in terms of the coal rank as this is the only variable between the two samples.

The high rank coal, that is, sample 10 has the highest adsorption capacity compared to sample 2. The adsorption capacity for sample 10 is 53.5 cm^3/g and the adsorption capacity for sample 2 is 50.06 cm^3/g. A closer look at the results shows that there is a difference of 6.4 % in the adsorption capacities of the two samples. This is a very small difference compared to the difference in the vitrinite reflectances of the two samples, that is, 2.28 % and 0.69 %. This suggests that the relationship between coal rank and adsorption capacity is not as strong as the relationship between the vitrinite content and adsorption capacity, as discussed in Figs. 7.5 and 7.6.

7.4 SUITABILITY OF THE LANGMUIR MODEL

The Langmuir adsorption model is widely used for the assessment of gas adsorption onto coal (Siemons and Busch, 2007). This model describes the dependence of the surface coverage of an adsorbed gas on the pressure of the gas above the surface at a fixed temperature. The Langmuir type equation 4.1 derived by Osborne (2008) was used for the assessment of the adsorptive capacity:

$$Vads = \frac{K_L P Vm}{1 + K_L P} \quad \ldots\ldots 4.1$$

Equation 4.1 can be written in the form given below

$$\frac{P}{Vads} = \frac{P}{Vm} + \frac{1}{K_L Vm} \quad \ldots\ldots 7.1$$

Graphs of (P/Vads) against P were plotted in Figs 7.11 to 7.14 for samples 10, 2, 1 and 9. Graphs for the rest of the samples can be found in Appendix B.

According to equation 7.1 a plot of (P/Vads) against P should yield a straight line with a gradient of (1/Vm) and intercept ($1/K_L Vm$).

Linear regression of the plots was used to obtain the gradient and intercept of the graph. The values obtained were used to calculate the monolayer capacity Vm and Langmuir constant K_L for each sample (Table 7.1)

The suitability of the Langmuir model in representing carbon dioxide adsorption onto coal was assessed by using the relative error. The relative error is defined as the standard deviation of measured and fitted values normalised to the Langmuir volume (Vm) (Saghafi et al, 2007).

The equation below was used to calculate the relative error.

$$r = \sqrt{\left(\Sigma \left(V_{exp} - V_{calc}\right)/\left(nV_m^2\right)\right)} \quad \ldots\ldots 7.2$$

r – relative error

V_{exp} - Volume of gas adsorbed - Experimental

V_{calc} - Volume of gas adsorbed - Calculated

n - number of measurement points

V_m - Langmuir volume

Table 7.1 Langmuir Parameters, relative error and correlation coefficient.

Sample I.D	Langmuir Parameters			
	Vm (m^3/g)	K_L (1/kPa)	r (%)	R^2
Sample 1	21.56	0.0082	2.3	0.9704
Sample 2	50.06	0.0063	0.9	0.9841
Sample 3	1.42	0.0622	0.8	0.9997
Sample 4	42.37	0.0078	0.6	0.9968
Sample 5	31.41	0.0075	0.8	0.9902
Sample 6	20.61	0.0088	3.0	0.9367
Sample 7	30.69	0.0094	0.6	0.9978
Sample 8	24.94	0.0080	1.8	0.9697
Sample 9	1.26	0.0844	0.9	0.9996
Sample 10	53.50	0.0108	1.2	0.9942
Sample 11	35.24	0.0129	1.8	0.9918
Sample 12	19.74	0.0038	1.3	0.8815
Sample 13	9.79	0.0045	5.3	0.6149

Table 7.1 above gives the Langmuir parameters as well as the relative error r and the correlation coefficient for each plot of (P/Vads) against P. The Langmuir volume ranges between 1.26 and 53.50 cm^3/g, with the highest volumes corresponding to the high vitrinite samples 2 and 10. The least volumes were for the high mineral matter samples 3 and 9.

The relative error of the measurements is less than 5.0 % for all samples except sample 13. These levels are acceptable errors since the recommended level for gas content errors is less than 10 % (Saghafi A. et al, 2007).

The correlation between the measured gas adsorbed and the calculated was used to further confirm the validity of the Langmuir model. Equation 4.1 was used to calculate gas adsorbed and the two parameters were plotted and the

coefficient of correlation computed. Fig. 7.10 shows the relationship between the measured volume of gas adsorbed and the calculated volume. As it can be seen from the graph the correlation coefficient is 0.9991 which shows that it's a perfect fit. This therefore confirms that the Langmuir adsorption model is a perfect representation of the carbon dioxide gas adsorption onto coal at subcritical conditions.

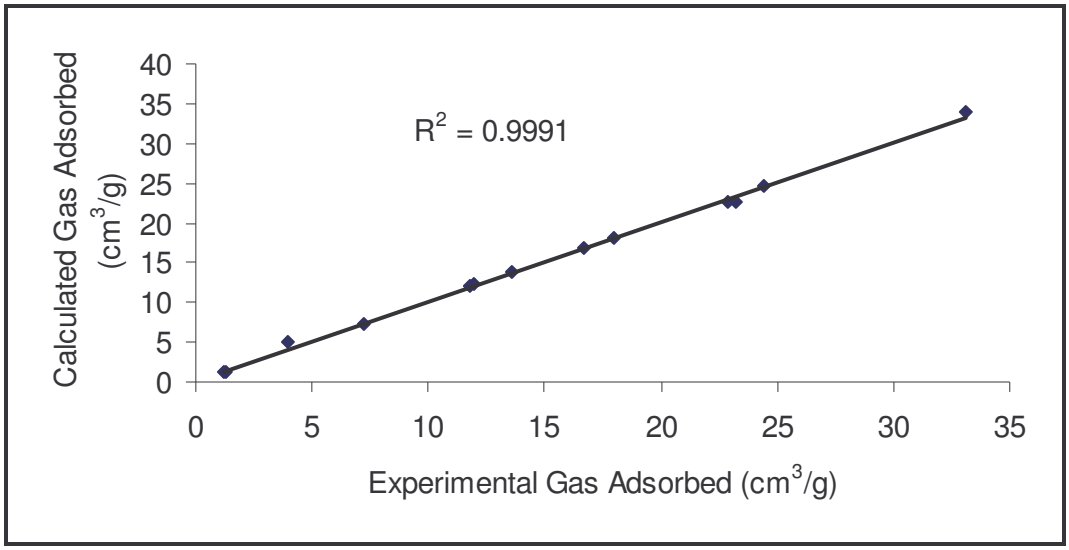

Fig. 7.10 Graph of calculated gas adsorbed vs experimental gas adsorbed.

Figs. 7.11 to 7.14 below are graphs of (P/Vads) versus P for 4 selected samples. The graphs show the Langmuir fit for the two samples with the highest adsorption capacity, a sample with medium adsorption capacity and another sample with the lowest adsorption capacity. The rest of the graphs can be found in Appendix B (Figs. B1 to B13)

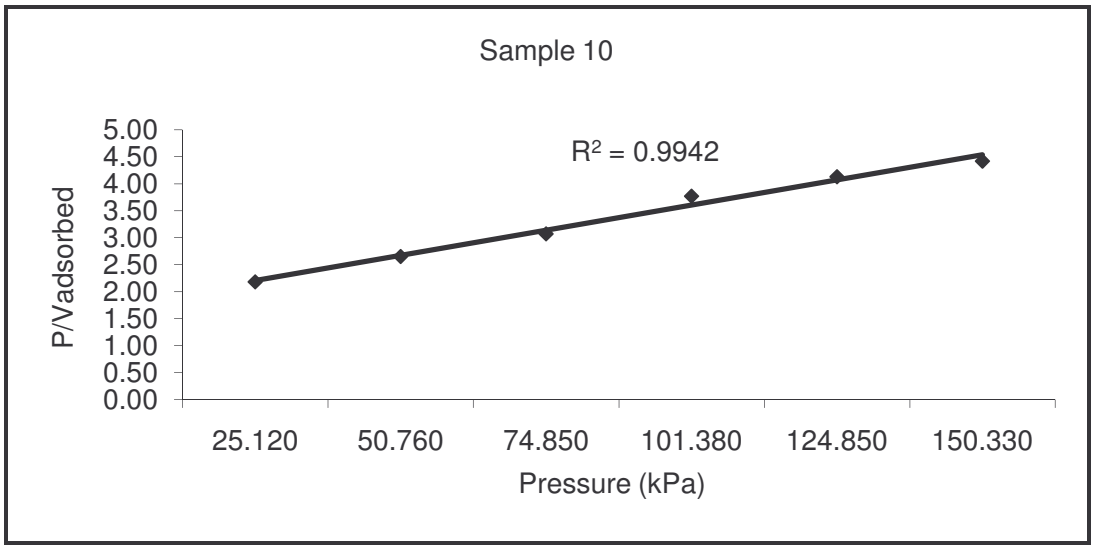

Fig. 7.11 Graph of (P/Vads) vs P for sample 10 (Vitrinite 92.8 %, RoVmr 2.28%)

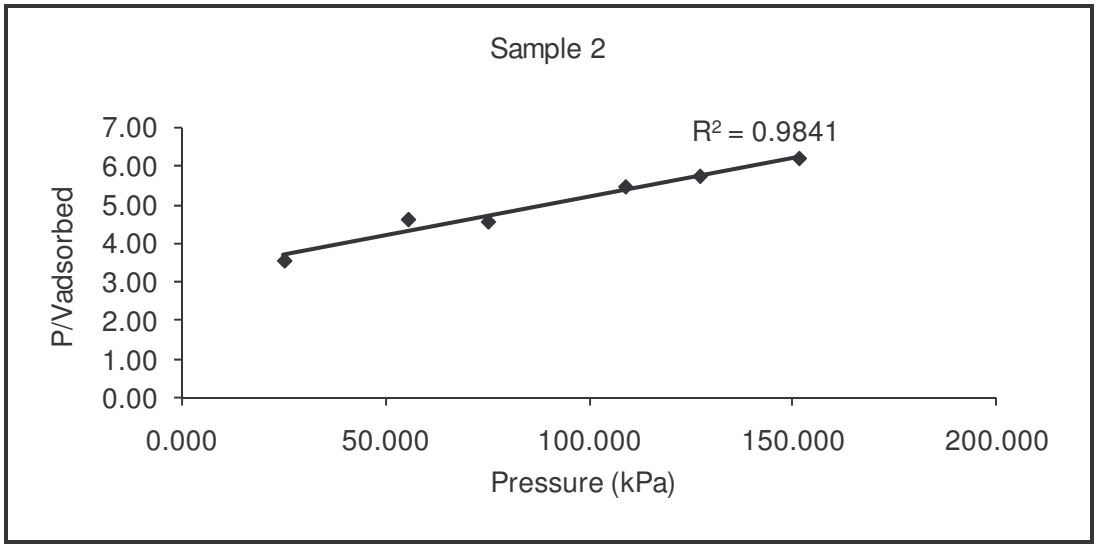

Fig. 7.12 Graph of (P/Vads) vs P for sample 2 (Vitrinite 92.0 %, RoVmr 0.69%)

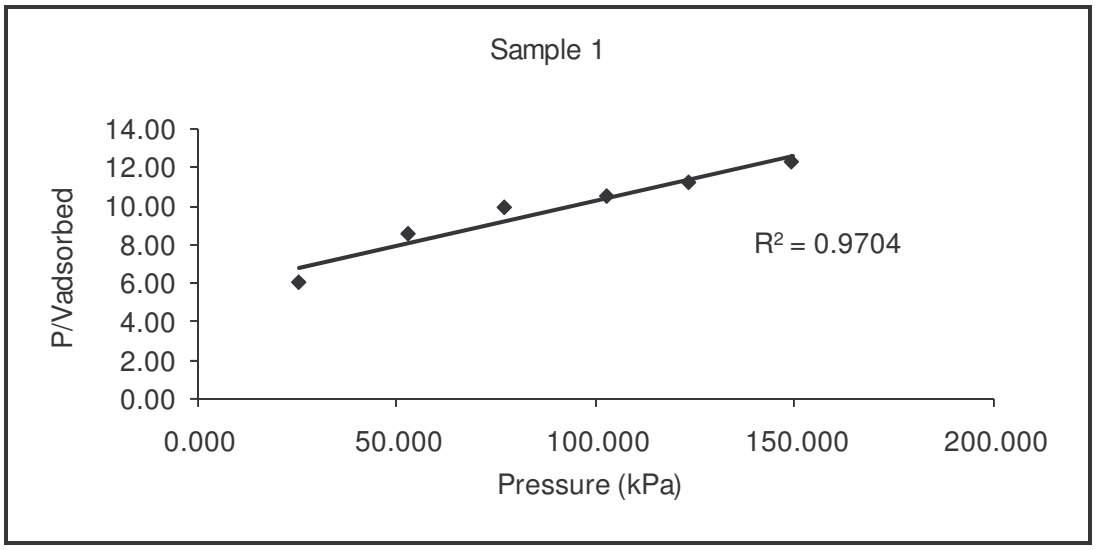

Fig. 7.13 Graph of (P/Vads) vs P for sample 1 (Inertinite 73.4 %, RoVmr 0.72%)

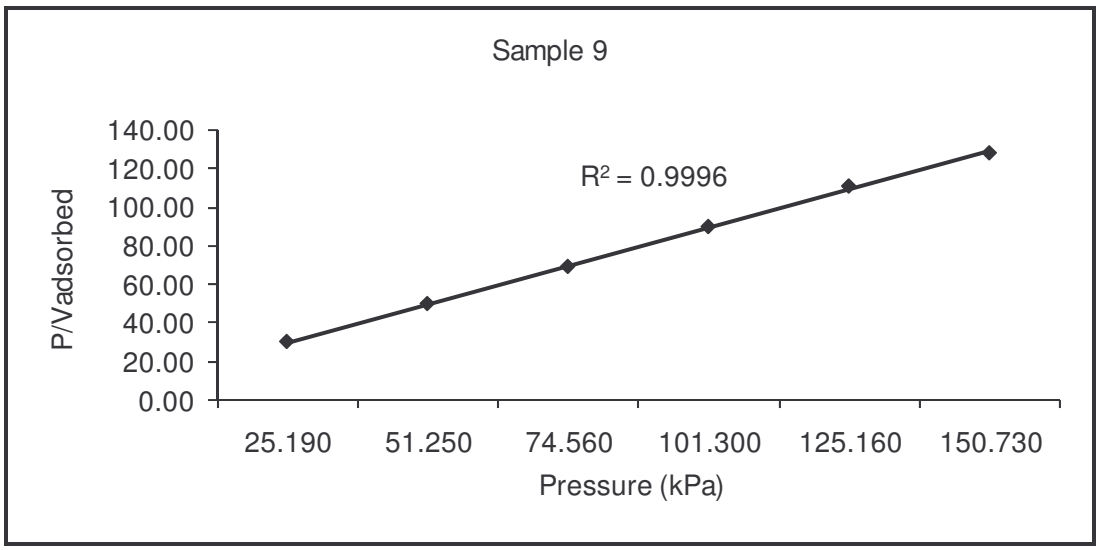

Fig. 7.14 Graph of (P/Vads) vs P for sample 9 (Mineral matter 92.8 %, RoVmr 0.69 %)

The graphs above present a very good correlation between the (P/Vads) and P, therefore confirming that the Langmuir adsorption model is a good model to be used for the coals studied at carbon dioxide subcritical conditions.

7.5 SURFACE AREA

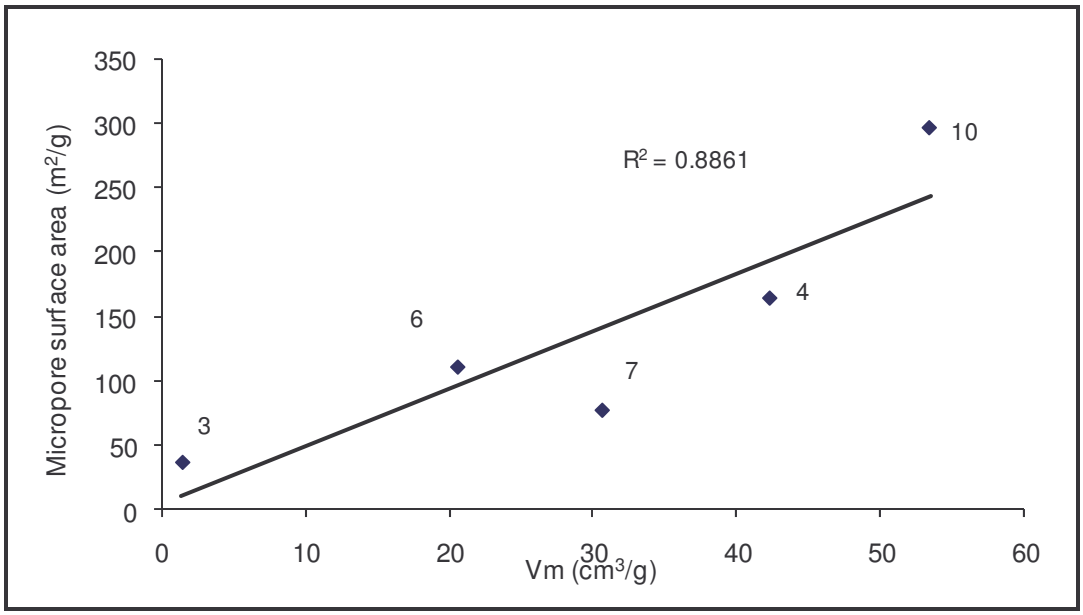

Fig. 7.15 Graph of Micropore surface area versus adsorption capacity.

The graph above presents the relationship between micropore surface area and the adsorption capacity. There appears to be a good correlation between adsorption capacity and micropore surface area. This confirms that adsorption mainly takes place on the surface of micropores as suggested by Saghafi (2007). A higher micropore surface area indicates that there are more vacant sites available for gas adsorption to take place.

Sample 10 is a vitrinite-rich and high rank coal (92.8 %, 2.28 %); therefore it has the highest micropore surface area. High rank and vitrinite rich coals have highly developed micropores (Stefanska, 2005). Sample 3 had the lowest micropore surface are because it has a very high mineral matter content (93.0 %) therefore a very small carbon content. Since carbon dioxide adsorption occurs mainly on micropores in the carbon matrix, the small quantity of fixed carbon available for adsorption limited the adsorption process resulting in a very low adsorption capacity of this sample.

7.6 REPEATABILITY TESTS

The graphs below show the original isotherm as well as the repeatability isotherm. The original isotherm is presented as Sample X and the repeat isotherm is presented as Sample X(2).

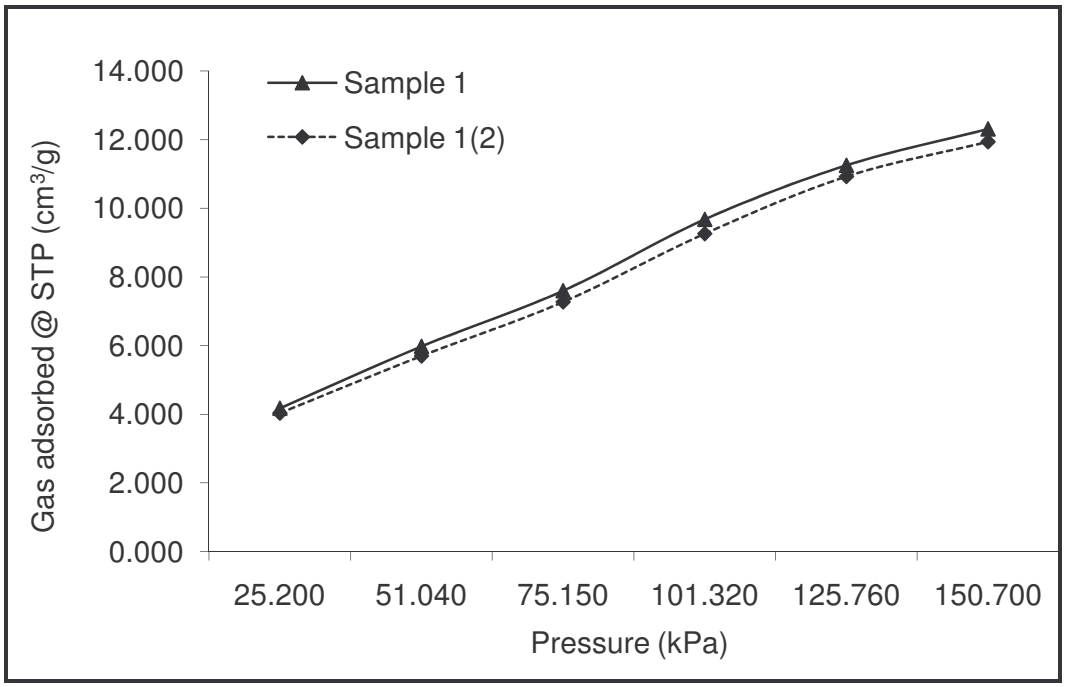

Fig. 7.16 Repeatability test isotherm for sample 1

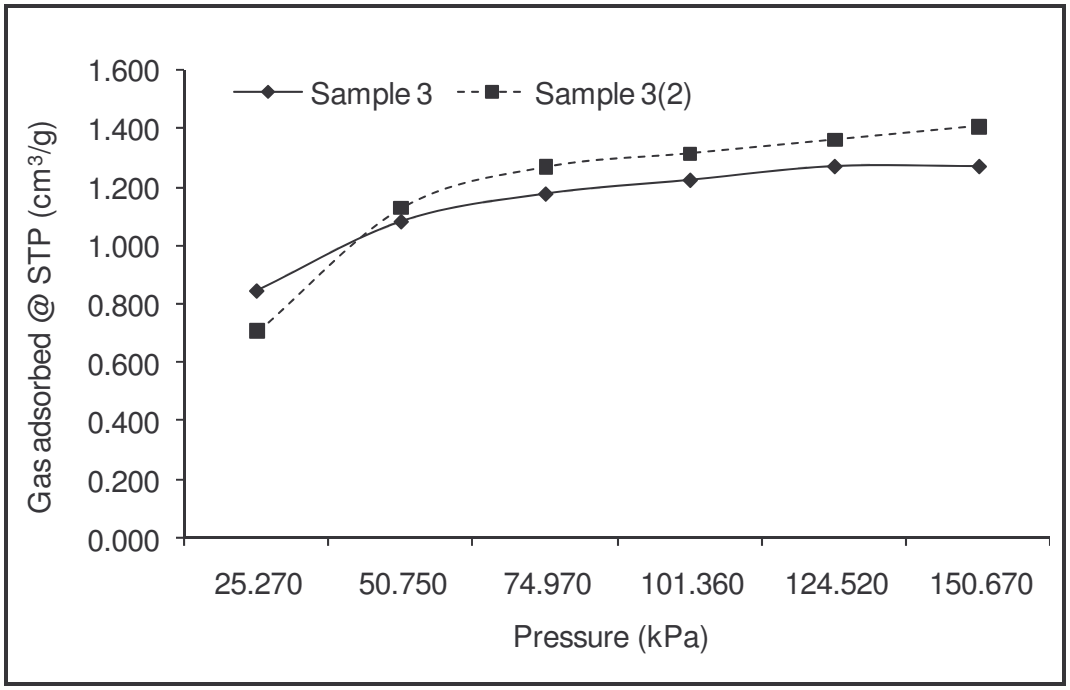

Fig. 7.17 Repeatability test for sample 3

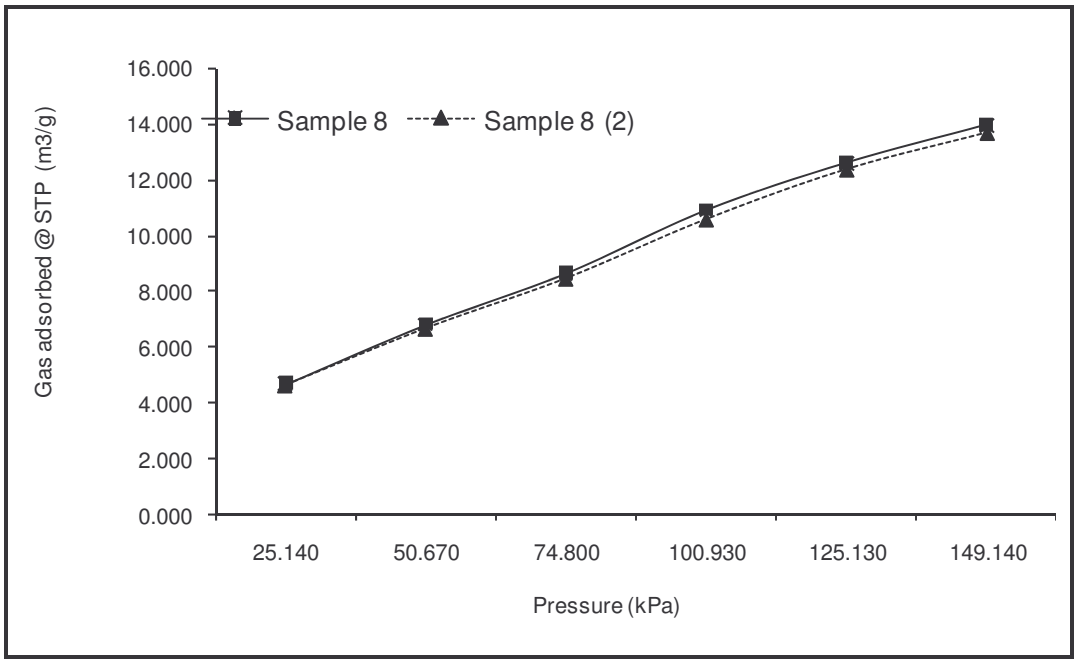

Fig. 7.18 Repeatability test for sample 8

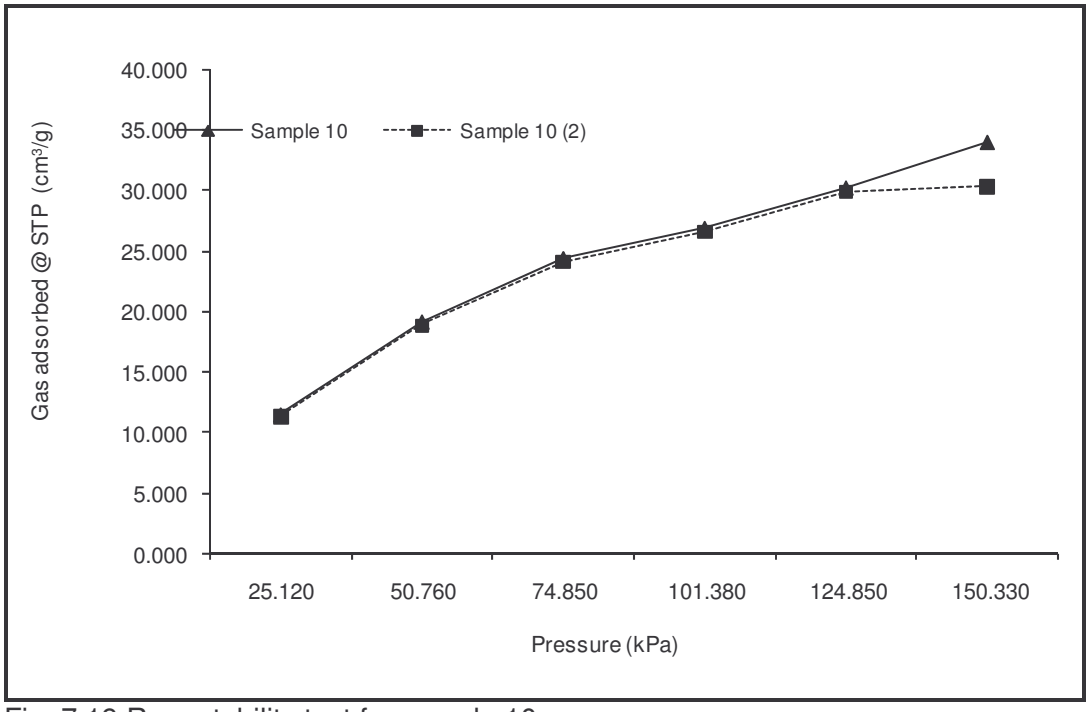

Fig. 7.19 Repeatability test for sample 10

Figs 7.16 to 7.19 show the results of repeatability tests. The tests were conducted on freshly prepared coal samples. The conditions for the adsorption, that is temperature and pressure, were maintained exactly the same as the initial measurements. The follow up tests for samples 1, 8 and 10 show nearly identical shapes of the measured isotherms.

The repeated adsorption isotherm for sample 3 has a shape similar to the initial measurement; however the adsorbed volumes differ at each pressure step. The pressure measurement was higher for the initial step but the subsequent pressure steps had much lower adsorbed volumes. This can be attributed to experimental errors, although all efforts were made to ensure that the conditions were exactly the same for both samples.

Despite the deviation in the repeatability tests for sample 3, it can be concluded that the repeatability tests were successful based on the results of the other 3 samples, therefore confirming that the procedure and equipment used for the measurements can be adopted for future tests as it is reliable.

The table below summarises the results of adsorption measurements conducted by other researchers as well as results from current work conducted.

Table 7.2 Langmuir volume for carbon dioxide adsorption onto coal reported in literature and present work.

Sample I.D	Pressure range (kPa)	Temperature (K)	Vm	Ref.
Argonne premium	0 - 5100	295	36.0 – 51.0 (mmol/g)	Busch et al., 2003
Bowen basin	-	-	28.0 – 44.0 (m^3/ton)	Crossdale et al., 1998
Sydney, Bowen, Argonne premium, Polish, New Zealand	0 - 16000	326	50.0 – 120.0 (kg/ton)	Day et al., 2008
Indiana basin	0 – 2800	290	19.5 – 24.6 (m^3/ton)	Mastalerz et al., 2004
Sydney basin	0 - 6000	300	41.0 – 72.0 (m^3/ton)	Saghafi et al., 2007
Tupton, Silesia, Warndt Brzeszcze, German creek Pocahontas, Selar Cornish	0 - 20000	318	1.30 – 4.02 (mmol/g)	Siemons and Busch, 2007
Witbank, Waterberg, Kwazulu Natal	0 - 150	303	1.20 – 54.0 (cm^3/g)	Present work

The table above presents a summary of the Langmuir volume obtained by different researchers on various coal samples. The current research shows that the adsorption capacity is within the same range as the adsorption capacities obtained by other researchers. The pressure range used was too low compared to pressures used by other researchers; therefore higher pressures need to be used in future.

7.7 SUMMARY

In this section the adsorption experimental results and discussion were given. The next chapter is on the conclusions drawn from the results and recommendations for future research.

CHAPTER 8: CONCLUSION AND RECOMMENDATIONS

In this chapter a conclusion is given based on the experimental results obtained. Recommendations on future work to be done are also given.

8.1 CONCLUSION

In this study a volumetric gas adsorption system was designed, constructed and used to conduct adsorption measurements on coal samples. The parent coal samples used were from the Witbank, Waterberg and Kwazulu Natal coalfields. Coals from different coal basins are difficult to compare since the coal basin evolution, that is the degree of metamorphism and the organic precursors, are different. This leads to variations in the composition of the coals of the same rank and therefore to variations in the adsorption capacity. In order overcome this problem each of the coal samples received was separated using heavy media separation to give vitrinite-rich samples, inertinite-rich samples and mineral matter–rich samples.

The adsorption isotherms were measured on either the float, sink and/or middling fractions of heavy media separation of the four parent samples. After the completion of each measurement the adsorbed volumes were normalised to the Australian standard P–T conditions (i.e. 20 ℃ and 101.325 kPa) (Saghafi et al., 2007). The Langmuir model was used to determine the adsorption capacity for each sample.

The highest adsorption capacity was obtained for the high rank vitrinite rich sample and the lowest adsorption capacity was obtained for the mineral matter rich sample. Correlation of the adsorption capacities with maceral composition showed a very strong correlation between vitrinite and the adsorption capacity. There seams to be no direct relationship between adsorption capacity and inertinite content. The presence of mineral matter was found to have a strong effect on the adsorption capacity. Samples with high mineral matter adsorbed the least gas volume while samples with low mineral matter adsorbed greater

volumes of gas. This confirms that gas adsorption takes place on the organic surface of coal and not the inorganic surface.

Coal rank was also found to be another factor that influences adsorption capacity. Studies of samples with similar maceral composition but with different rank showed that higher rank coals adsorb more than low rank coals. However the effect of vitrinite content is more profound than the effect of rank.

The Langmuir adsorption model was fit to the experimental data and was found to be a good fit. In general, the relative error was less than 5.0 %, therefore the Langmuir monolayer mechanism is a good representation of carbon dioxide adsorption at sub critical conditions.

Repeatability tests were conducted and these showed that the procedure and instrument used are reliable since adsorption isotherms of repeat samples were almost the same as the original sample.

The following conclusions can be drawn from this research work:

1. The vitrinite rich coals adsorb more carbon dioxide than inertinite rich coals.
2. A very strong correlation exists between vitrinite content and adsorption capacity.
3. There is no clear relationship between carbon dioxide adsorption capacity and inertinite content.
4. Mineral matter reduces carbon dioxide adsorption capacity.
5. High rank coals adsorb more carbon dioxide than low rank coals.
6. When modeling carbon dioxide sequestration it is important to consider the vitrinite content as this has a profound effect on the quantity of carbon dioxide that can be stored.
7. The Langmuir adsorption isotherm is an appropriate model for predicting gas adsorption in sub critical conditions.

Vitrinite is the key maceral that affects carbon dioxide adsorption onto coal. The hypothesis that inertinite adsorbs more coal than carbon dioxide was found not to be true, because most of the adsorption is occurring on the micropores found in

mainly in vitrinite. Coal rank also plays a role in adsorption capacity; high rank samples adsorb more carbon dioxide than low rank samples.

8.1.1 Contribution Of This Study

The design and construction of the volumetric equipment is a significant contribution that was achieved in this study, as this equipment can be used for other studies on gas adsorption.

The results of the experimental work conducted may be included in the database for carbon dioxide sequestration research in South Africa. The results showed that coal maceral composition and coal rank are very important factors to be considered when modeling carbon dioxide sequestration in coal seams.

Coal is a reservoir for natural gases and most of the gases are stored in the micropores. The results from the research work show that coal seams can be very good storage sites for anthropogenic carbon dioxide.

8.2 RECOMMENDATIONS

Deep unminable coal seams have pressures and temperatures which are well above the critical temperature and pressure that is 304 K and 73.8 bar. For the purposes of modeling storage capacities it is necessary to measure the adsorption properties of the coal under supercritical conditions which closely resemble conditions in deep coal seams (Day et al., 2007). This will require constructing more robust equipment that can withstand the high pressures.

Since coal exhibits variable chemical and physical properties it is necessary to conduct adsorption tests on coal seams targeted for storage purposes.

Dry coal samples were used for this study, but in application some coal seams are likely to be saturated with water. Hence more tests need to be conducted to determine the effect of water on the adsorption capacity of each coal maceral.

REFERENCES:

Alexander, M., 2005. From Kyoto to Khayelitsha. South Africa. Info. http://www.southafrica.info/about/sustainable/kuyasa-121205.htm

Barker, O.B., 1999. A Techno-Economic and Historical Review of the South African Coal Industry in the 19th And 20th Centuries.

Belmabkhout, Y., Frere, M., De Weireld, G., 2004. High Pressure Adsorption Measurements. A Comparative Study of the Volumetric and Gravimetric Methods. Measurement Science and Technology (15) pp 848 – 858.

Birol, F., van Hulst, N., 2006. World Energy Outlook. International Energy Agency Publications Service, Paris. http://www.worldenergyoutlook.org/2006.asp

BOM (Bureau of Meteorology), Australia, 2003. The Greenhouse Effect and Climate Change pp 74. http://www.bom.gov.au/info/GreenhouseEffectAndClimateChange.pdf

Braasch, G., 2008. Glaciers and Glacial Warming, Receding Glaciers. World View of Global Warming. Portland. http://www.worldviewofglobalwarming.org/pages/glaciers.html

Busch, A., Gensterblum, Y., Krooss, B.M., 2003. Methane and Carbon Dioxide Sorption and Desorption Measurements on Dry Argonne Premium Coals: Pure Components and Mixtures. International Journal of Coal Geology 55, pp 205-224.

CARMA (Carbon Monitoring for Action), 2007. 5 Highest Carbon Dioxide Emitting Power Companies in the World. http://carma.org/company

Chemical Technology, July 2006. Carbon Dioxide Utilisation and Storage. Air Emissions. Chemical Technology, Crown Publications, Johannesburg.

Coulson, J.M., Richardson, J.F., Sinnott, R.K., 1991 Chemical Engineering Volume 6 Design. Pergamon Press, Oxford.

Crawford, F., 2007. 10 Worst Polluted Cities. http://rcrawford79.files.wordpress.com/2007/09/air-pollution-systems.jpg

Crosdale, P.J., Beamish, B.B., Valix, M., 1997. Coalbed Methane Sorption Related to Coal Composition. International Journal of Coal Geology 35, pp 147-158.

Cui, X., Bustin, R.M., Dipple, G., 2004. Selective Transport of CO2, CH4, and N2 in Coals: Insights from Modeling of Experimental Gas Adsorption Data. Fuel, 83 pp 293-303.

Day, S., Duffy, G., Sakurovs, R., Weir, S., 2007. Effect of Coal Properties on CO_2 Sorption Capacity under Supercritical Conditions. International Journal of Greenhouse Gas Control 72.

DEAT (Department of Environmental Affairs and Tourism), 2006. South Africa Environment Outlook. A report on the state of the environment. Executive summary and key findings. Department of Environmental Affairs and Tourism, Pretoria. 42pp. http://soer.deat.gov.za/docport.aspx?m=97

DME (Department of minerals and energy), 2003. White Paper on the Renewable Energy Policy of the Republic of South Africa. Department of minerals and energy, Pretoria.

DMP (Division of Mine Permits), 2008. Where does coal come from? Division of Mine Permits, Kentucky. http://www.minepermits.ky.gov/miningeducation/coal_formation.htm

Engelbrecht, A., Golding, A., Hietkamp, S., Scholes, B., 2004. The Potential for Sequestration of Carbon Dioxide in South Africa. CSIR (File 86DD/HT339), Pretoria. http://www.dme.gov.za/pdfs/energy/coal/carbon_dioxide.pdf

Eskom, 2007. Eskom Annual Report, Climate change. Eskom Holdings Ltd., Johannesburg. http://www.eskom.co.za/annreport07/annreport07/info_sheets/climate.htm

Falcon, R.M.S., 1986[a]. A Brief Review of the Origin, Formation, and Distribution of Coal in Southern Africa. Mineral Deposits of Southern Africa, pp 1879-1898.

Falcon, R.M.S., 1986[b]. Classification of Coals in Southern Africa. Mineral Deposits of Southern Africa, pp 1899-1921.

Flory, A., 2005. Legal Aspects of Storing CO_2. International Energy Agency Publication.

Francis, W., 1961. Coal; Its formation and Composition, 2nd ed. E. Arnold, London.

Handley, J.F., 2006. Global Warming & Climate Chaos - Health Tips for Planet Earth. Heart Spring. http://heartspring.net/global_warming_greenhouse.html

Houghton, J., 2004. Global Warming; The complete briefing 3rd ed. Cambridge University Press.

ICCP (International Committee for Coal and Organic Petrology), 1994[a]. The new vitrinite classification system. Fuel, 77 (5) pp 349-358.

ICCP (International Committee for Coal and Organic Petrology), 1994[b]. The new inertinite classification system. Fuel, 80 (2001) pp 459-471.

IPCC, 2007. Technical Summary in Climate Change 2007: The Physical Science Basis. Contribution of Working Group 1 to the Fourth Assessment Report of the Intergovernmental Panel on Climate Change. Cambridge University press, Cambridge.

(ISO 11760) International Organisation of Standardisation, ISO 11760, 2005 (E) Classification of coals.

(ISO 7404) International Organisation of Standardisation, ISO 7404, 1985 (E). Method of preparing coal samples.

(ISO 7404) International Organisation of Standardisation, ISO 7404, 1994 (E). Method of determining maceral group composition.

Jacobs, M., 2005. Carbon dioxide pressure- temperature phase diagram. Wikimedia http://commons.wikimedia.org/wiki/Image:Carbon_dioxide_pressure-temperature_phase_diagram.svg

Karacan, C.O., Mitchell, G.D., 2003. Behaviour and Effect of Different Coal Microlithotypes During Gas Transport for Carbon Dioxide Sequestration into Coal Seams. International Journal of Coal Geology 53, pp 201-217.

Karr, C., 1978. Analytical Methods for Coal and Coal Products Volume I, Academic Press, New York.

Kirk, R.E., Othmer, D.F., 1991[a]. Encyclopedia of Chemical Technology Vol.1, pp 493-524 4th ed. J. Wiley, New York.

Kirk, R.E., Othmer, D.F., 1991[b]. Encyclopedia of Chemical Technology Vol.5, pp 35-53 4th ed. J. Wiley, New York.

Kirk, R.E., Othmer, D.F., 1991[c]. Encyclopedia of Chemical Technology Vol.6, pp 423-489 4th ed. J. Wiley, New York.

Larsen, J., 9 October 2003. Record Heat Wave in Europe Takes 35,000 Lives Far Greater Losses May Lie Ahead. Earth Policy Institute. www.earth-policy.org/Updates/Update29.htm.

Levin, K., Pershing, J., 2006. Climate Science Major New Discoveries. World Resources Institute Issue Brief January 2007. http://www.wri.org/publication/climate-science-2006.

Marczewski, A.W., 2004. Carbon dioxide in air/water. http://www.adsorption.org/awm/utils/CO2.htm

Martin., S.C., 2008. Evaluation Matrix, Business Solutions. http://www.positive-way.com/business/evaluati.htm

Metz, B., Ogunlade, D., Heleen de, C., Manuela, L., Leo, M., 2005. Carbon dioxide Capture and Storage. IPCC Special Report. Cambridge University Press, Cambridge.

NCDC (National Climatic Data Centre), 2006. Global Surface Temperature Anomalies, National Climatic Data Centre. http://www.ncdc.noaa.gov/oa/climate/research/anomalies/anomalies.html

NETL (National Energy Technology Laboratory), 2008. Weyburn Carbon dioxide Sequestration project. Carbon Sequestration. National Energy Laboratory, Pittsburgh. http://www.netl.doe.gov/publications/factsheets/project/Proj282.pdf

Osborne, M., accessed 2008. Surface Science. Langmuir and BET Isotherms. Department of Chemistry, University of Sussex. http://www.sussex.ac.uk/Users/kaf18/SurfSci2.pdf

Pearce, F., 2007. But here is what they didn't tell us. New Scientist 10/02/2007 pp 6-9.

Perry, R.H., Green. D.W., Maloney, J.O., 1997. Perry's Chemical Engineers Handbook, 7th Ed. McGraw-Hill, New York.

Pringle, B., Eldridge, M., May 2007. The Twin Pillars of Sustainable Energy: Synergies between Energy Efficiency and Renewable Energy Technology and Policy. American Council for an Energy Efficient Economy. www.aceee.org/pubs/e074.htm

Rekacewicz, P., 2002. The Greenhouse Effect. UNEP/GRID-Arendal. http://maps.grida.no/go/graphic/greenhouse-effect.

Saghafi, A., Pinetown, K. L., Grobler, P., van Heerden, J. H., 2006. CO_2 Storage Potential of South African Coals and Gas Entrapment Enhacement due to Igneous Intrusions. International Journal of Coal Geology TSOP Special Publication.

Saghafi, A., Faiz, M., Roberts, D., 2007. CO_2 Storage and Gas Diffusivity Properties of Coals from Sydney Basin, Australia. International Journal of Coal Geology 70, pp 240-254.

Schlumberger, 2008. Carbon dioxide sources. Global Climate Change and Energy.

http://www.seed.slb.com/en/scictr/watch/climate_change/sources.htm

Siemons, N., Busch, A., 2007. Measurement and Interpretation of Supercritical Carbon dioxide Sorption on Various Coals. International Journal of Coal Geology 69 pp 229 – 242.

Stach, E., Mackowsky, M., Teichmuller, M., Taylor, G.H., Chandra, D., Teichmuller, R., 1982. Coal Petrology, 2nd ed. Gebruder Borntraeger, Berlin.

Stefanska, G.C., Zarebska, K., 2005. Sorption of carbon dioxide-methane mixtures. International Journal of Coal Geology 62, pp 211-222.

Thomas, T., Schmidt, S., Gerling, J.P., 2007. Lignite and hard coal: Energy suppliers for world needs until the year 2100 — An outlook. International Journal of Coal Geology 72 pp 1 – 14.

UIG (Universal Industrial Gases), 2003. Carbon Dioxide (CO_2) Properties, Uses, Applications CO_2 Gas and Liquid Carbon Dioxide. Universal Industrial Gases, Inc, Pennsylvania.

Van Wyk, J., Weidema, J., Fikela, N., 2006. Digest of South African Statistics. Department of Minerals and Energy, Pretoria. http://www.dme.gov.za/pdfs/energy/planning/2006%20Digest.pdf

Ward, C.R., 1984. Coal Geology and Coal Technology, Blackwell Scientific Publications, Melbourne.

Wills, B. A., 1992. Mineral Processing Technology – An introduction to the practical aspects of ore treatment and mineral recovery 5th ed. Pergamon Press, Oxford.

Yu, H., Zhou, G., Fan, W., Ye, J., 2006.Predicted CO_2 enhanced coal bed methane recovery and CO_2 sequestration in China. International Journal of Coal Geology 71 pp 345-357.

APPENDIX A: ADSORPTION RESULTS

Table A1.1 Sample 1- Adsorption Measurement Results

Initial Pressure (bar)	0.2520	0.5104	0.7515	1.0132	1.2576	1.5070
Final Pressure (bar)	0.2430	0.5065	0.7480	1.0087	1.2542	1.5047
Temperature (°C)	30.6	30.7	30.7	30.7	30.7	30.8

Table A1.2 Sample 1 - Volume of Gas Adsorbed Per Unit Mass

	Sample 1					
Pressure (kPa)	25.20	51.04	75.15	101.32	125.76	150.70
Gas adsorbed (cm^3/g)	4.18	5.98	7.60	9.68	11.25	12.31

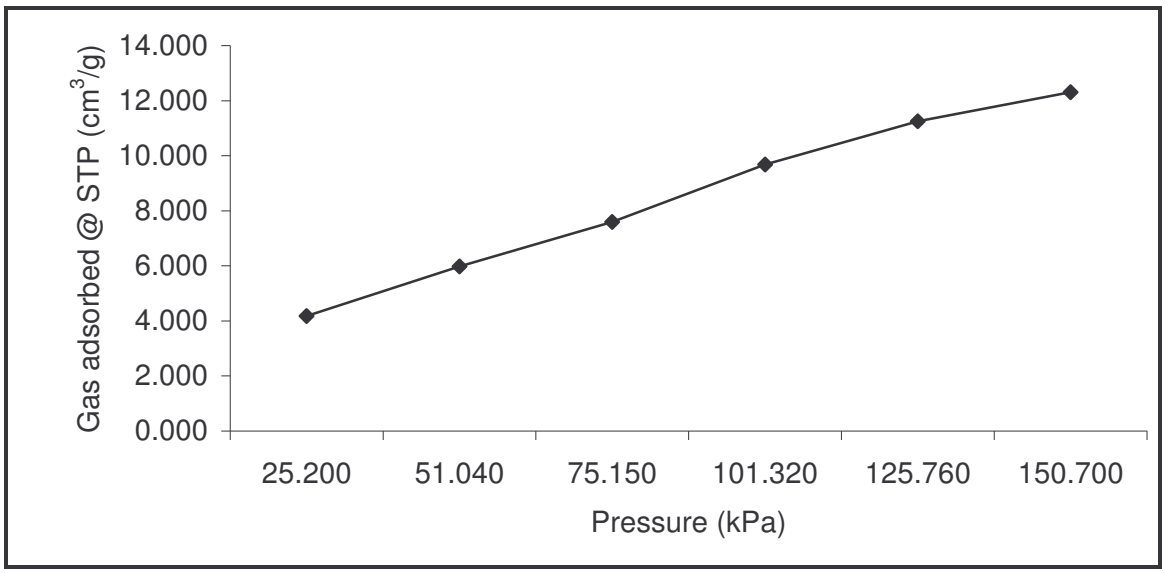

Fig. A.1 Sample 1- Volume of Gas Adsorbed Per Unit Mass Vs Pressure.

Table A2.1 Sample 2- Adsorption Measurement Results

Initial Pressure (bar)	0.2510	0.5552	0.7517	1.0891	1.2722	1.5156
Final Pressure (bar)	0.2359	0.5446	0.7421	1.0817	1.2674	1.5107
Temperature (^oC)	30.1	30.2	30.3	30.4	30.4	30.4

Table A2.2 Sample 2 - Volume of Gas Adsorbed Per Unit Mass

Sample 2						
Pressure (kPa)	25.10	55.52	75.17	108.91	127.22	151.56
Gas adsorbed (cm^3/g)	7.12	12.11	16.61	20.06	22.31	24.59

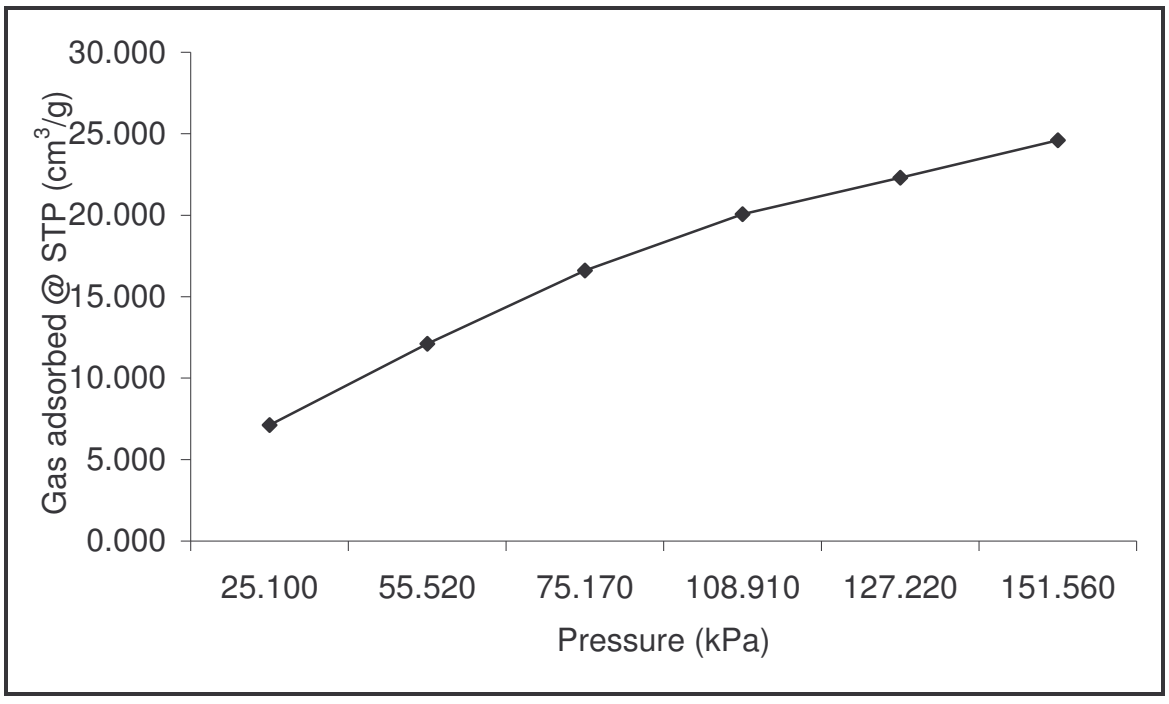

Fig. A.2 Sample 2- Volume of Gas Adsorbed Per Unit Mass Vs Pressure.

Table A3.1 Sample 3- Adsorption Measurement Results

Initial Pressure (bar)	0.2527	0.5075	0.7497	1.0136	1.2452	1.5067
Final Pressure (bar)	0.2509	0.5070	0.7495	1.0135	1.2451	1.5067
Temperature (^oC)	30.2	30.2	30.3	30.3	30.4	30.4

Table A3.2 Sample 3 - Volume of Gas Adsorbed Per Unit Mass

Sample 3						
Pressure (kPa)	25.27	50.75	74.97	101.36	124.52	150.67
Gas adsorbed (cm^3/g)	0.85	1.08	1.18	1.22	1.27	1.27

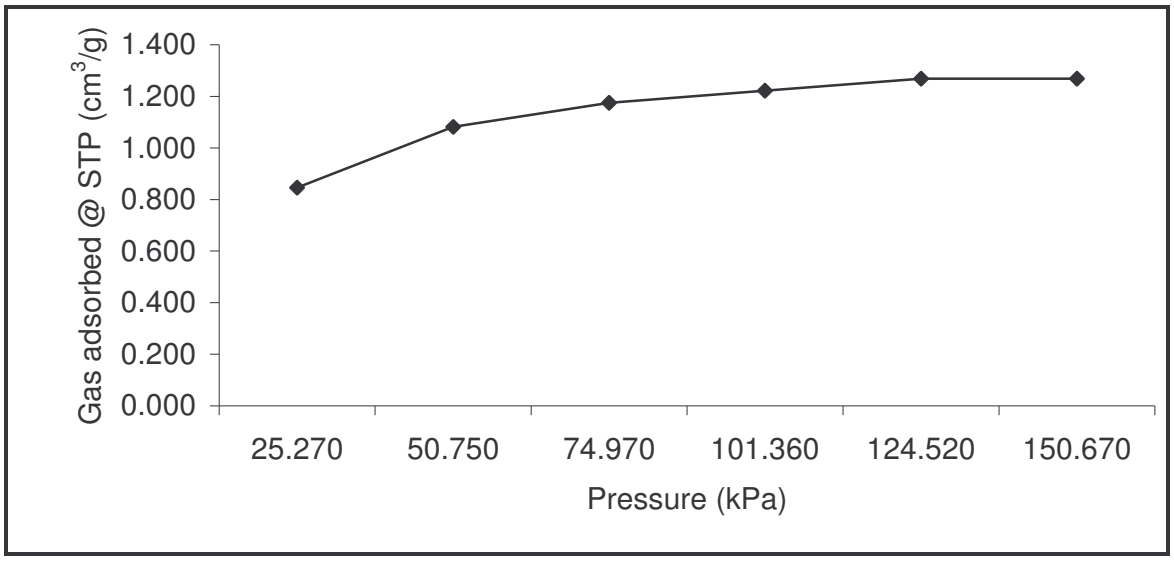

Fig. A.3 Sample 3 - Volume of Gas Adsorbed Per Unit Mass Vs Pressure.

Table A4.1 Sample 4 - Adsorption Measurement Results

Initial Pressure (bar)	0.2497	0.5221	0.7618	1.0169	1.2327	1.5012
Final Pressure (bar)	0.2348	0.5113	0.7529	1.0104	1.2289	1.4975
Temperature (^oC)	30.5	30.5	30.5	30.5	30.6	30.7

Table A4.2 Sample 4 - Volume of Gas Adsorbed Per Unit Mass

Sample 4						
Pressure (kPa)	24.97	52.21	76.18	101.69	123.27	150.12
Gas adsorbed (cm^3/g)	6.94	11.97	16.11	19.13	20.90	22.61

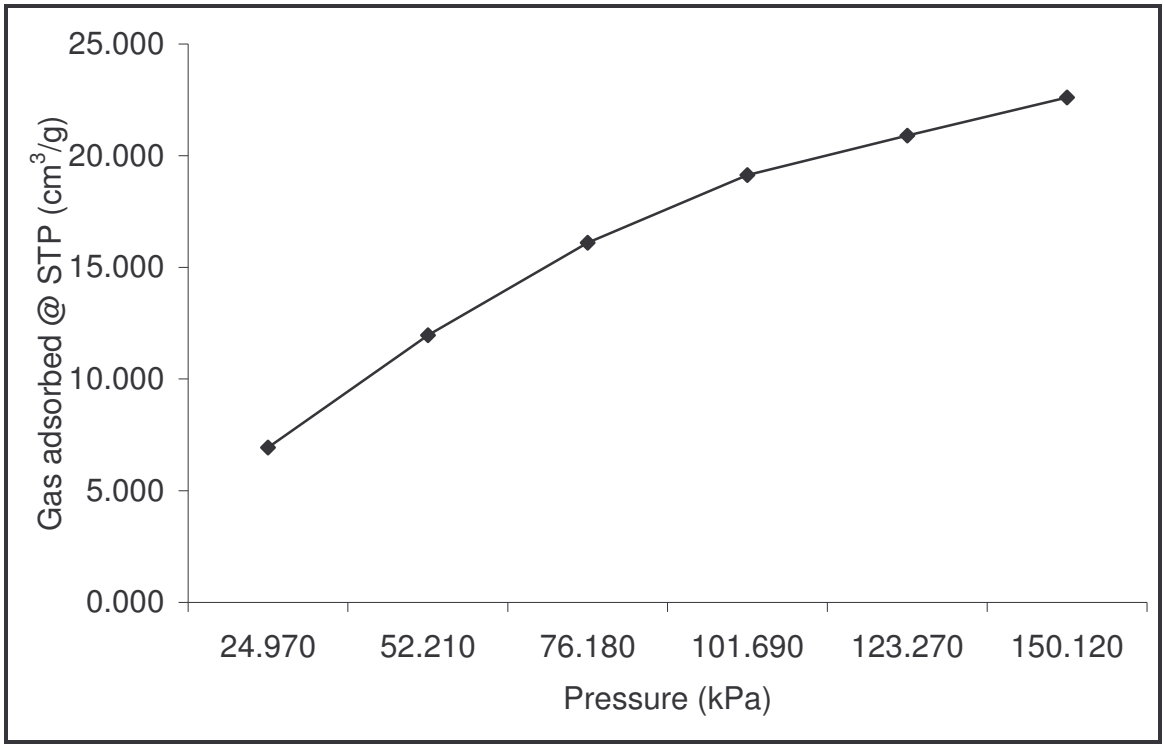

Fig. A.4 Sample 4 - Volume of Gas Adsorbed Per Unit Mass Vs Pressure.

Table A5.1 Sample 5- Adsorption Measurement Results

Initial Pressure (bar)	0.2467	0.5035	0.7467	1.0225	1.2532	1.5112
Final Pressure (bar)	0.2356	0.4973	0.7403	1.0175	1.2493	1.5080
Temperature (^oC)	30.2	30.2	30.2	30.3	30.3	30.4

Table A5.2 Sample 5 - Volume of Gas Adsorbed Per Unit Mass

Sample 5						
Pressure (kPa)	24.67	50.35	74.67	102.25	125.32	151.12
Gas adsorbed (cm^3/g)	5.22	8.13	11.14	13.49	15.31	16.81

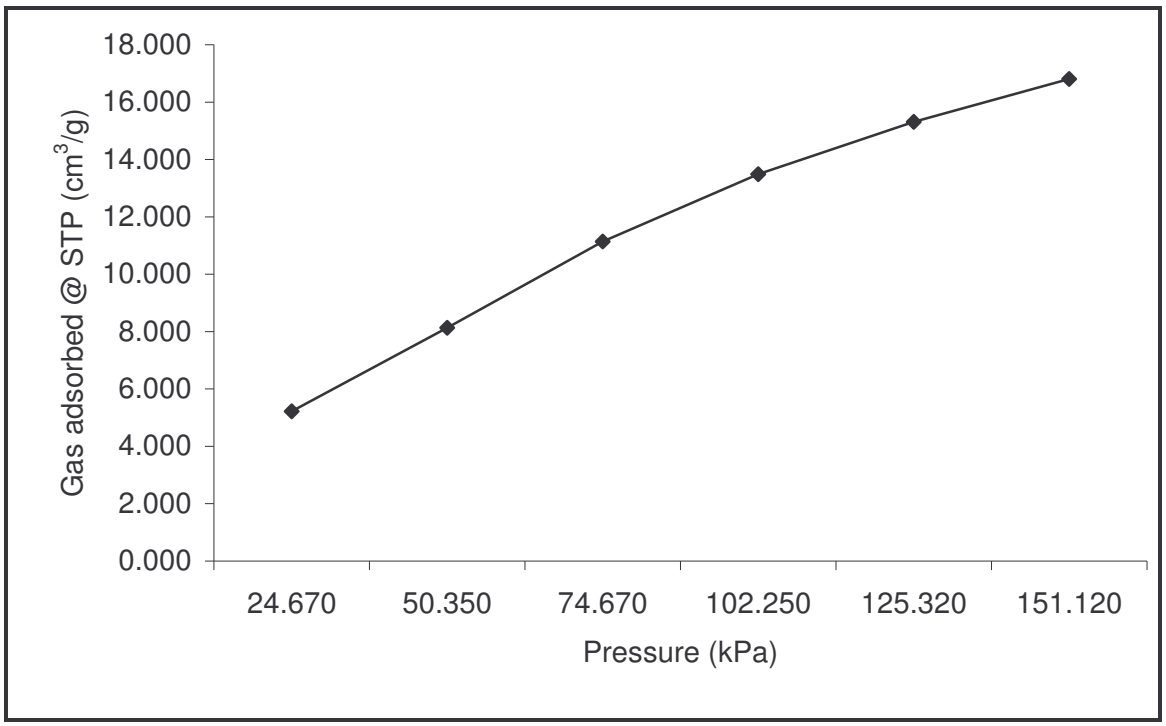

Fig. A.5 Sample 5 - Volume of Gas Adsorbed Per Unit Mass Vs Pressure.

Table A6.1 Sample 6 - Adsorption Measurement Results

Initial Pressure (bar)	0.2510	0.5107	0.7424	1.0157	1.2453	1.5130
Final Pressure (bar)	0.2414	0.5076	0.7395	1.0115	1.2405	1.5119
Temperature (^oC)	30.2	30.3	30.4	30.4	30.4	30.5

Table A6.2 Sample 6 - Volume of Gas Adsorbed Per Unit Mass

Sample 6						
Pressure (kPa)	25.10	51.07	74.24	101.57	124.53	151.30
Gas adsorbed (cm^3/g)	4.51	5.97	7.32	9.28	11.53	12.04

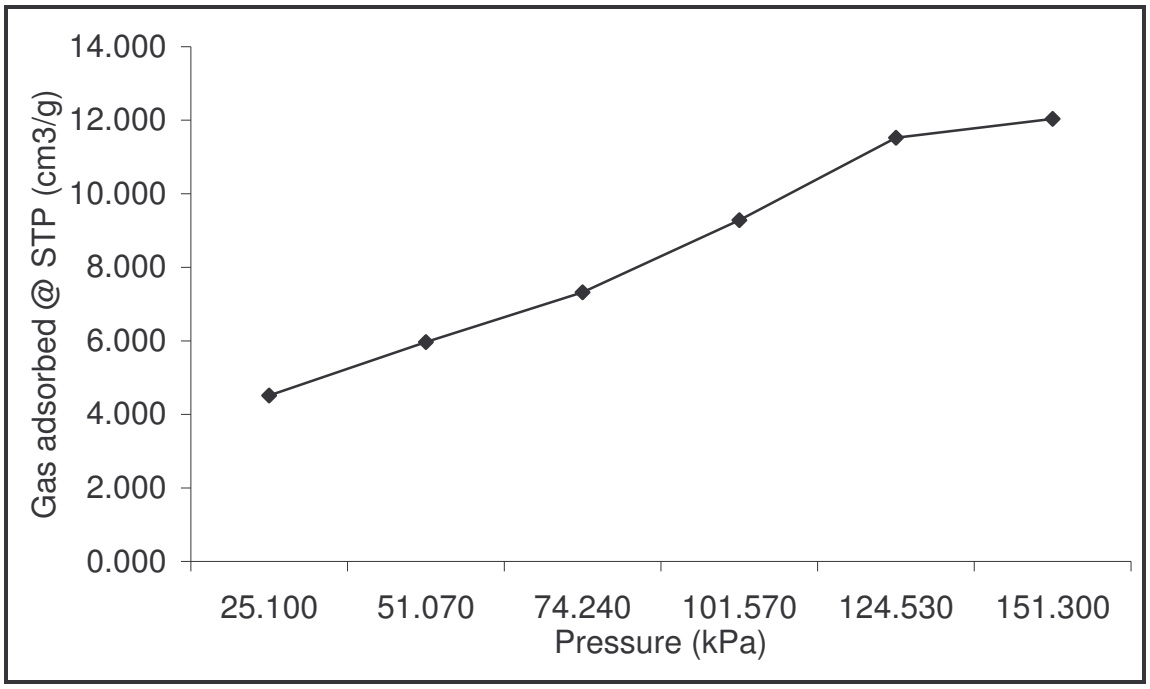

Fig. A.6 Sample 1- Volume of Gas Adsorbed Per Unit Mass Vs Pressure.

Table A7.1 Sample 7- Adsorption Measurement Results

Initial Pressure (bar)	0.2508	0.5090	0.7440	1.0128	1.2482	1.5101
Final Pressure (bar)	0.2382	0.5011	0.7373	1.0085	1.2400	1.5062
Temperature (^oC)	30.0	30.1	30.2	30.2	30.2	30.3

Table A7.2 Sample 7 - Volume of Gas Adsorbed Per Unit Mass

Sample 7						
Pressure (kPa)	25.08	50.90	74.40	101.28	124.82	151.01
Gas adsorbed (cm^3/g)	5.96	9.69	12.84	14.86	16.37	18.20

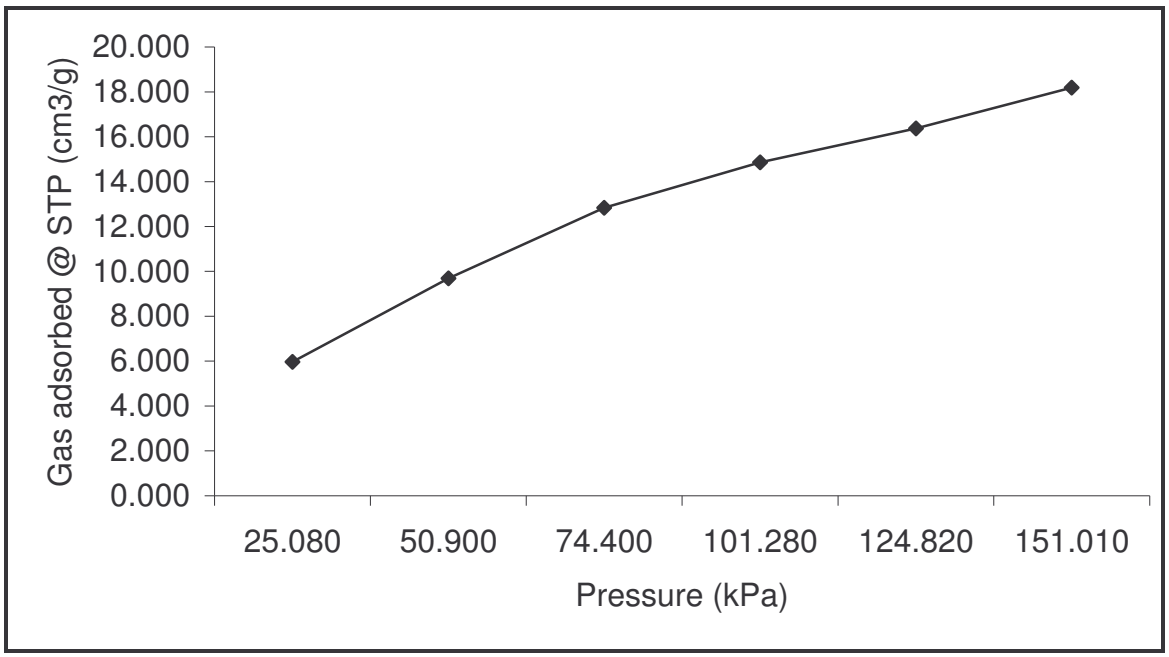

Fig. A.7 Sample 7 - Volume of Gas Adsorbed Per Unit Mass Vs Pressure.

Table A8.1 Sample 8 - Adsorption Measurement Results

Initial Pressure (bar)	0.2514	0.5067	0.7480	1.0093	1.2513	1.4914
Final Pressure (bar)	0.2415	0.5022	0.7441	1.0045	1.2477	1.4885
Temperature (^oC)	30.0	30.1	30.2	30.2	30.2	30.3

Table A8.2 Sample 8 - Volume of Gas Adsorbed Per Unit Mass

	Sample 8					
Pressure (kPa)	25.14	50.67	74.80	100.93	125.13	149.14
Gas adsorbed (cm^3/g)	4.69	6.81	8.64	10.90	12.59	13.95

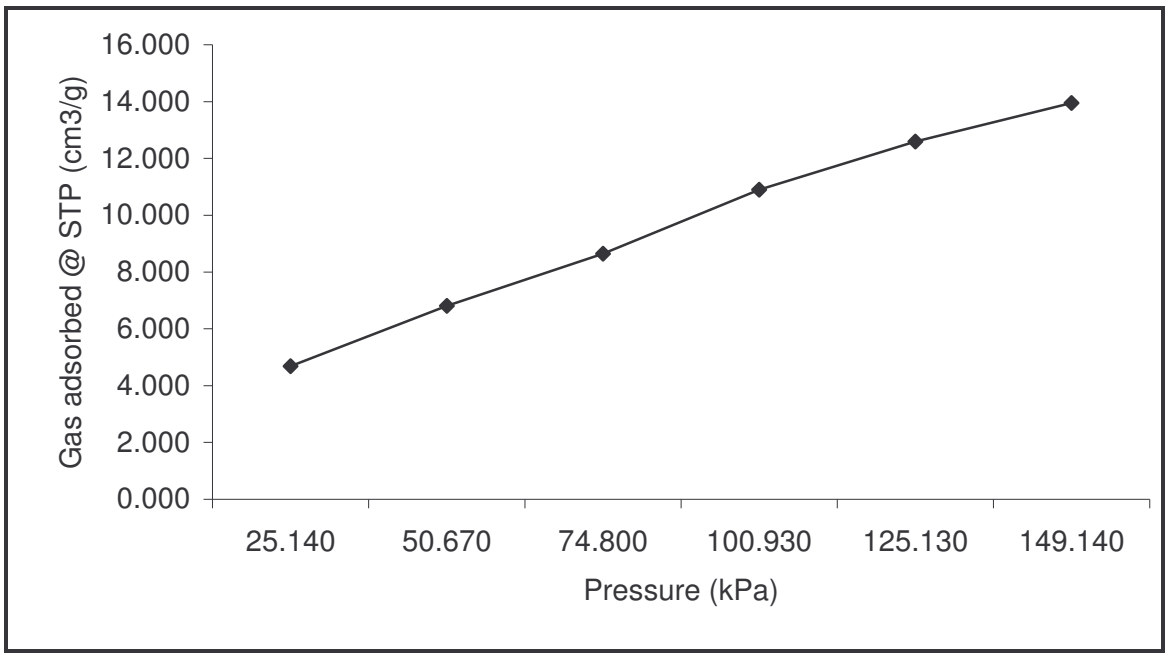

Fig. A.8 Sample 8- Volume of Gas Adsorbed Per Unit Mass Vs Pressure.

Table A9.1 Sample 9 - Adsorption Measurement Results

Initial Pressure (bar)	0.2519	0.5125	0.7456	1.0130	1.2516	1.5073
Final Pressure (bar)	0.2501	0.5121	0.7455	1.0129	1.2516	1.5072
Temperature (^oC)	30.0	30.1	30.2	30.2	30.2	30.3

Table A9.2 Sample 9 - Volume of Gas Adsorbed Per Unit Mass

Sample 9						
Pressure (kPa)	25.19	51.25	74.56	101.30	125.16	150.73
Gas adsorbed (cm^3/g)	0.85	1.04	1.09	1.14	1.14	1.18

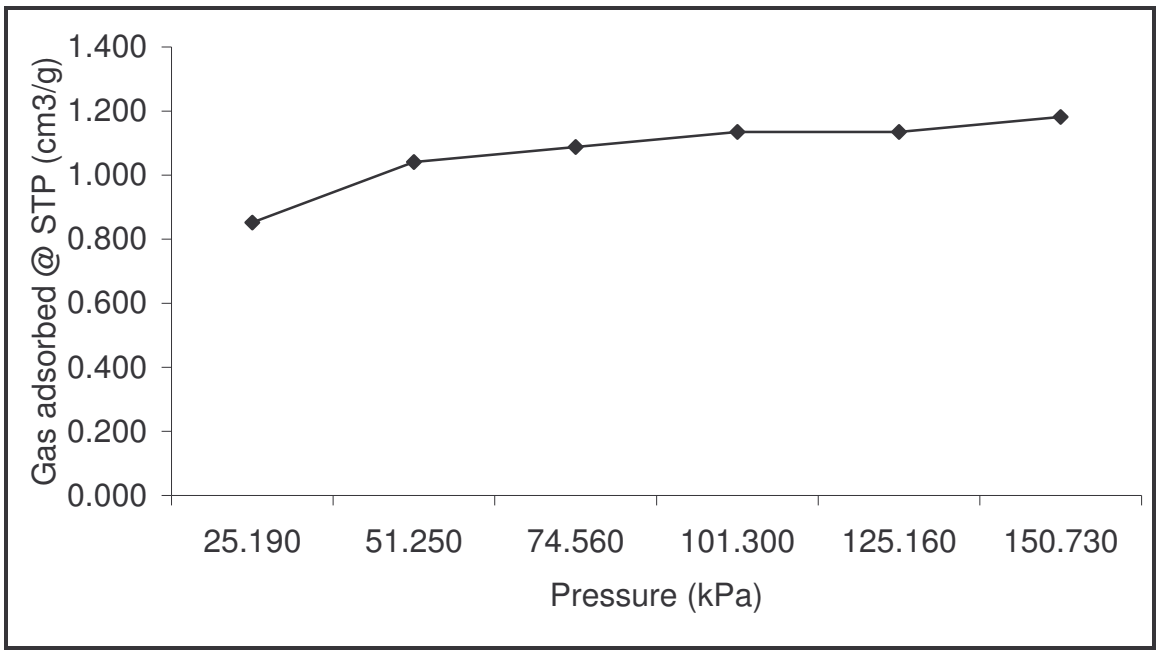

Fig. A.9 Volume of gas adsorbed against pressure for sample 1

Table A10.1 Sample 10 - Adsorption Measurement Results

Initial Pressure (bar)	0.2512	0.5076	0.7485	1.0138	1.2485	1.5033
Final Pressure (bar)	0.2267	0.4913	0.7374	1.0085	1.2414	1.4953
Temperature (^oC)	30.2	30.2	30.2	30.2	30.3	30.2

Table A10.2 Sample 1 - Volume of Gas Adsorbed Per Unit Mass

Sample 10						
Pressure (kPa)	25.12	50.76	74.85	101.38	124.85	150.33
Gas adsorbed (cm^3/g)	11.52	19.18	24.40	26.89	30.22	33.98

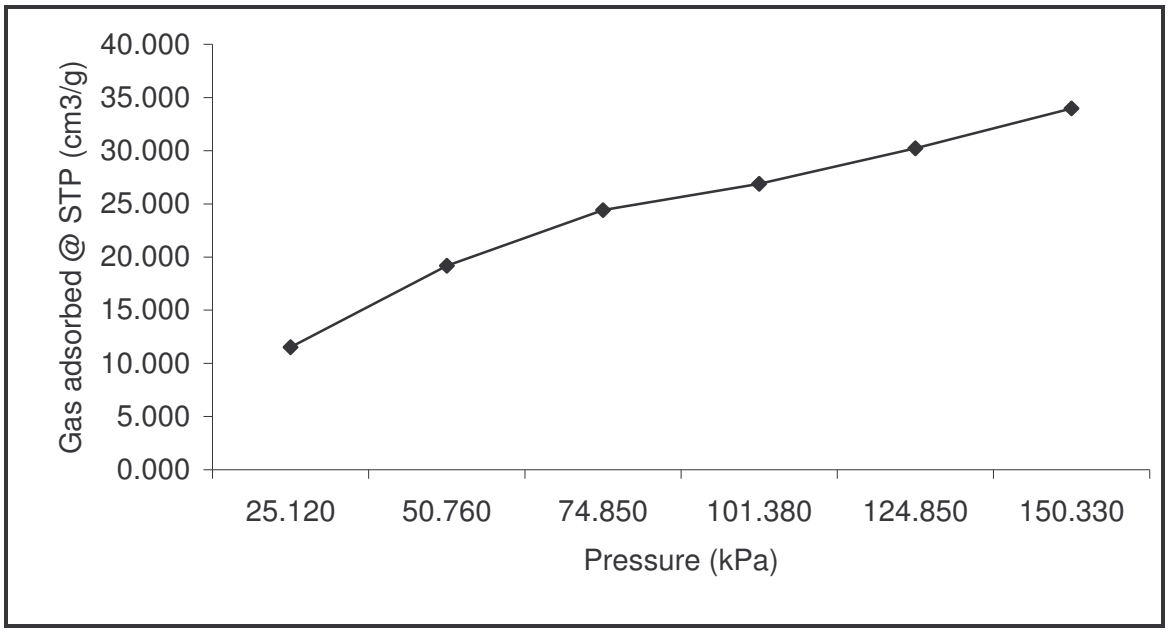

Fig. A.10 Sample 10 - Volume of Gas Adsorbed Per Unit Mass Vs Pressure

Table A11.1 Sample 11 - Adsorption Measurement Results

Initial Pressure (bar)	0.2526	0.5070	0.7519	1.0153	1.2494	1.5053
Final Pressure (bar)	0.2346	0.4958	0.7412	1.0105	1.2473	1.5030
Temperature (^oC)	30.8	30.7	30.7	30.6	30.6	30.6

Table A11.2 Sample 11 - Volume of Gas Adsorbed Per Unit Mass

Sample 11						
Pressure (kPa)	25.26	50.70	75.19	101.53	124.94	150.53
Gas adsorbed (cm^3/g)	8.30	13.48	18.43	20.66	21.63	22.70

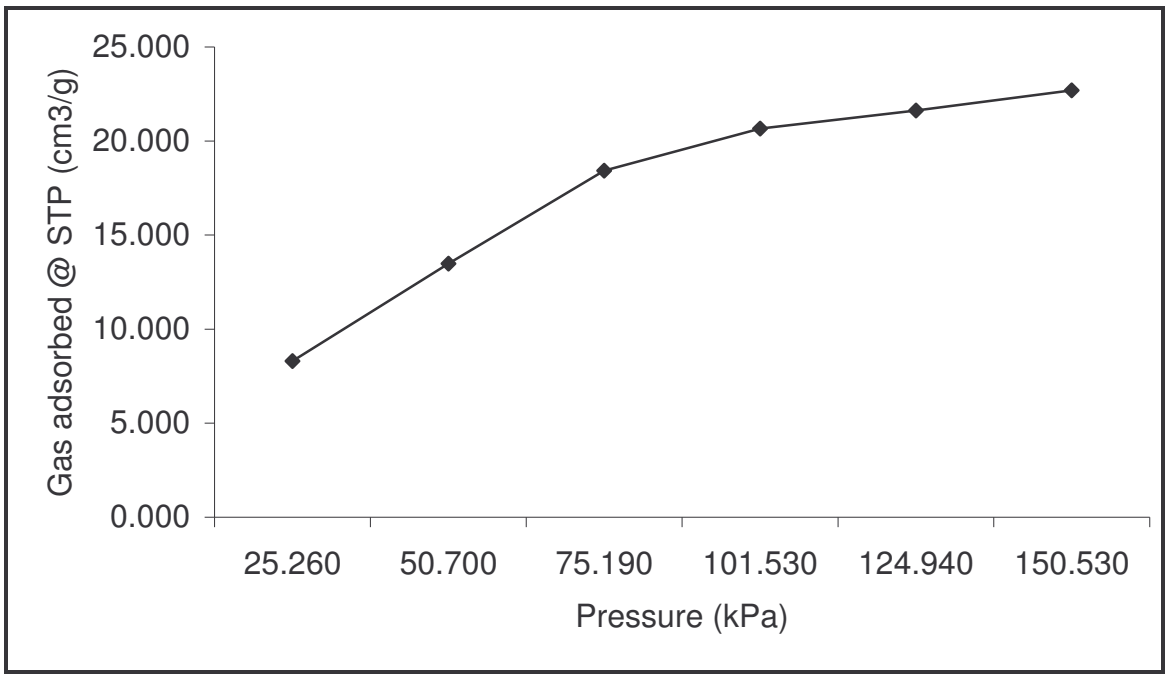

Fig. A.11 Sample 11- Volume of Gas Adsorbed Per Unit Mass Vs Pressure.

Table A12.1 Sample 12 - Adsorption Measurement Results

Initial Pressure (bar)	0.2500	0.5124	0.7516	1.0067	1.2498	1.5083
Final Pressure (bar)	0.2459	0.5101	0.7495	1.0036	1.2470	1.5074
Temperature (^oC)	30.2	30.2	30.3	30.3	30.3	30.4

Table A12.2 Sample 12 - Volume of Gas Adsorbed Per Unit Mass

Sample 12						
Pressure (kPa)	25.00	51.24	75.16	100.67	124.98	150.83
Gas adsorbed (cm^3/g)	1.93	3.01	3.99	5.45	6.76	7.18

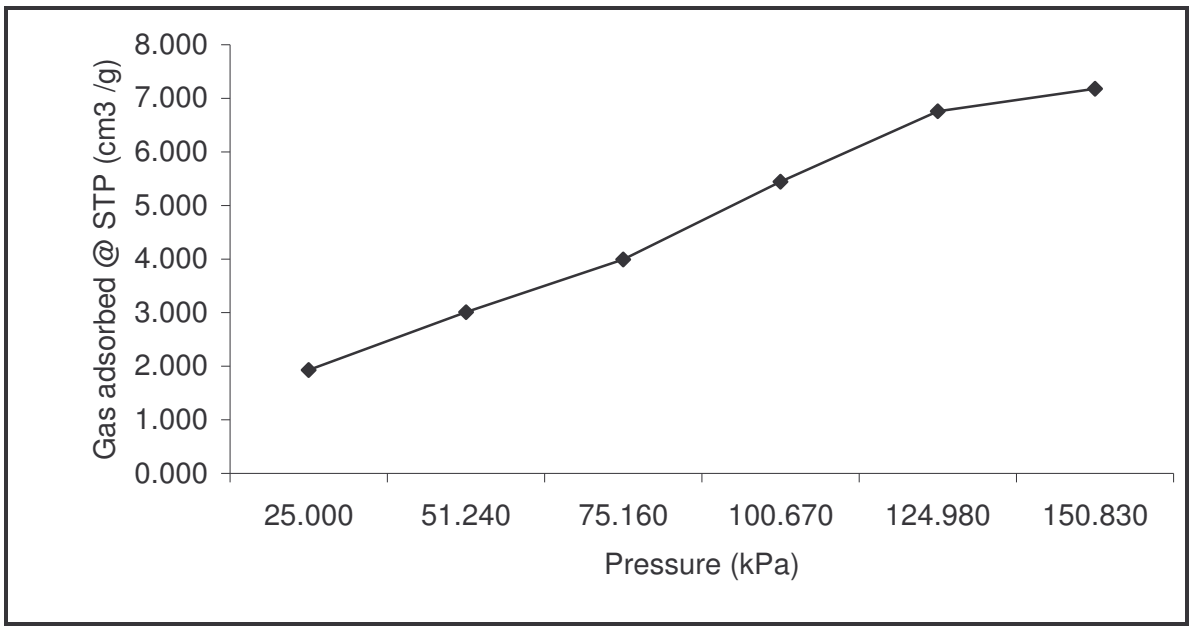

Fig. A.12 Sample 12 - Volume of Gas Adsorbed Per Unit Mass Vs Pressure.

Table A13.1 Sample 13 - Adsorption Measurement Results

Initial Pressure (bar)	0.2528	0.5082	0.7433	1.0096	1.2413	1.5098
Final Pressure (bar)	0.2499	0.5072	0.7427	1.0087	1.2395	1.5063
Temperature (^oC)	30.7	30.7	30.7	30.7	30.6	30.6

Table A13.2 Sample 13 - Volume of Gas Adsorbed Per Unit Mass

Sample 13						
Pressure (kPa)	25.28	50.82	74.33	100.96	124.13	150.98
Gas adsorbed (cm^3/g)	1.34	1.81	2.08	2.50	3.33	4.96

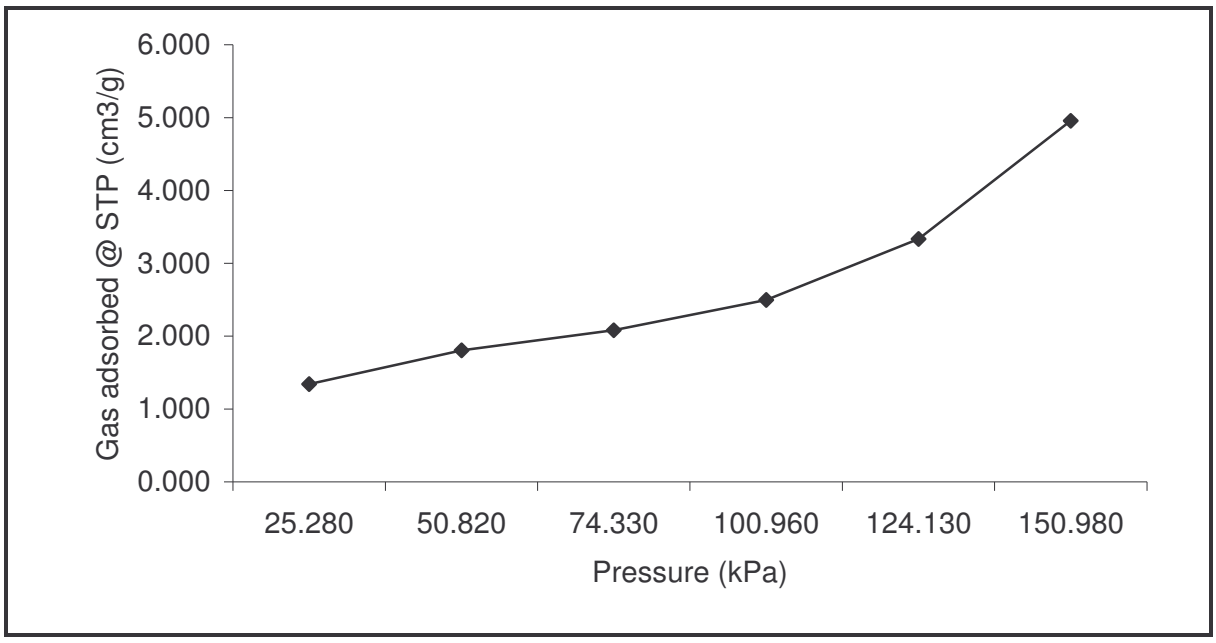

Fig. A.13 Sample 13 - Volume of Gas Adsorbed Per Unit Mass Vs Pressure.

APPENDIX B: LANGMUIR FIT

Table B.1 Sample 1 – P/Vadsorbed and Pressure.

Sample 1						
P/Vads (kPa/cm^3g^{-1})	6.03	8.53	9.89	10.47	11.18	12.24
P (kPa)	25.20	51.04	75.15	101.32	125.76	150.70

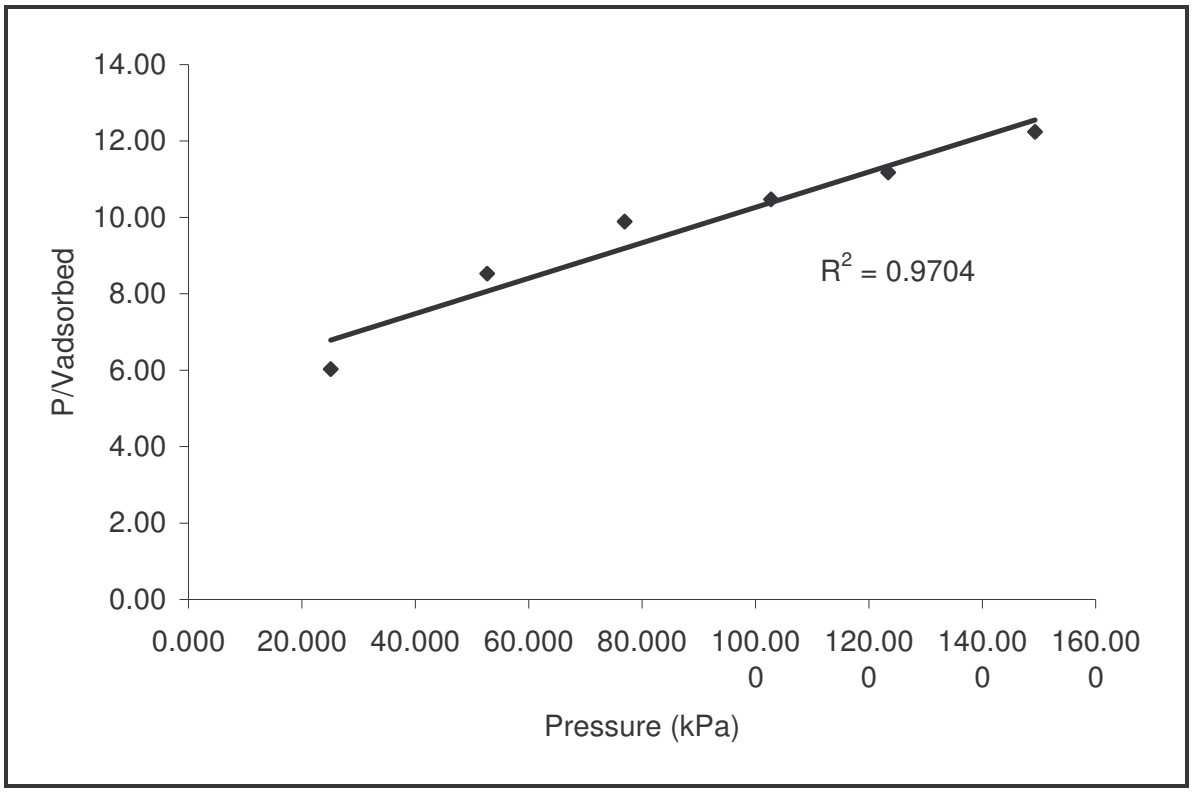

Fig. B.1 Sample 1 - P/Vadsorbed vs Pressure.

Table B.2 Sample 2 – P/Vadsorbed and Pressure.

Sample 2						
P/Vads (kPa/cm^3g^{-1})	3.52	4.59	4.53	5.43	5.70	6.16
P (kPa)	25.10	55.52	75.17	108.91	127.22	151.56

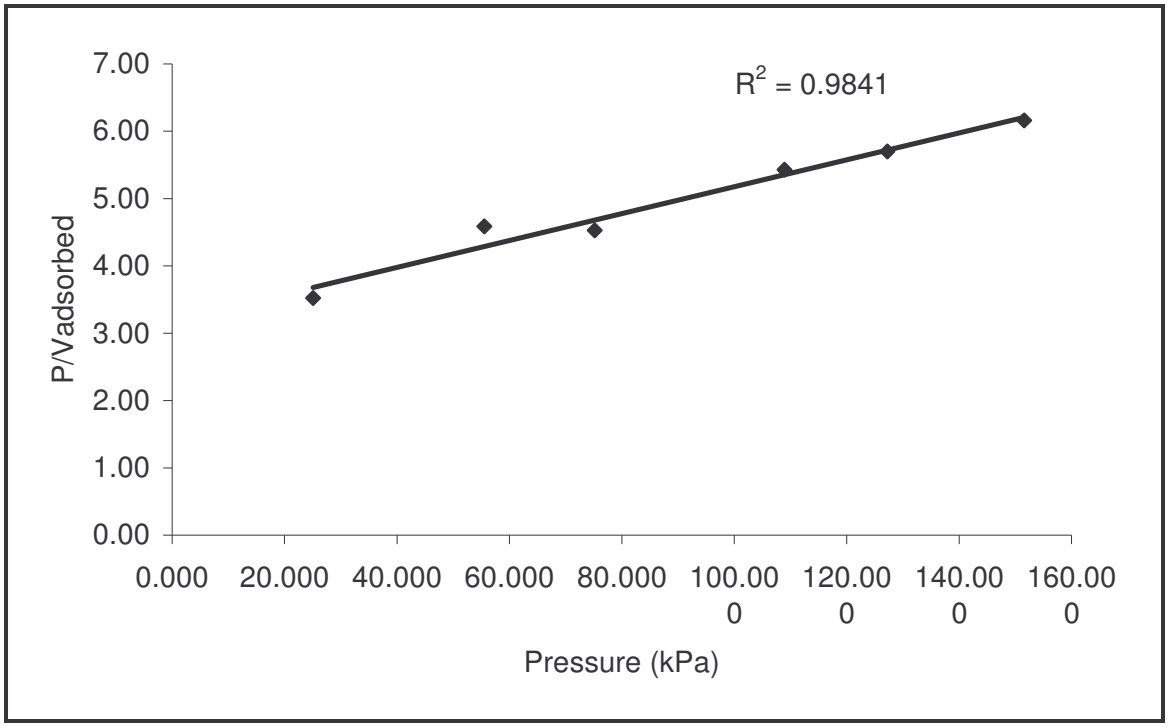

Fig. B.2 Sample 2 - P/Vadsorbed vs Pressure.

Table B.3 Sample 3 – P/Vadsorbed and Pressure.

Sample 3						
P/Vads (kPa/cm^3g^{-1})	29.86	46.93	63.8	82.93	98.15	118.76
P (kPa)	25.27	50.75	74.97	101.36	124.52	150.67

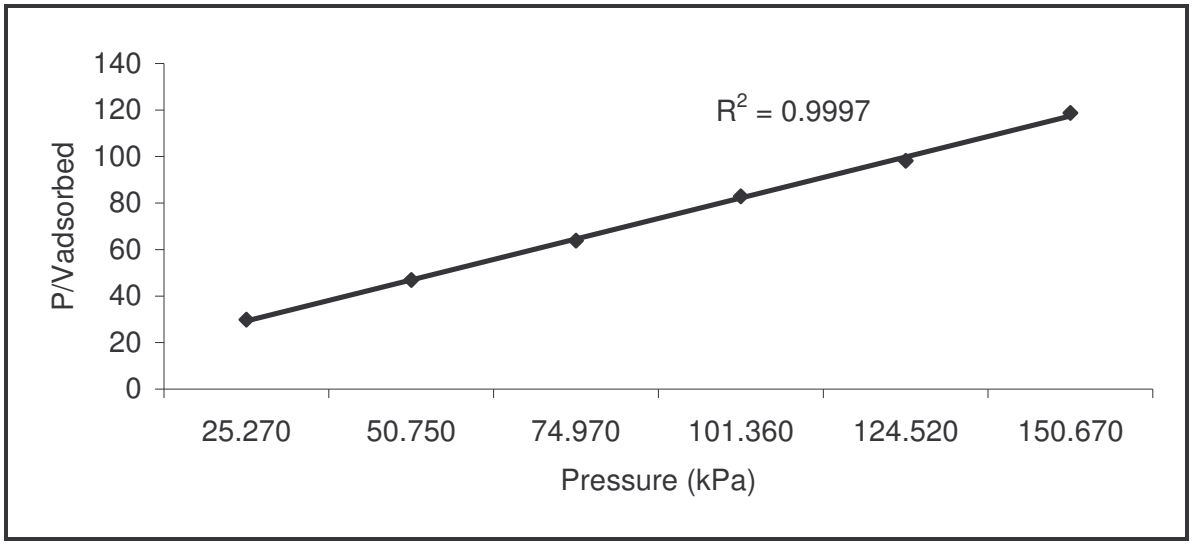

Fig. B.3 Sample 3 - P/Vadsorbed vs Pressure.

Table B.4 Sample 4 – P/Vadsorbed and Pressure.

Sample 4						
P/Vads (kPa/cm^3g^{-1})	3.60	4.36	4.73	5.31	5.90	6.64
P (kPa)	24.97	52.21	76.18	101.69	123.27	150.12

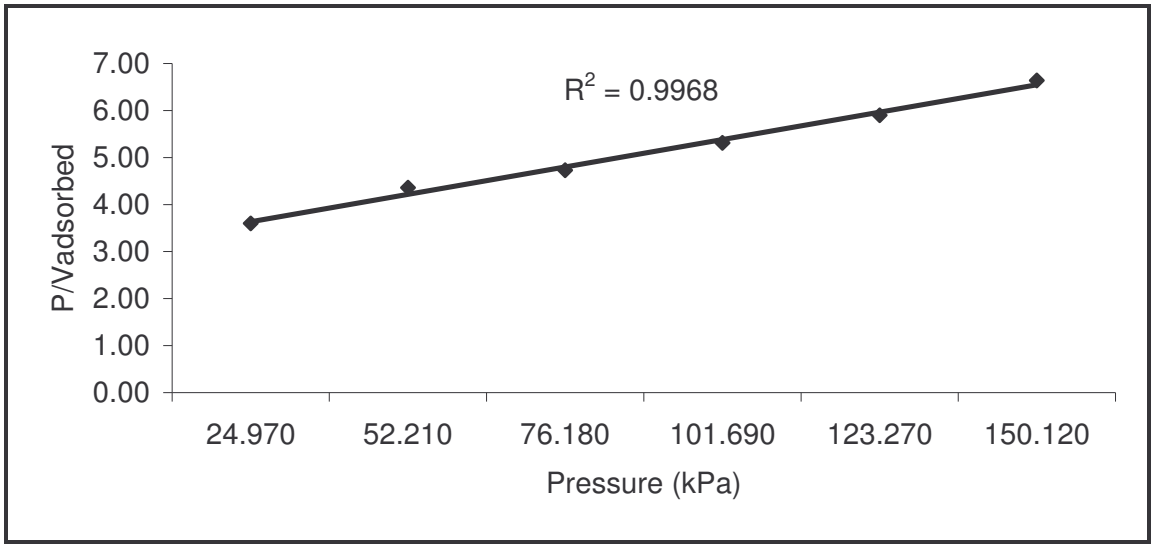

Fig. B.4 Sample 4 - P/Vadsorbed vs Pressure.

Table B.5 Sample 5 – P/Vadsorbed and Pressure.

Sample 5						
P/Vads (kPa/cm^3g^{-1})	4.73	6.19	6.70	7.58	8.18	8.99
P (kPa)	24.67	50.35	74.67	102.25	125.32	151.12

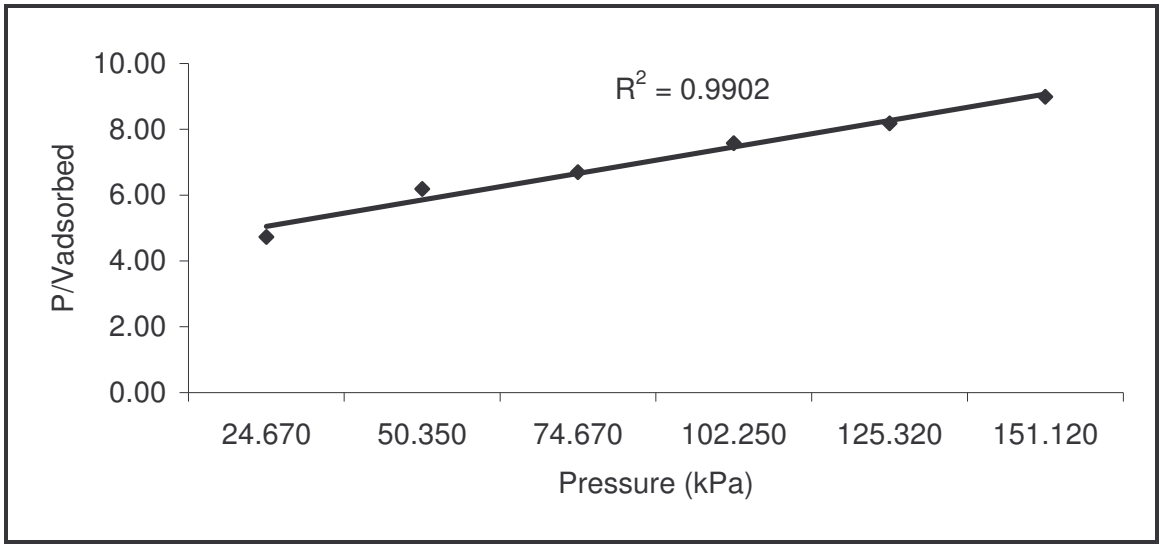

Fig. B.5 Sample 5 - P/Vadsorbed vs Pressure.

Table B.6 Sample 6 – P/Vadsorbed and Pressure.

Sample 6						
P/Vads (kPa/cm^3g^{-1})	5.56	8.56	10.14	10.94	10.81	12.57
P (kPa)	25.10	51.07	74.24	101.57	124.53	151.30

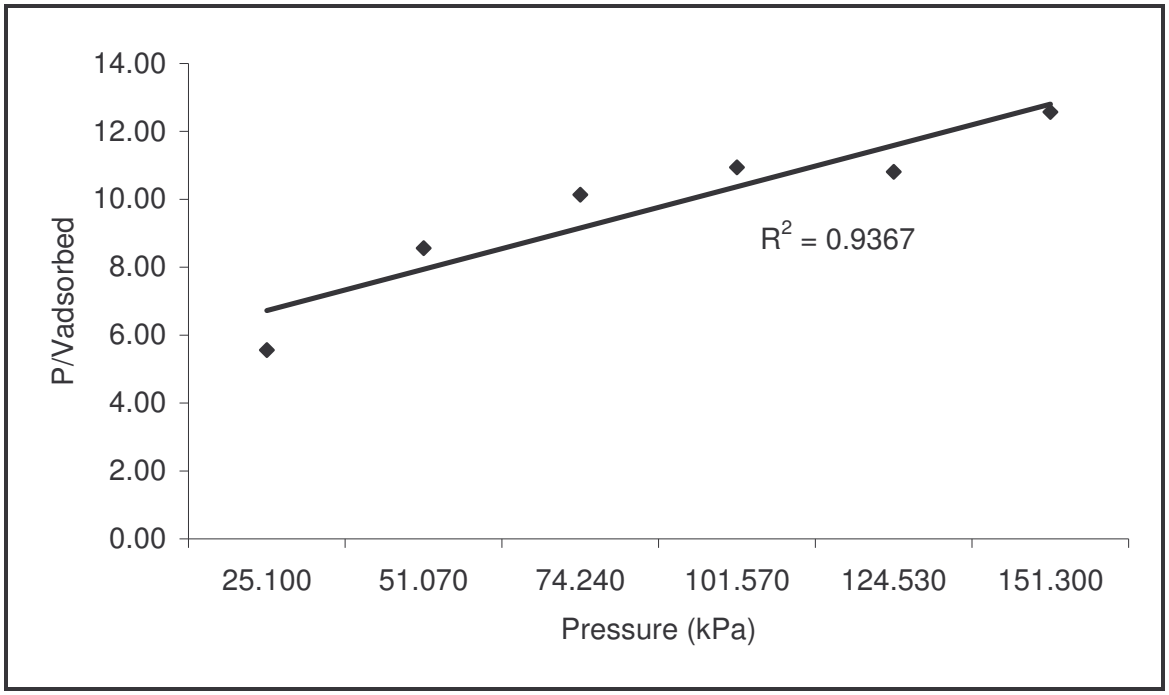

Fig. B.6 Sample 6 - P/Vadsorbed vs Pressure.

Table B.7 Sample 7 – P/Vadsorbed and Pressure.

Sample 7						
P/Vads (kPa/cm^3g^{-1})	4.21	5.25	5.79	6.81	7.63	8.30
P (kPa)	25.08	50.90	74.40	101.28	124.82	151.01

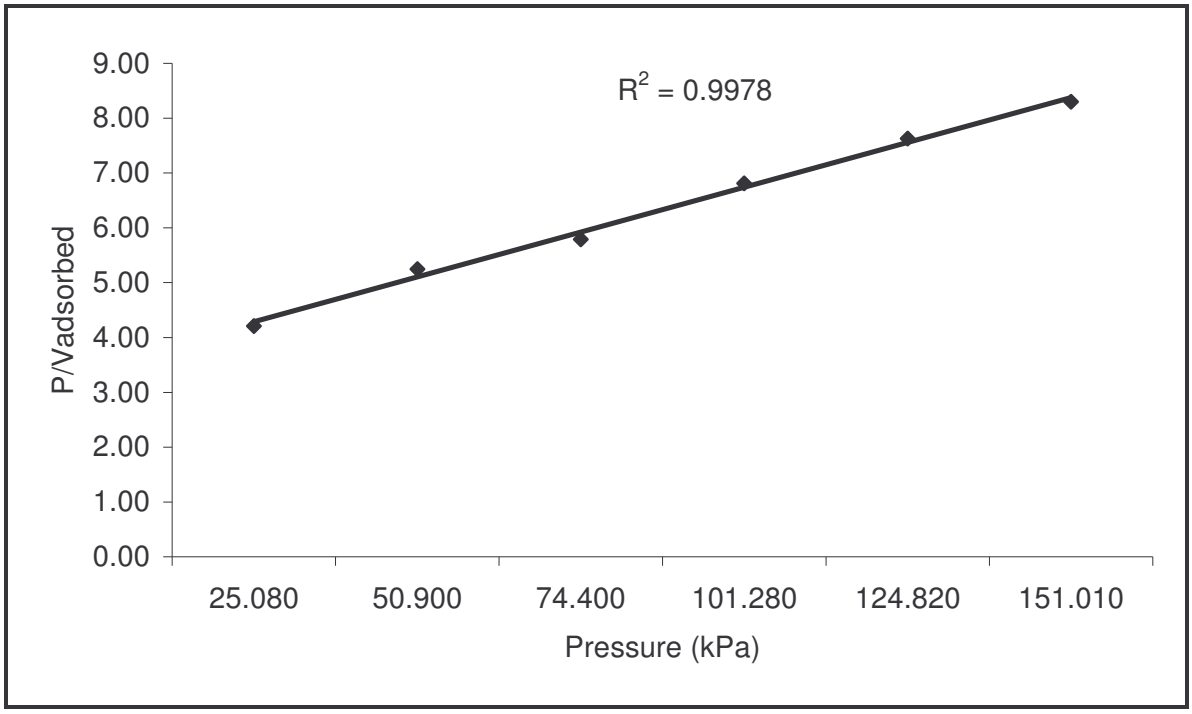

Fig. B.7 Sample 7 - P/Vadsorbed vs Pressure.

Table B.8 Sample 8 – P/Vadsorbed and Pressure.

Sample 8						
P/Vads (kPa/cm^3g^{-1})	5.37	7.44	8.65	9.26	9.94	10.69
P (kPa)	25.14	50.67	74.80	100.93	125.13	149.14

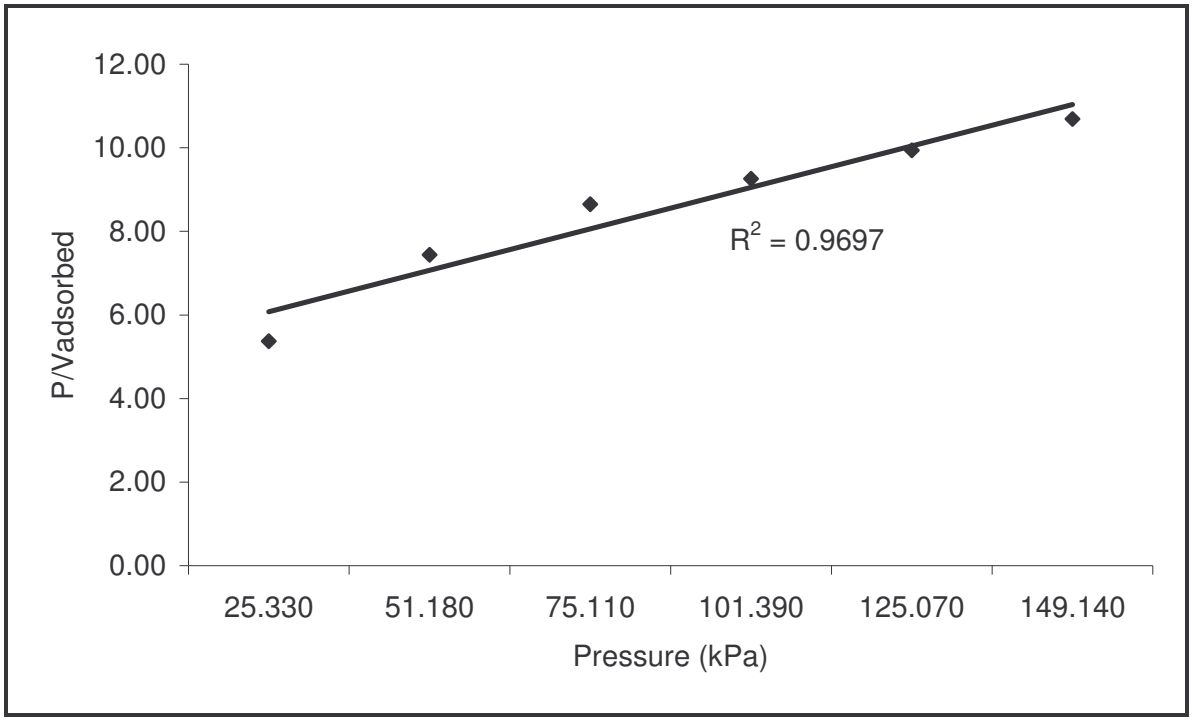

Fig. B.8 Sample 8 - P/Vadsorbed vs Pressure.

Table B.9 Sample 9 – P/Vadsorbed and Pressure.

Sample 9						
P/Vads (kPa/cm^3g^{-1})	29.57	49.25	68.55	89.27	110.30	127.57
P (kPa)	25.19	51.25	74.56	101.30	125.16	150.73

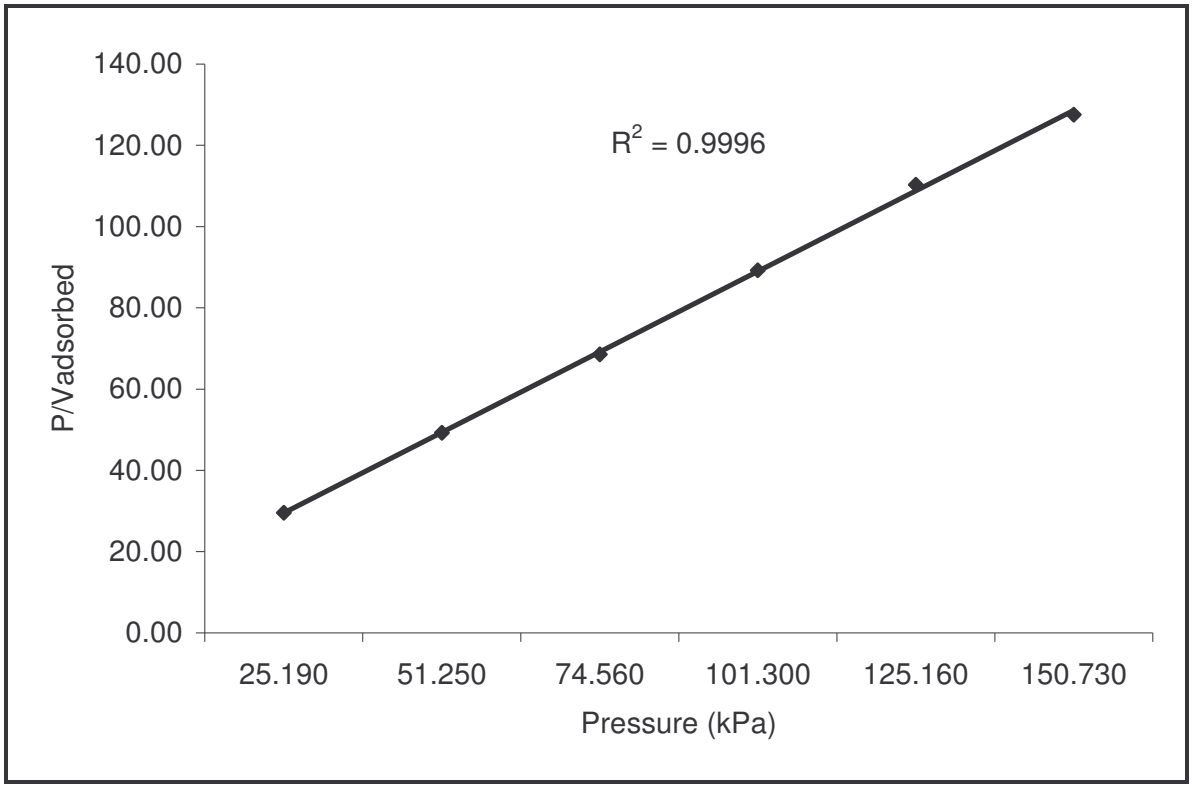

Fig. B.9 Sample 9 - P/Vadsorbed vs Pressure.

Table B.10 Sample 10 – P/Vadsorbed and Pressure.

Sample 10						
P/Vads (kPa/cm^3g^{-1})	2.18	2.65	3.07	3.77	4.13	4.42
P (kPa)	25.12	50.76	74.85	101.38	124.85	150.33

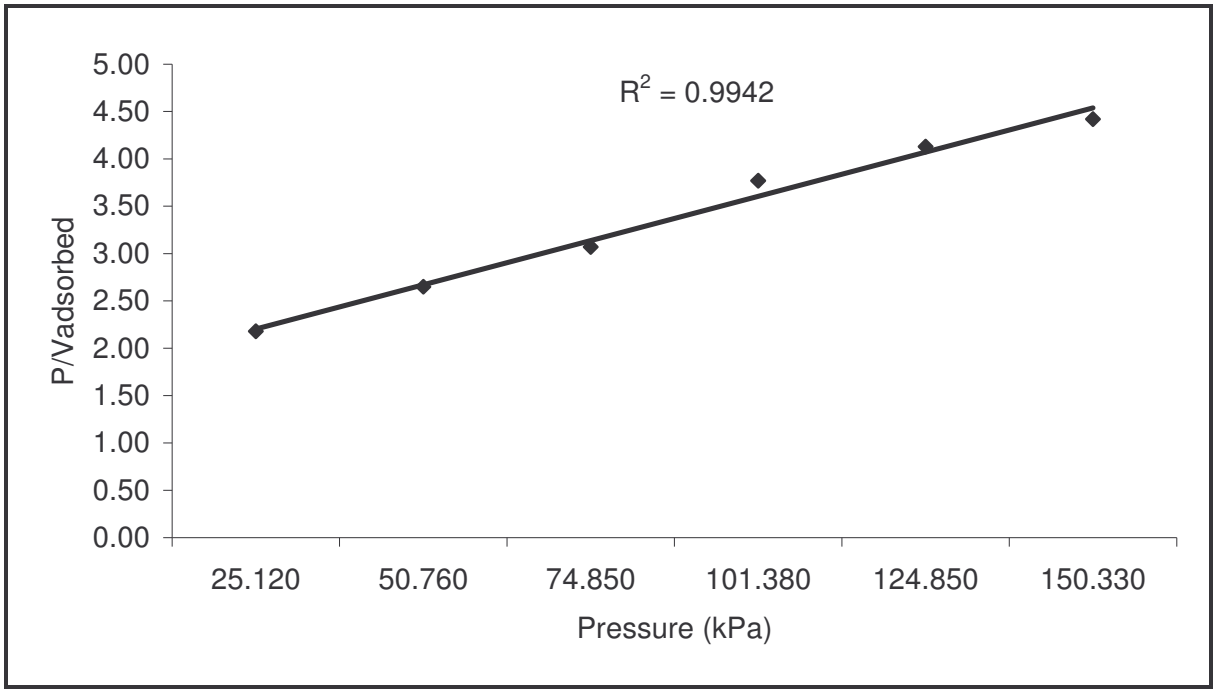

Fig. B.10 Sample 10 - P/Vadsorbed vs Pressure.

Table B.11 Sample 11 – P/Vadsorbed and Pressure.

Sample 11						
P/Vads (kPa/cm^3g^{-1})	3.04	3.76	4.08	4.92	5.78	6.63
P (kPa)	25.26	50.70	75.19	101.53	124.94	150.53

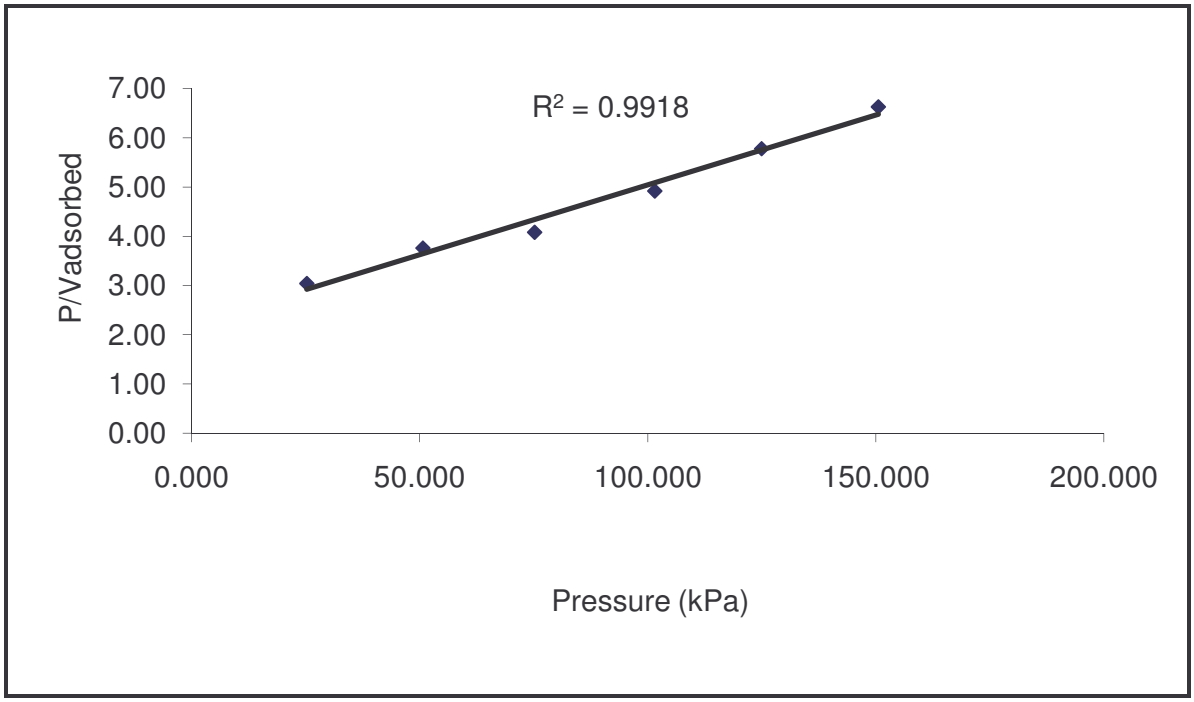

Fig. B.11 Sample 11 - P/Vadsorbed vs Pressure.

Table B.12 Sample 12 – P/Vadsorbed and Pressure.

Sample 12						
P/Vads (kPa/cm^3g^{-1})	12.97	17.03	18.82	18.48	18.49	21.01
P (kPa)	25.00	51.24	75.16	100.67	124.98	150.83

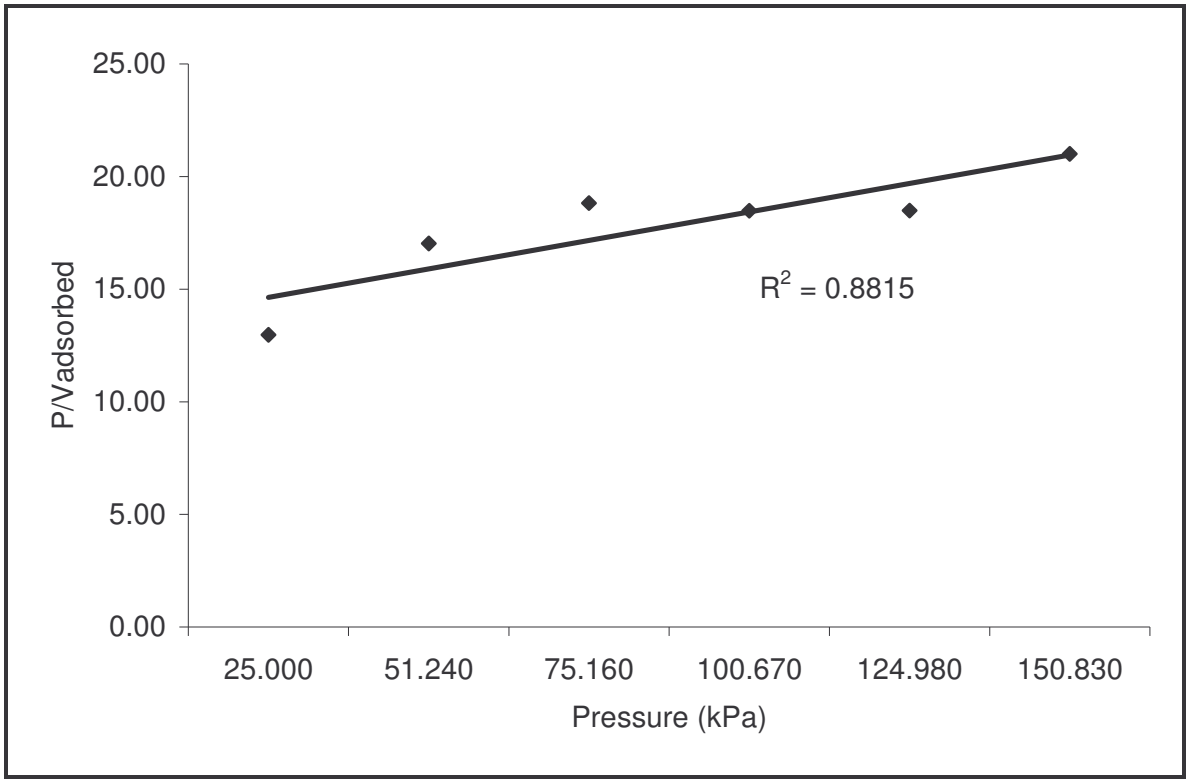

Fig. B.12 Sample 12 - P/Vadsorbed vs Pressure.

Table B.13 Sample 13 – P/Vadsorbed and Pressure.

Sample 13						
P/Vads (kPa/cm^3g^{-1})	18.85	28.17	35.71	40.42	37.24	30.46
P (kPa)	25.28	50.82	74.33	100.96	124.13	150.98

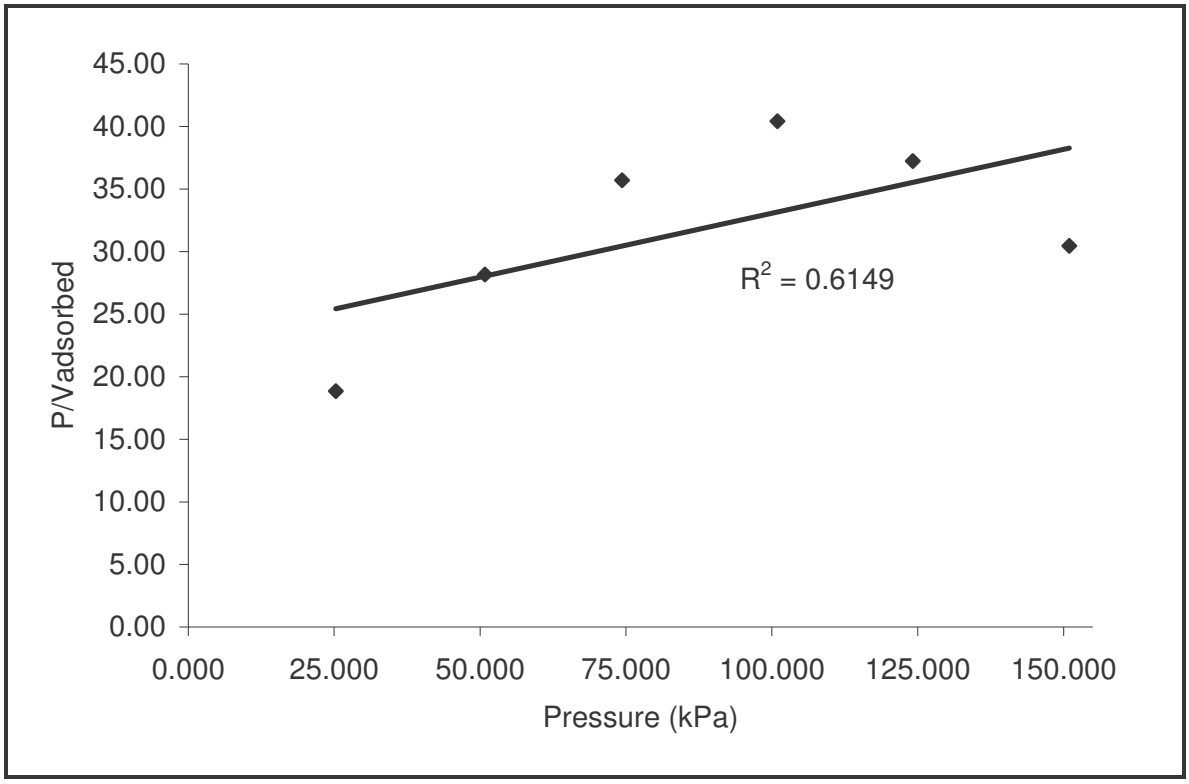

Fig. B.13 Sample 13 - P/Vadsorbed vs Pressure.

APPENDIX C: GENERAL RESULTS

Table C.1. Petrographic Analysis Results of Parent Samples

Parent Sample I.D	Petrographic Analysis Results (%)				
	Vitrinite	Inertinite	Liptinite	Mineral matter	RoVmr
Witbank	13.8	56.8	4.0	25.4	0.72
Waterberg	46.2	4.80	1.4	47.6	0.69
KZN Sample A	80.0	16.3	0	3.7	2.28
KZN Sample B	49.8	46.5	0	4.6	2.21

Table C.2. Table of Experimental and Calculated Gas Adsorbed

Sample I.D	Gas adsorbed (cm^3/g)	
	Experimental	Calculated
Sample 1	12.31	11.92
Sample 2	24.59	24.45
Sample 3	1.27	1.28
Sample 4	22.61	22.85
Sample 5	16.81	16.69
Sample 6	12.04	11.77
Sample 7	18.2	18.01
Sample 8	13.95	13.57
Sample 9	1.18	1.17
Sample 10	33.98	33.11
Sample 11	22.7	23.26
Sample 12	7.18	7.19
Sample 13	4.96	3.96